SCHISTOSOMA MANSONI : LOCALISATION OF SCHISTOSOME ANTIGENS USING MONOSPECIFIC ANTIBODIES RAISED AGAINST ADULT WORM TEGUMENT MEMBRANES

VOLUME 2 (2 VOLS.)

SUDA RIENGROJPITAK

Thesis submitted for the degree of

DOCTOR OF PHILOSOPHY

University of York

Department of Biology

July, 1987

TO MY PARENTS AND FAMILY

TABLE OF CONTENTS

VOLUME 2

LIST OF ABBREVIATIONS

A	Apical end or anterior end
B	Body
BI	Basal invagination
BL	Basal lamina
C	Cytoplasmic connections
CM	Circular muscle fibres
d	Duct
D	Digestive tract
DB	Discoid body
ER	Endoplasmic reticulum
F	Female worm
g	Postacetabular gland
G	Gland cells
GA	Golgi apparatus
GD	Gland duct
H	Head capsule
Hb	Haemoglobin
I	Internal tissues
L	Lamellae
LM	Longitudinal muscle fibres
M	Muscle layer
MF	Muscle fibres or myofilaments
MT	Mitochondria
n	Nephridia
N	Nucleus
p	The point where the cercarial tail detached from the body
P	Packets
PE	Posterior end
PM	Plasma membrane
PT	Parenchymal tissues
SB	Secretory body
sp	Surface pit
T	Tail
TM	Tegument
V	Vacuole

CHAPTER 2

MONOCLONAL ANTIBODIES REACTING AGAINST TEGUMENT ANTIGENS

FIGURE 2.1

Acetone-fixed cryostat sections of adult male S. mansoni were incubated in a 1:100 dilution of AMS followed by FITC conjugated rabbit anti-mouse Ig (RAM/Ig/FITC, 1:64) as described in detail in Materials & Methods. Transverse section showing an intense and homogeneous fluorescence throughout, with strongest reactivity in the tegument. The gut epithelium is also positive. The cytoplasm of the muscle cells beneath the tegument is unlabelled but the muscle cell membrane or the interstitial material around the muscle fibres is fluorescently labelled. Sections of female adult worms (not shown) exhibit a similar staining pattern to that of male worms except for the vitelline cells in the parenchyma which autofluoresce bright yellow. x 130.

FIGURE 2.2

Paraformaldehyde-fixed frozen section of S. mansoni cercaria stained with AMS and RAM/Ig/FITC at dilutions of 1:100 and 1:64, respectively. The tegument of the cercaria is strongly labelled. The internal tissues are less positive. The spines within the tegument are also fluorescently labelled. The gland cells (G) inside the cercarial body are negative and appear as a dark area in section. Sections of tail (T) also show positive fluorescence, the label in the tegument being stronger than in the internal tissues. x 520.

FIGURE 2.3

Paraformaldehyde-fixed section of 3h in vitro skin-transformed schistosomulum stained with AMS (1:100) and RAM/Ig/FITC (1:64). The whole section exhibits fluorescence, brightest in the tegument and the peripheral area beneath the tegument. The gland cells (G) are unlabelled. x 520.

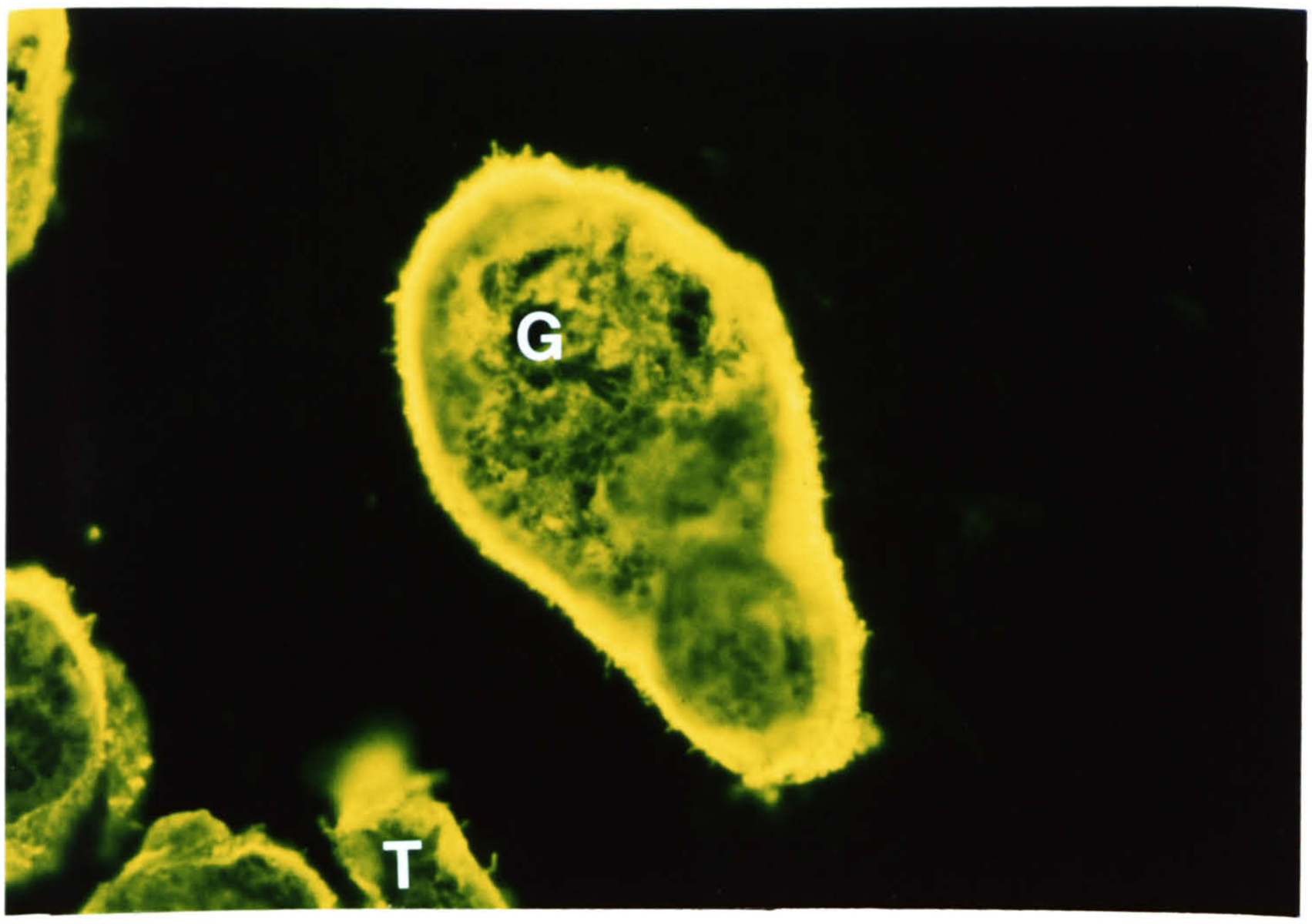
G
T

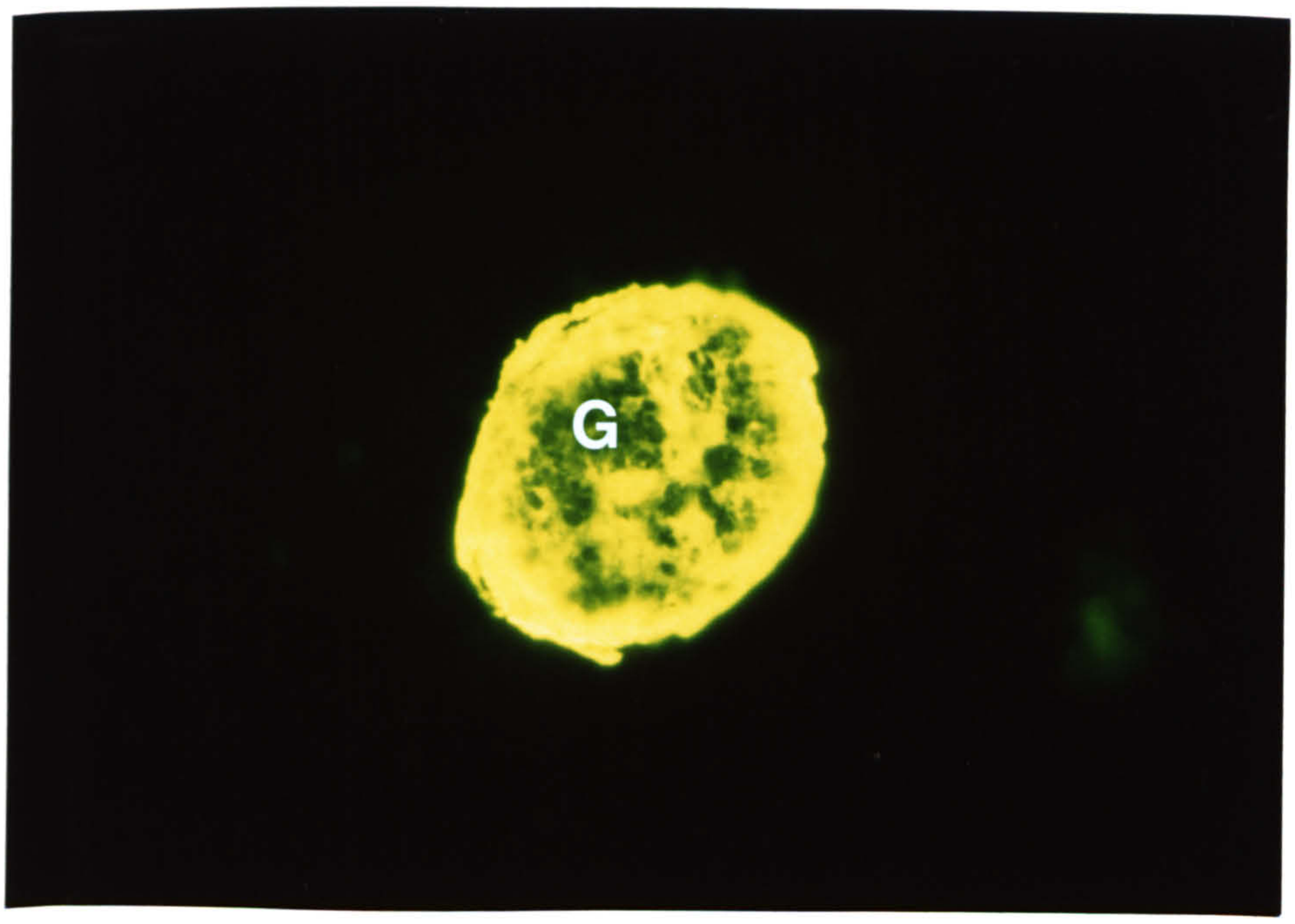
G

FIGURE 2.4

Immunofluorescence of paraformaldehyde-fixed intact cercaria labelled with AMS (1:100) plus RAM/Ig/FITC (1:64). The antibodies bind strongly to the entire surface of the cercarial body and tail (T). The apical end (A) of the body shows very bright fluorescence. The staining pattern of some parasites exhibited a patchy appearance (not shown). x 520.

FIGURE 2.5

Surface membrane binding of AMS (1:100) and RAM/Ig/FITC (1:64) to PF-fixed intact 3h skin-transformed schistosomulum. The antibody binds uniformly to the parasite surface. In some parasites, the posterior end of the body is more strongly fluorescent than the apical area. x 520.


A
T

FIGURE 2.6

AMS does not bind to the surface of intact PF-fixed 5-day-lung worms. Autofluorescence is seen in the digestive tract. Similar results were obtained with all the 50 MABs used in the present study. x 130.

FIGURE 2.7

PF-fixed intact, cultured (24 h) 21-day-liver worm labelled with AMS (1:40) and RAM/Ig/FITC (1:25). The binding of antibodies gave a patchy appearance to the worm surface. Fluorescent label is stronger in the rough areas (*) than on the smooth surface. Some areas are unstained. AMS binds to approximately 50% or less of the parasite surface. Uncultured liver worms were weakly positive or negative (not shown). x 520.

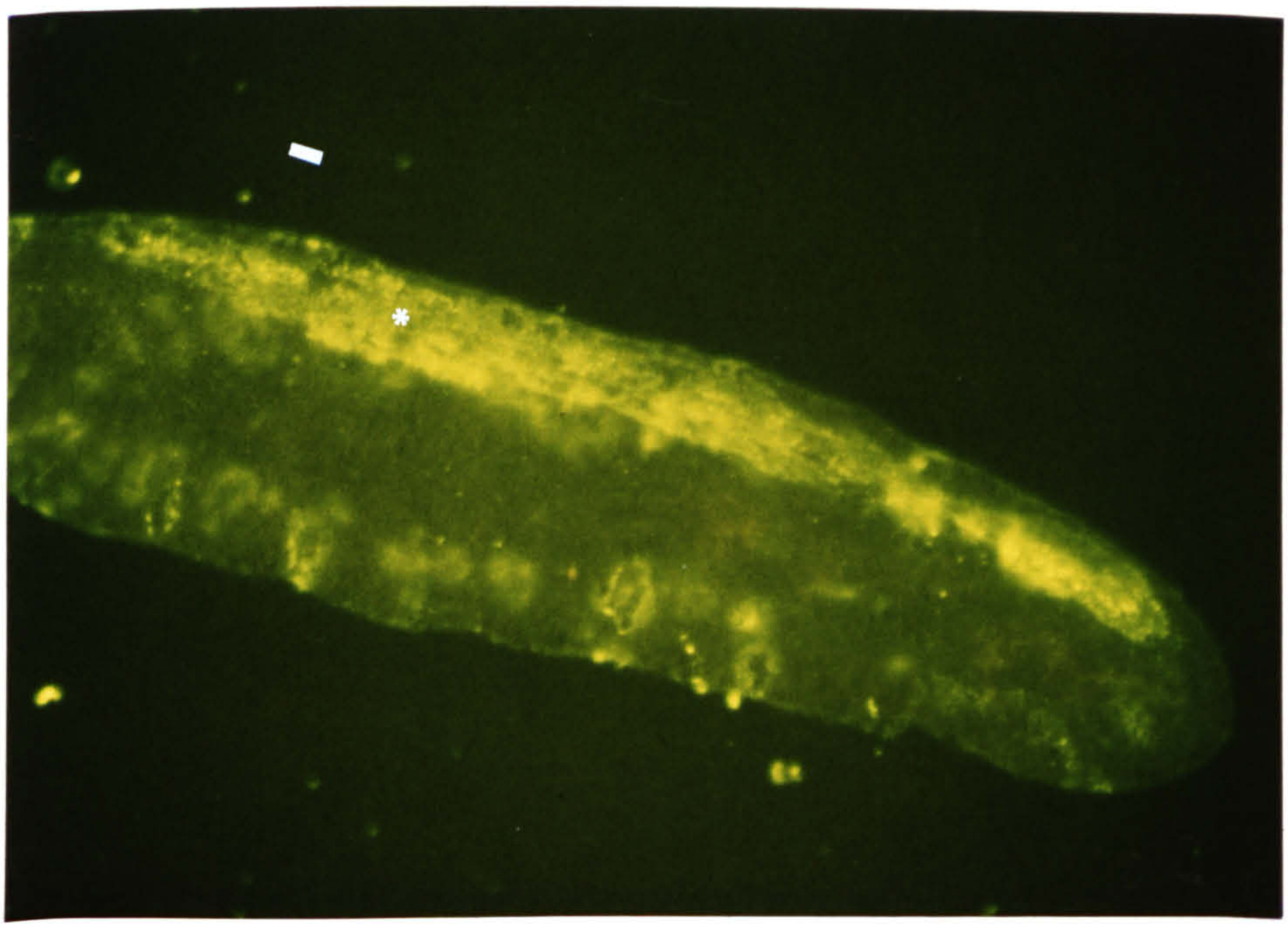

FIGURE 2.8

PF-fixed intact cercaria reacted with NMS (1:100) and RAM/Ig/FITC (1:64). No specific fluorescence is observed on the parasite surface. Similar results were obtained with NS-1 ascites. x 520.

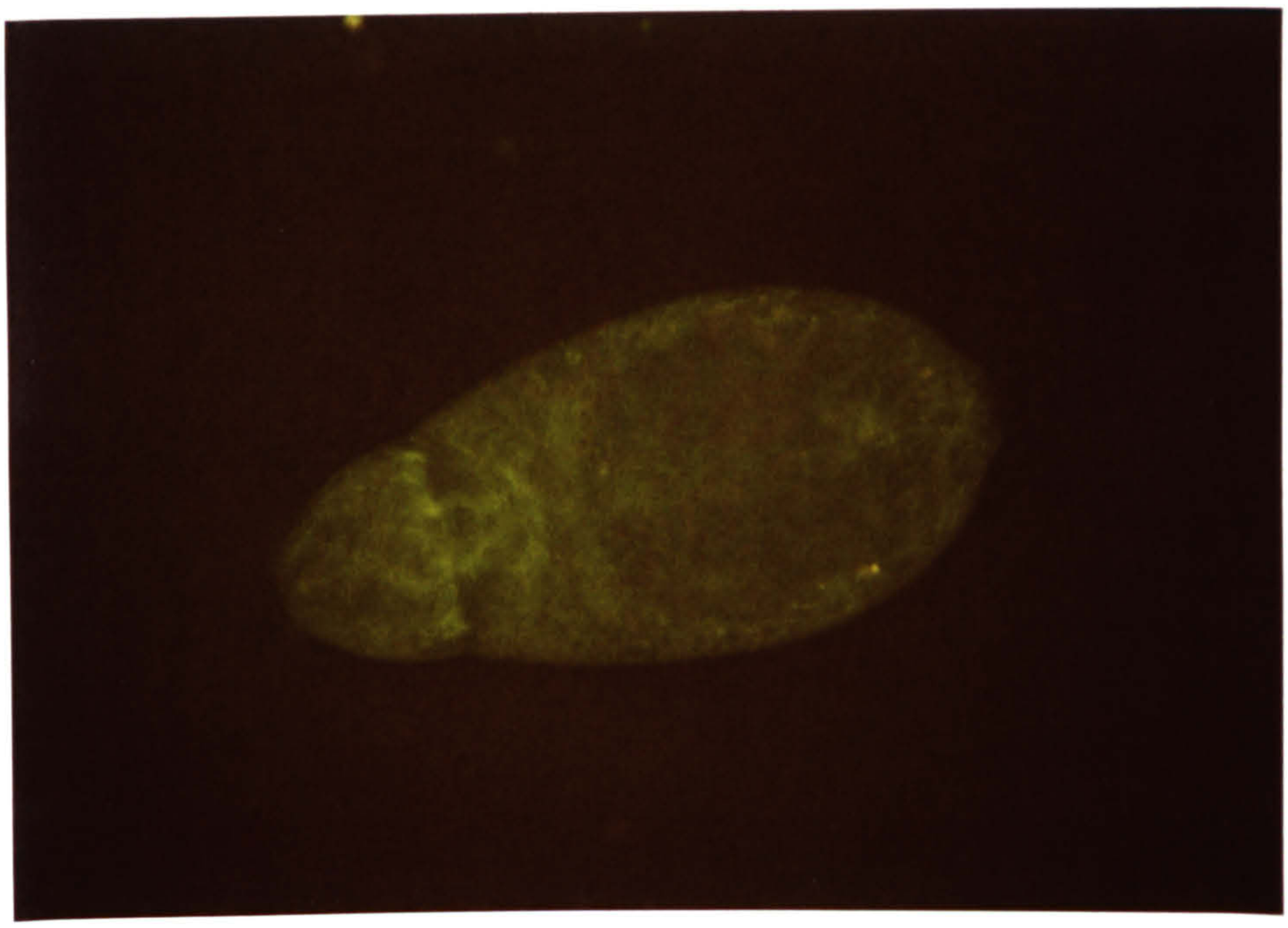

FIGURE 2.9

Indirect immunofluorescent localisation of the antigenic targets recognized by MAB M7.5. At low magnification, acetone-fixed adult worm section exhibits fluorescence only in the tegument of the parasite. Internal tissues are all unlabelled. x 130.

FIGURE 2.10

High magnification of Fig. 2.9 showing the MAB M7.5 reacts predominantly against the tegument of the adult worm. Internal structures are all unlabelled. x520.

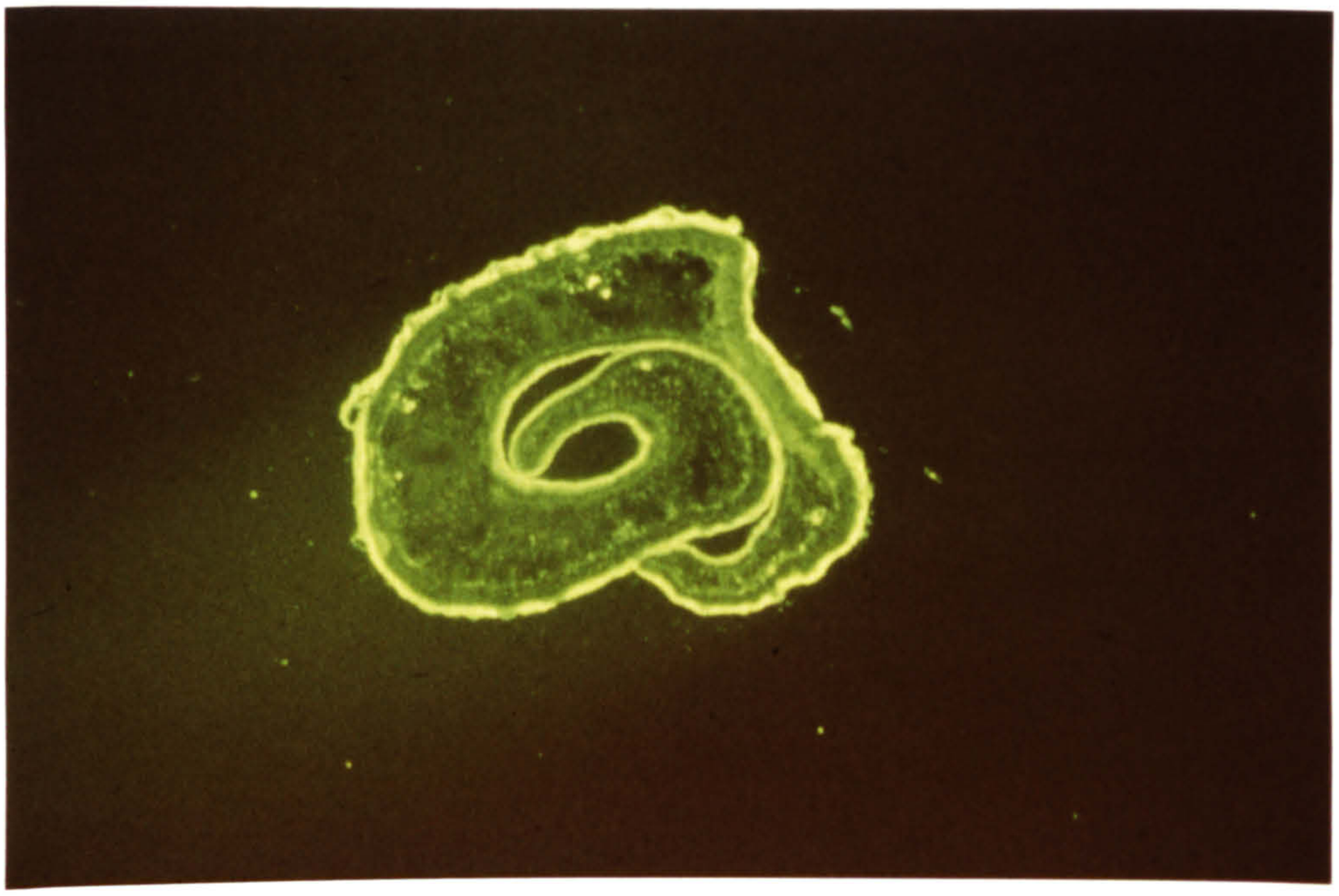

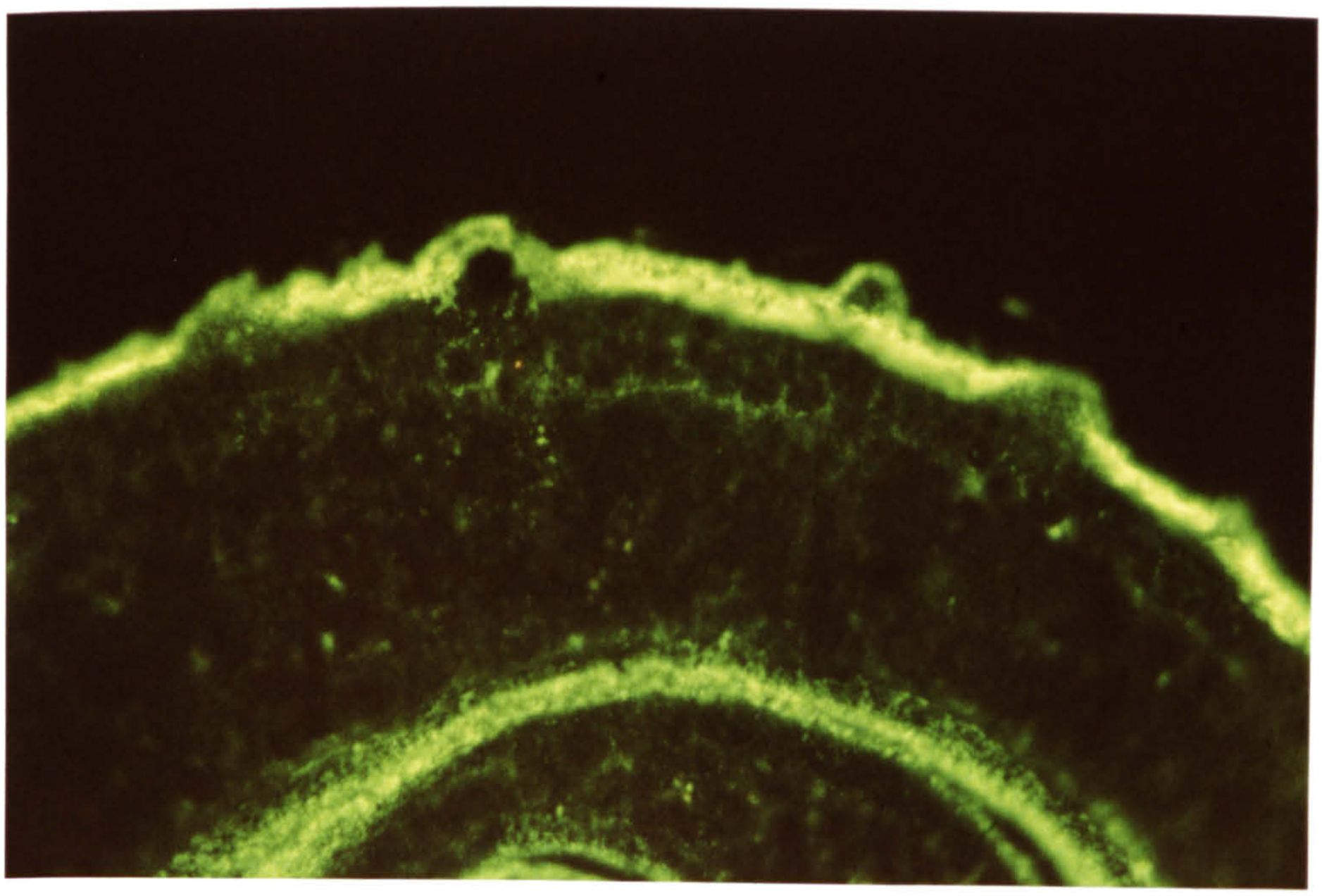

FIGURE 2.11

Indirect immunofluorescence on frozen section of PF-fixed adult male worm using MAB G3.12 at low magnification. Tegument fluorescence is very strong with a weaker reaction in the tegument cell bodies beneath the unstained muscle layers. The gut and parenchymal cells of the worm are negative. x 130.

FIGURE 2.12

Higher magnification of Fig. 2.11 showing specific fluorescence in the tegument, particularly bright towards the apical surface. The muscle layers and parenchyma are unlabelled. x 520.

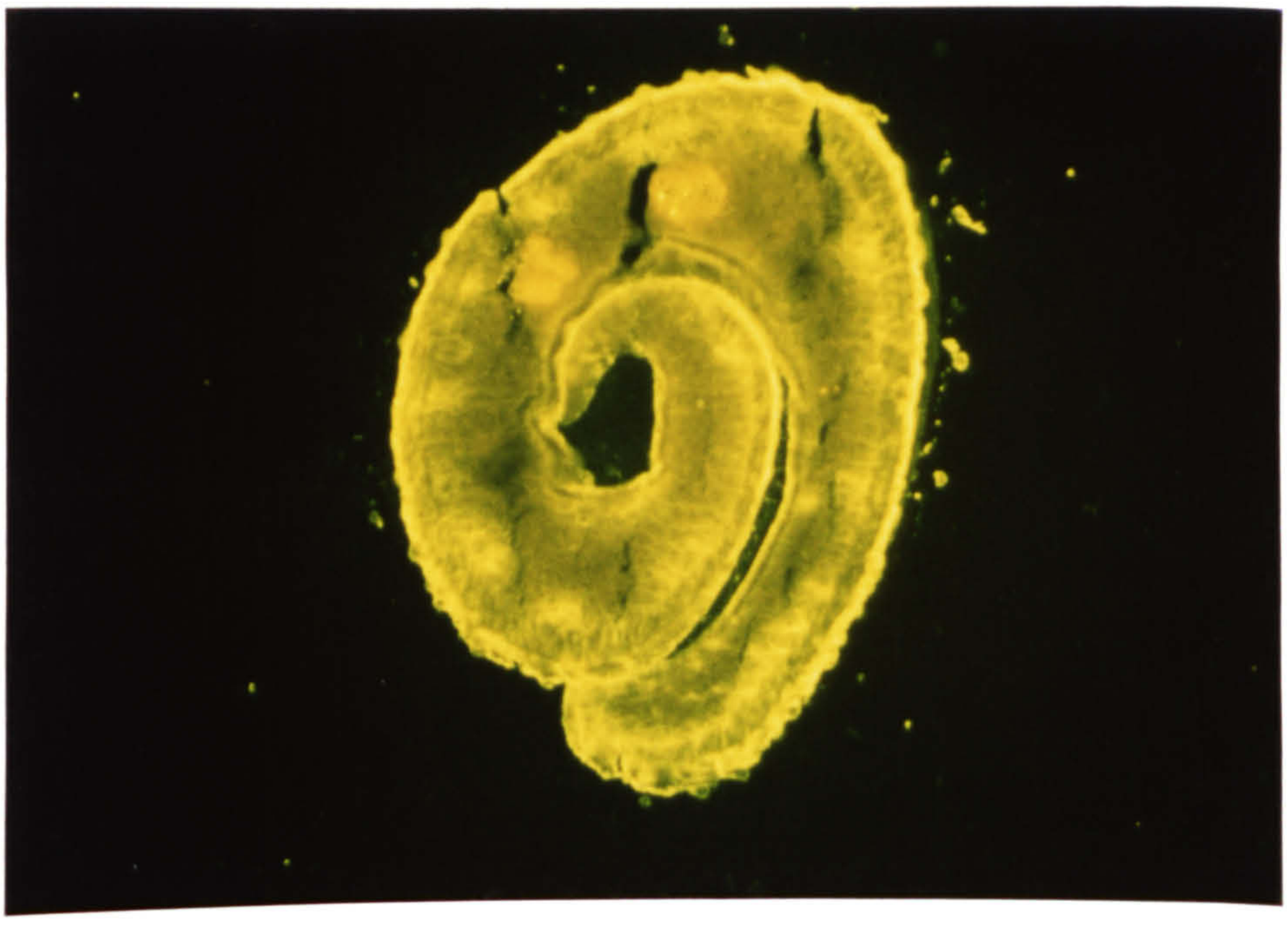

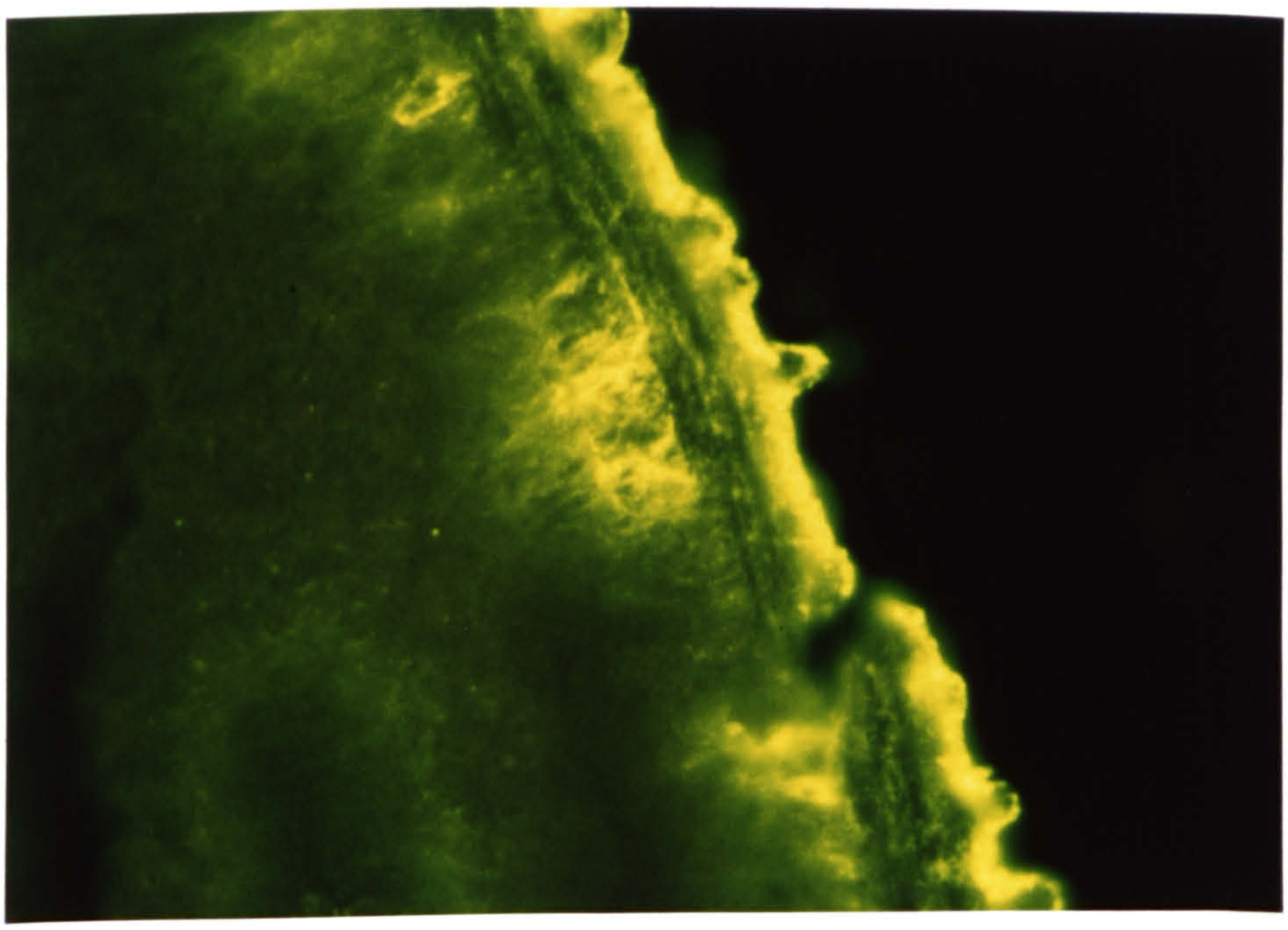

FIGURE 2.13

Acetone-fixed frozen section of adult male worm reacted with MAB D7.2 followed by RAM/Ig/FITC. Specific fluorescence is seen in the tegument and tegumental cell bodies; the latter appear as regions of bright fluorescent dispersed over the parenchyma of the worm. On transverse sections of the female worm (F) the tegument is also fluorescently labelled. The vitelline cells inside the female worm show nonspecific autofluorescence of egg shell granules. x 130.

FIGURE 2.14

Higher magnification of Fig. 2.13, the tegument is brightly fluorescent with the strongest reaction at the surface. Either the "interstitial material" around the muscle fibres or the muscle cell plasma membrane is also fluorescently labelled whereas the cytoplasm of muscle cells is unstained. This gives to the muscle layers a honey-comb appearance. The tegument cell bodies beneath the muscle layers are also positive. x 520.

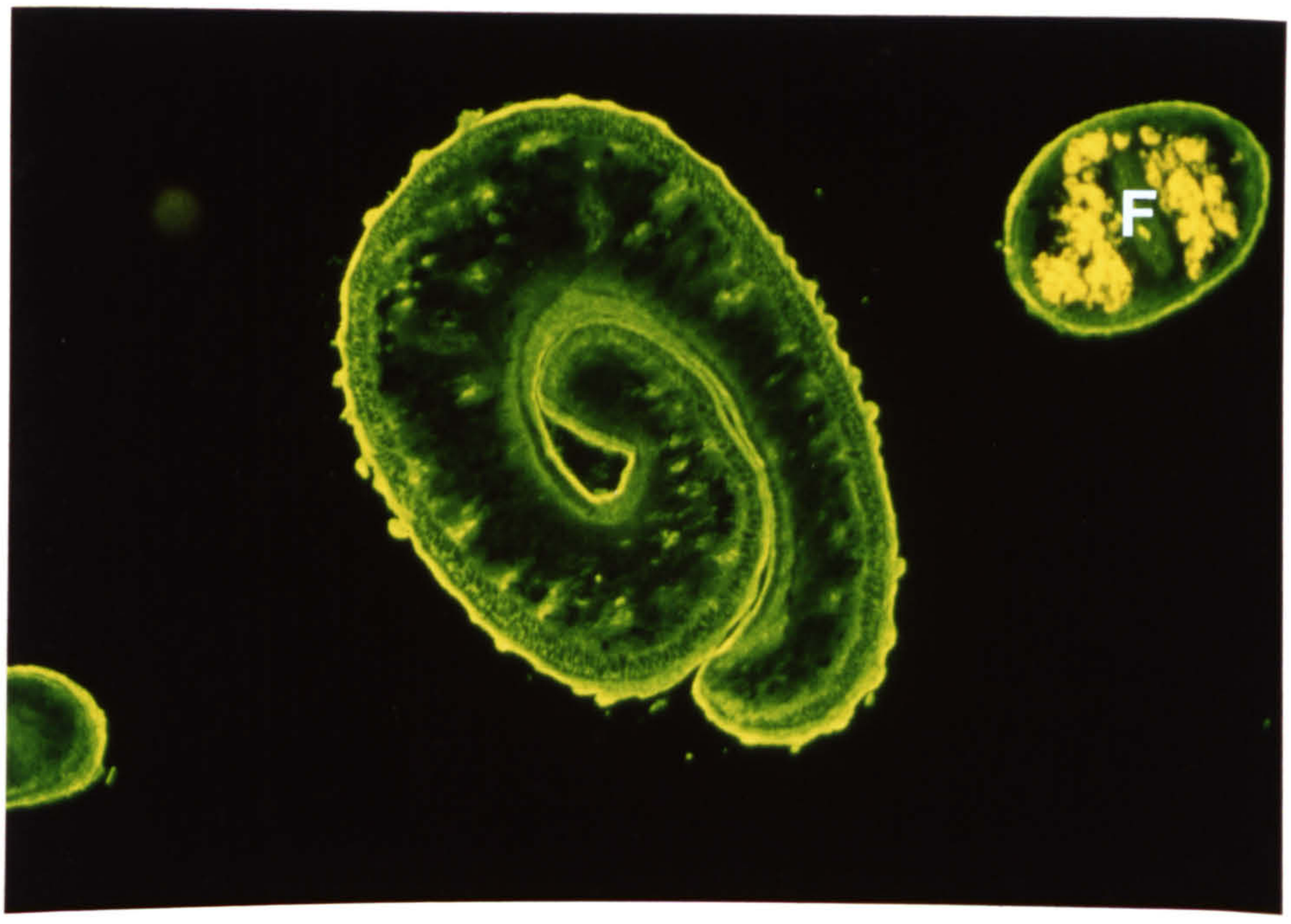
F

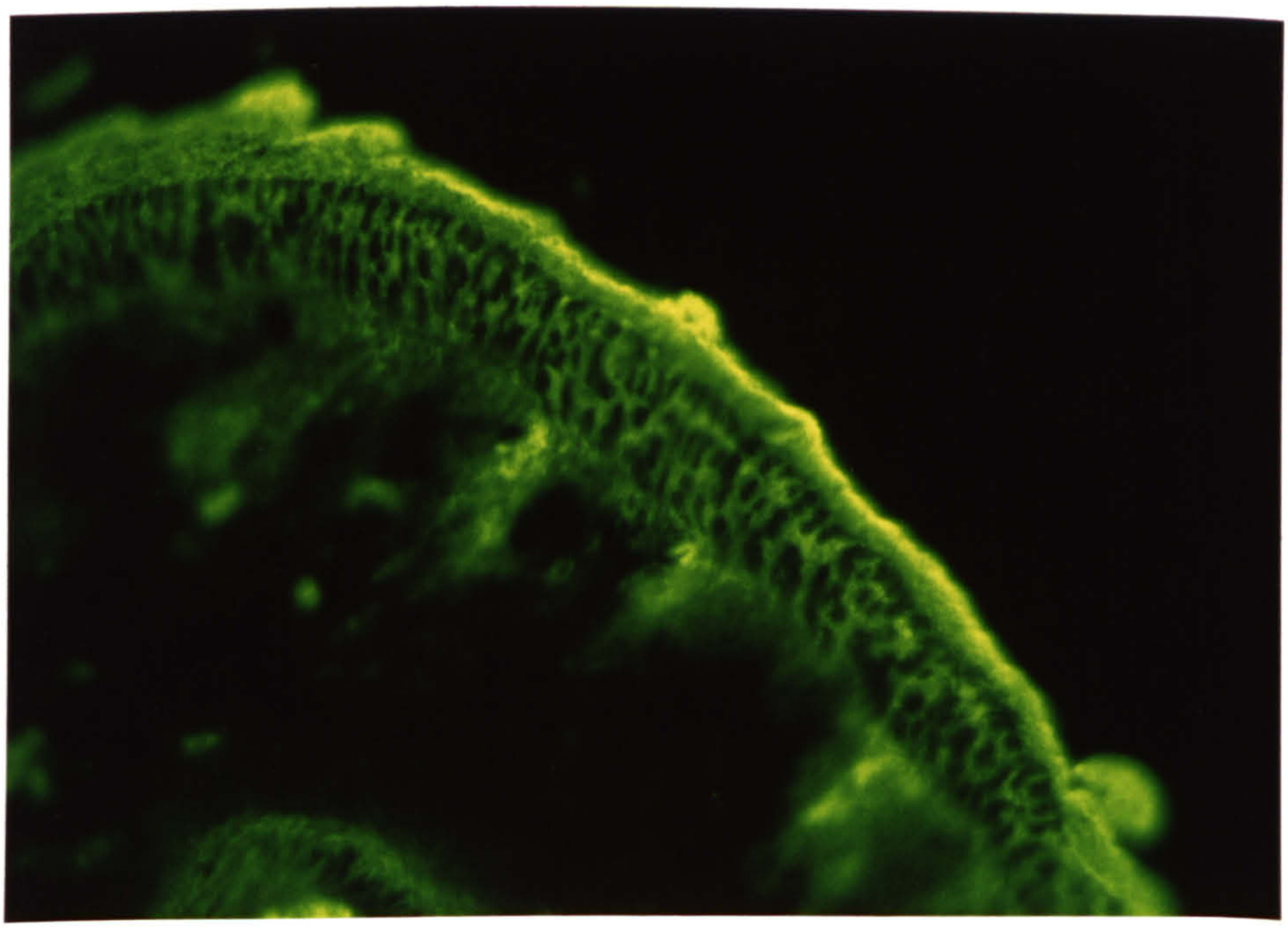

FIGURE 2.15

Acetone-fixed frozen section of adult male worm reacted with MAB G6.6 (1:60) and RAM/Ig/FITC (1:64). The parasite shows an overall fluorescence, brightest on the tegument. The parenchyma is also positive. x 130.

FIGURE 2.16

Higher magnification of Fig. 2.15, the tegument and the parenchymal cells are fluorescently labelled. The gut is also positive. The muscle cells are unstained. x 520.

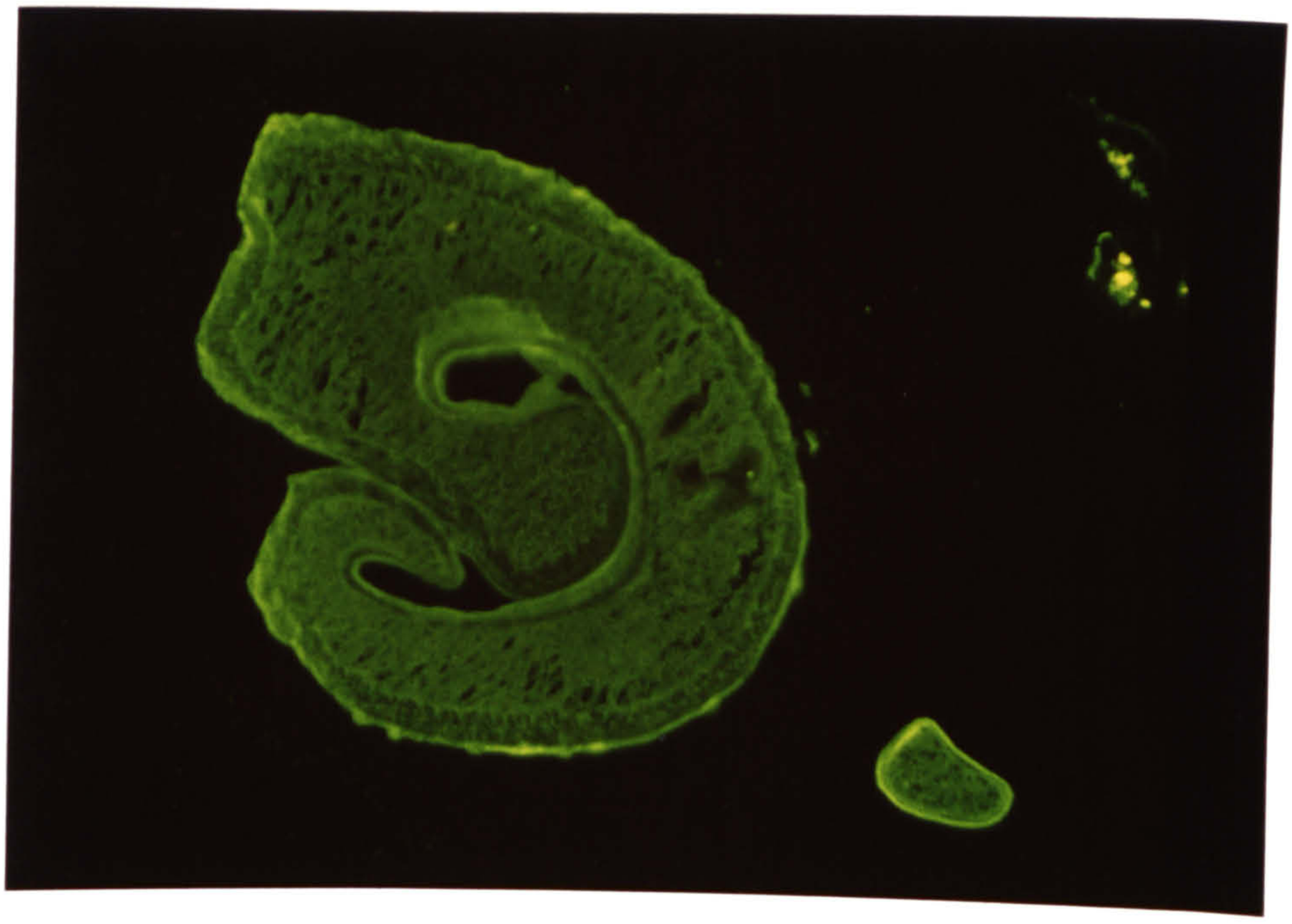

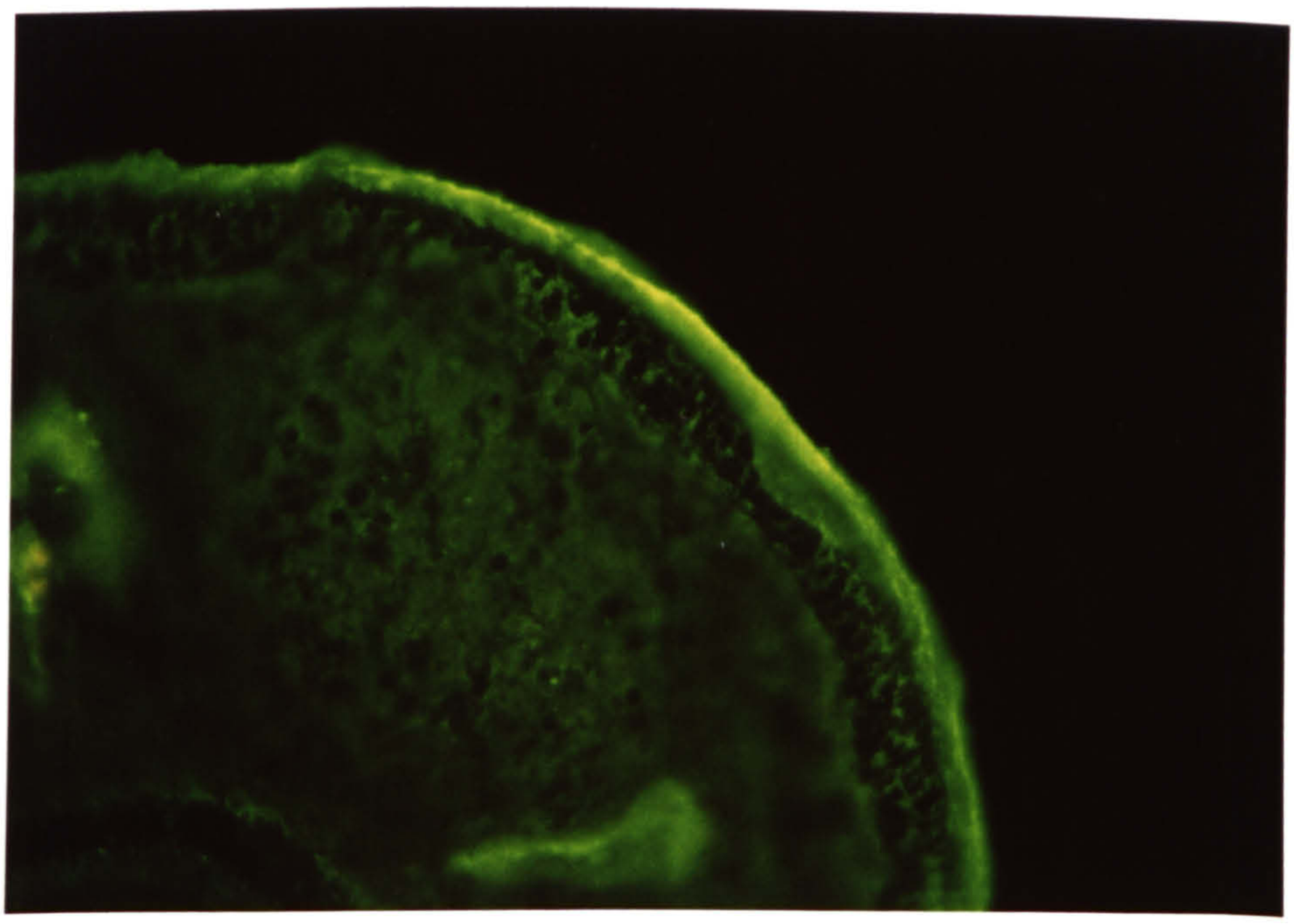

FIGURE 2.17

Acetone-fixed frozen section of adult male worm treated with MAB M7.6 (1:60) and subsequently labelled with RAM/Ig/FITC (1:64). The tegument is brightly fluorescent. Specific fluorescence is also observed in the tegument cell bodies just beneath the muscle layers and in the interstitial material around the muscle fibres. The parenchymal cells are unlabelled while nephridia (n) which are embedded in the parenchyma are fluorescently stained. Nephridia appear as spiral- or vermiform-structures in the section. x 130.

FIGURE 2.18

Higher magnification of Fig. 2.17 shows strong specific fluorescence in the tegument, and weaker reactions in the tegument cell bodies, the interstitial material around the muscle fibres, and a nephridium (n) of the adult worm. The nephridium is a long, thin wavy structure in the unstained parenchyma of the worm in the section. x 520.

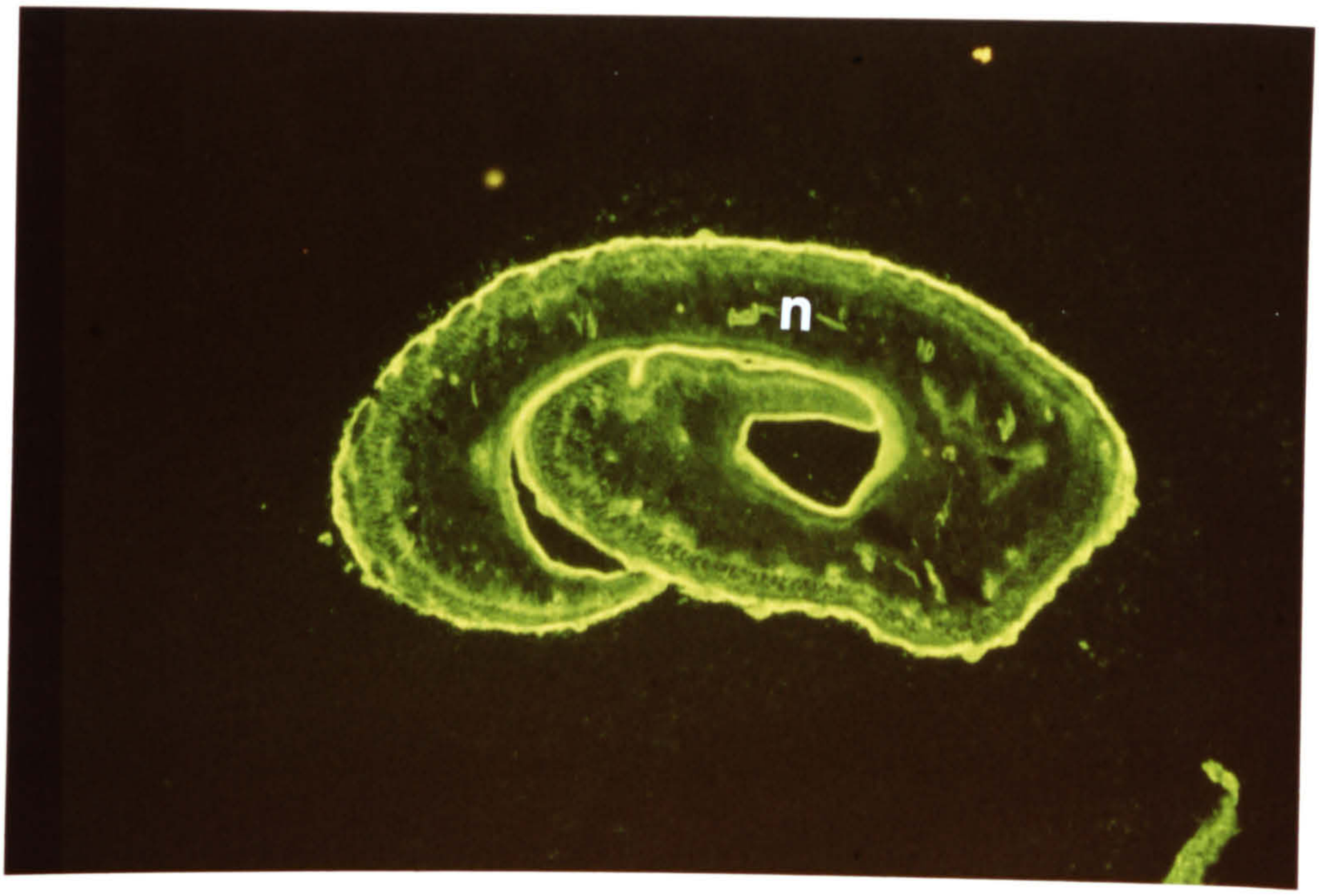
n

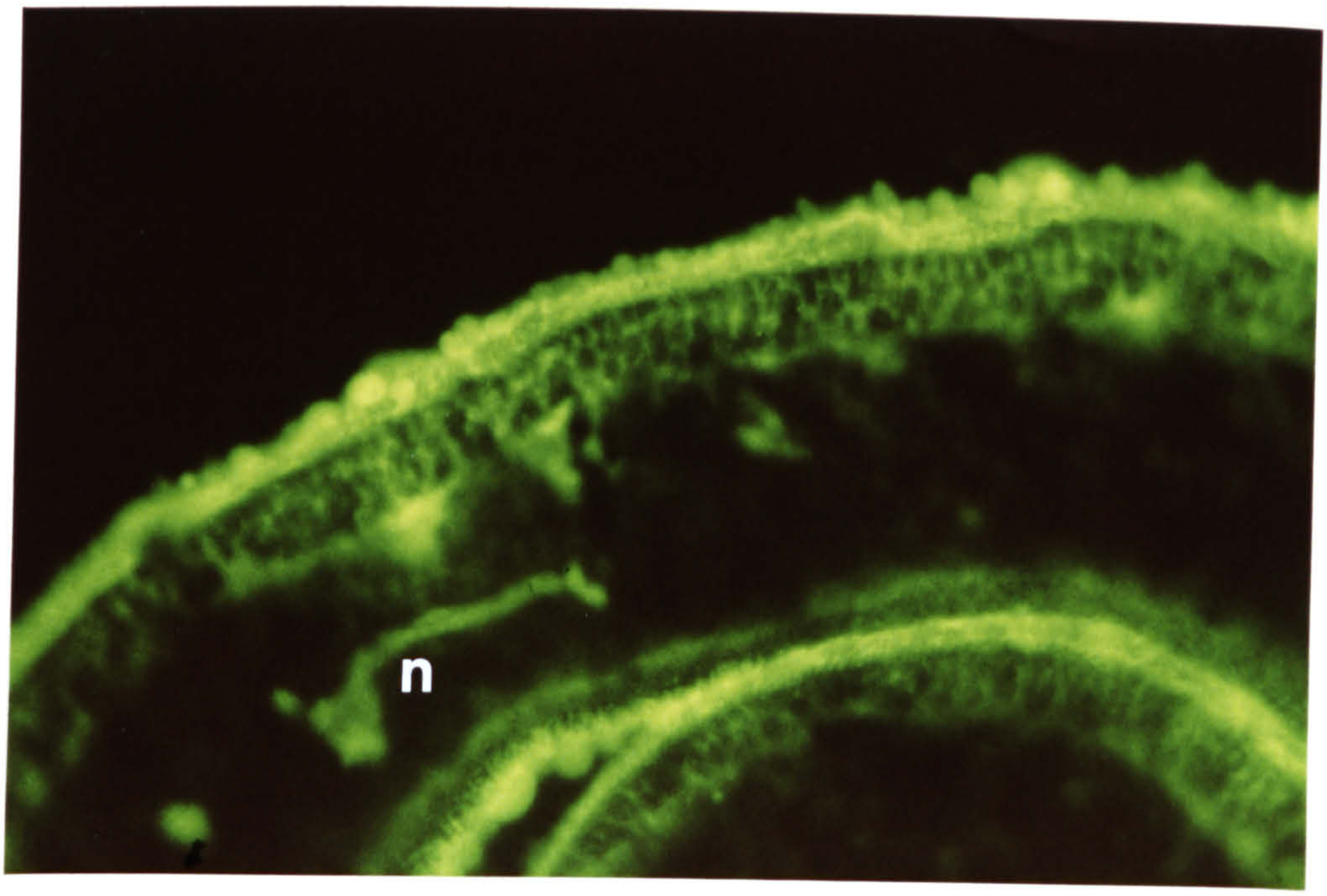
n

FIGURE 2.19

Anatomic localisation of the antigenic targets recognized by MAB M7.4. Indirect immunofluorescence microscopy of frozen section of PF-fixed S. mansoni adult male worm shows strong fluorescence within the tegument. The parenchymal tissues are also positive but show less fluorescent label. The gut epithelium is slightly positive, the gut contents are negative. x 130.

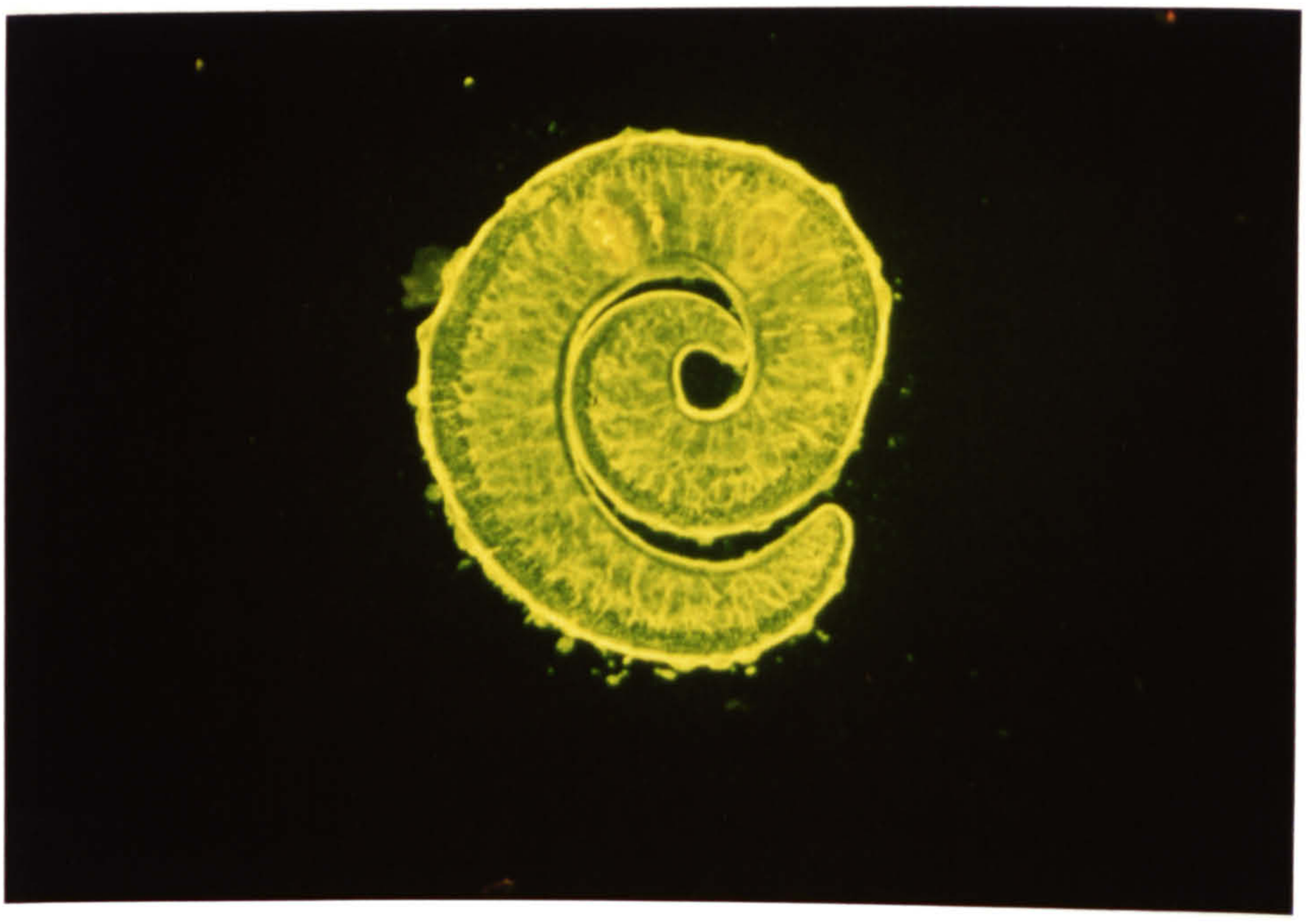

FIGURES 2.20 & 2.21

Higher magnification of Fig. 2.19 shows bright fluorescence within the tegument. The plasma membranes of parenchymal cells are brighter than their cytoplasm. The membranes of muscle fibres are fluorescently labelled while the muscle cytoplasm is unstained. It is likely that MAB M7.4 recognized membranes of muscle fibres, not the interstitial material around them (see Fig. 2.22). x 520.

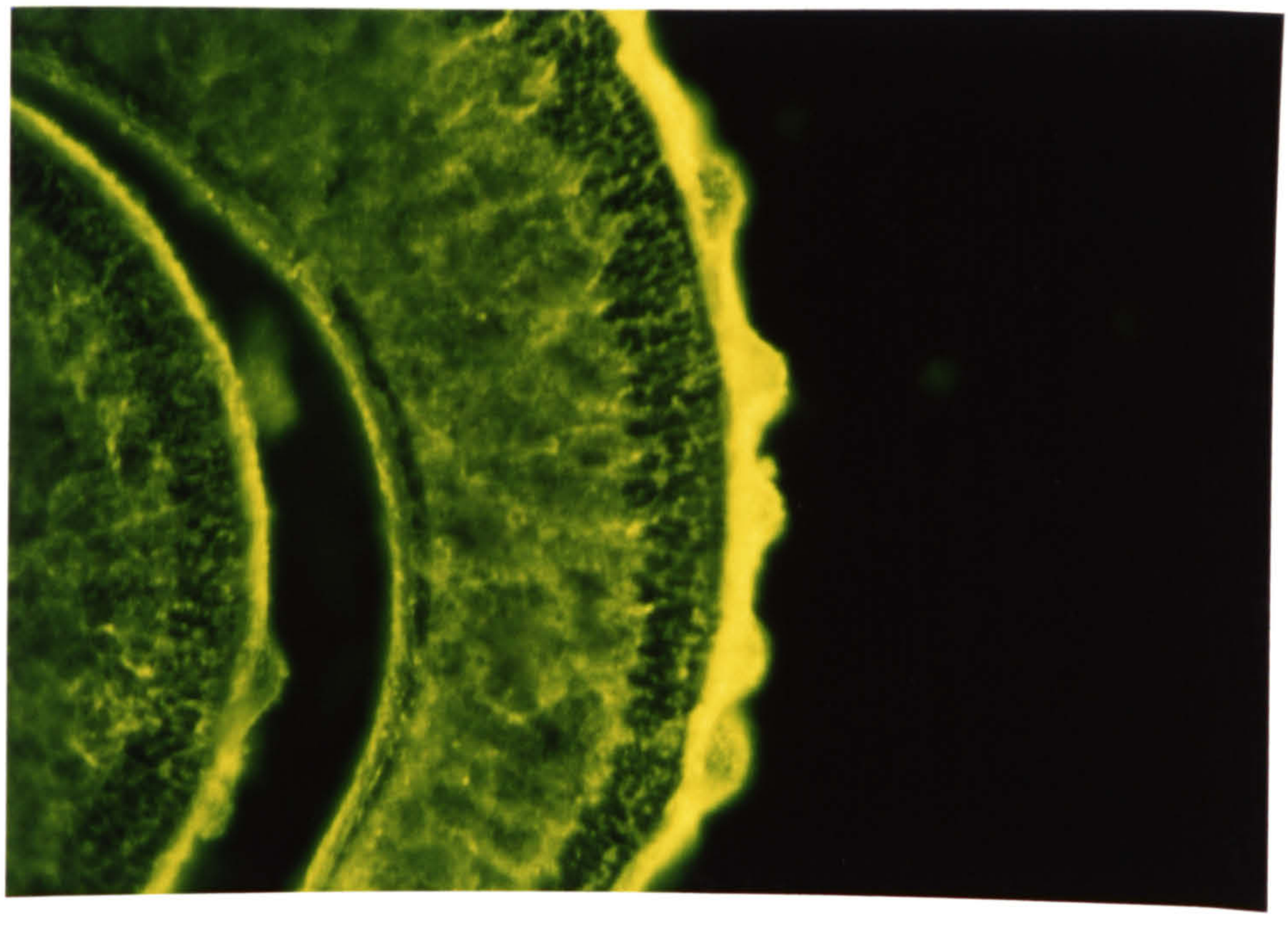

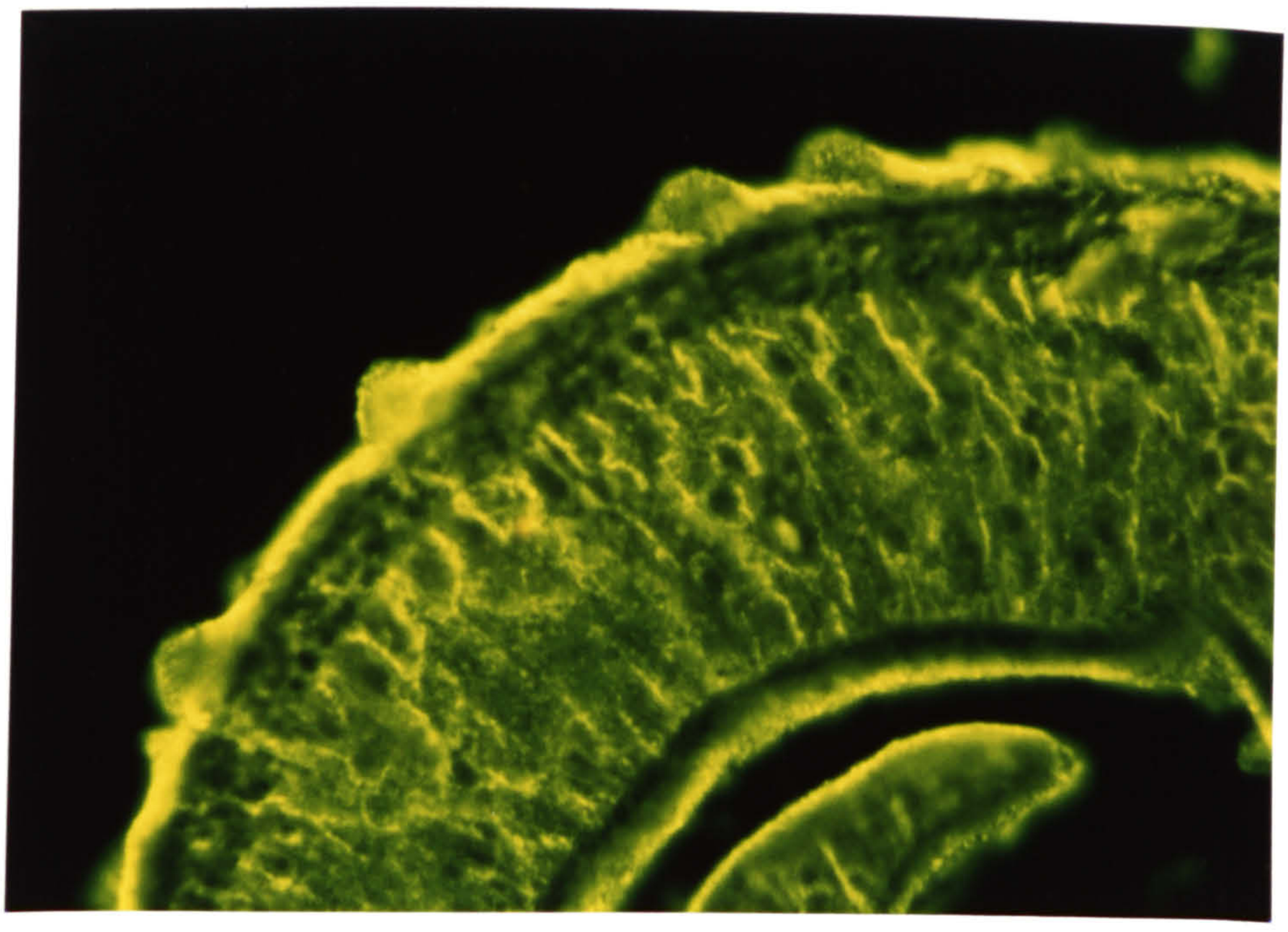

FIGURE 2.22

PF-fixed frozen section of adult male worm reacted with MAB M7.4 at high magnification; a longitudinal section showing the tegument on tubercles is brightly fluorescent. The centre of the section shows strong fluorescence in the plasma membranes (arrow) of longitudinal muscle fibres but the muscle cytoplasm is non-antigenic. x 520.

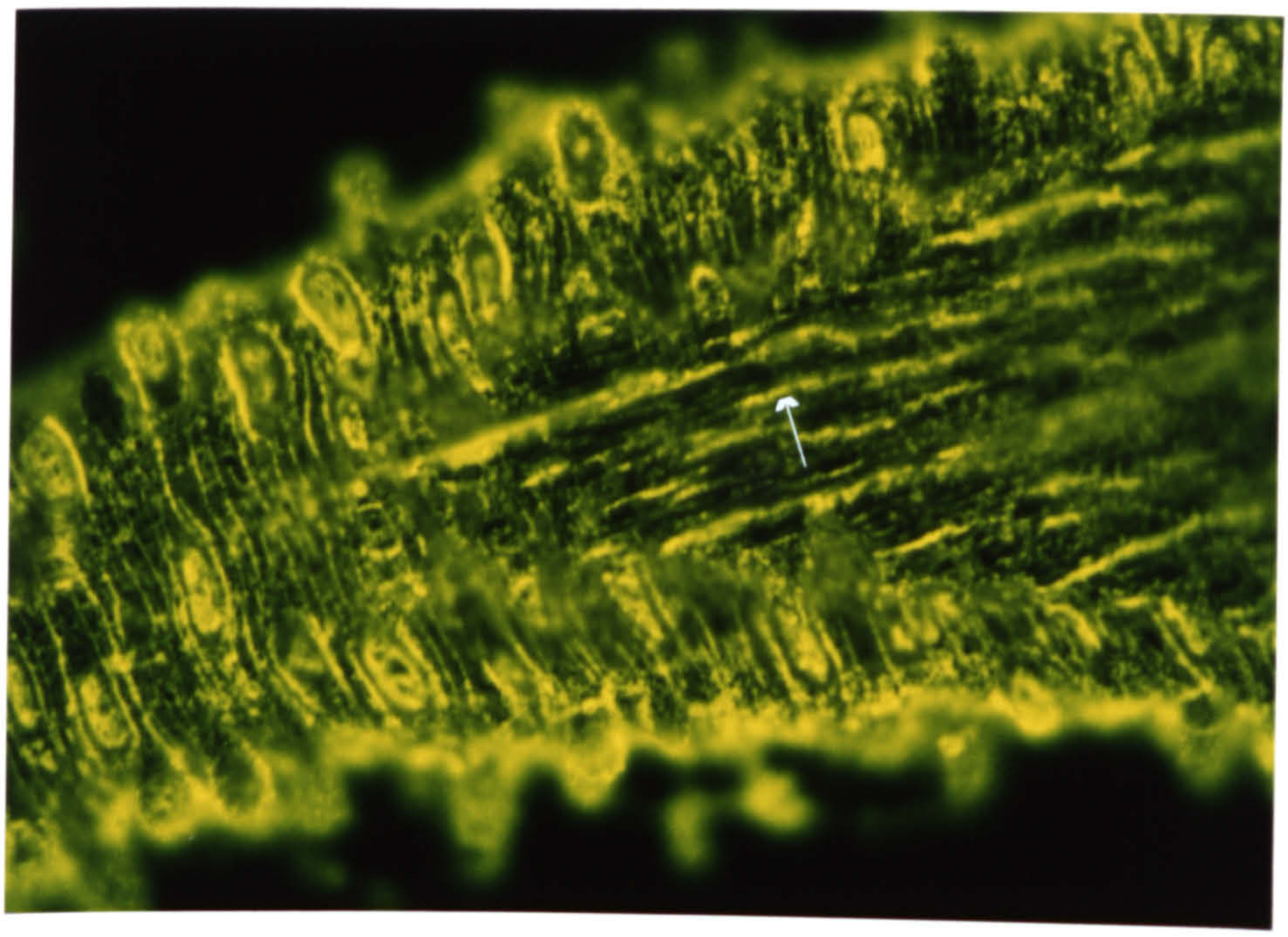

FIGURES 2.23 & 2.24

Acetone-fixed frozen sections of cercariae reacted with MAB G6.7 (1:60) and RAM/Ig/FITC (1:64) showing specific fluorescence in the tegument and the periphery of the body. The tegument appears as a thin line. Packets (P) of fluorescence are seen in the peripheral area beneath the tegument. On some sections the packets are not distinctly identified. They are recognized more easily on longitudinal than transverse sections. The head gland (H) is also brightly fluorescent but the penetration gland cells inside the body are non-antigenic. The oesophagus (*) appears fluorescent within the cercarial body. Sections of tail (T) are all negative. x 520.

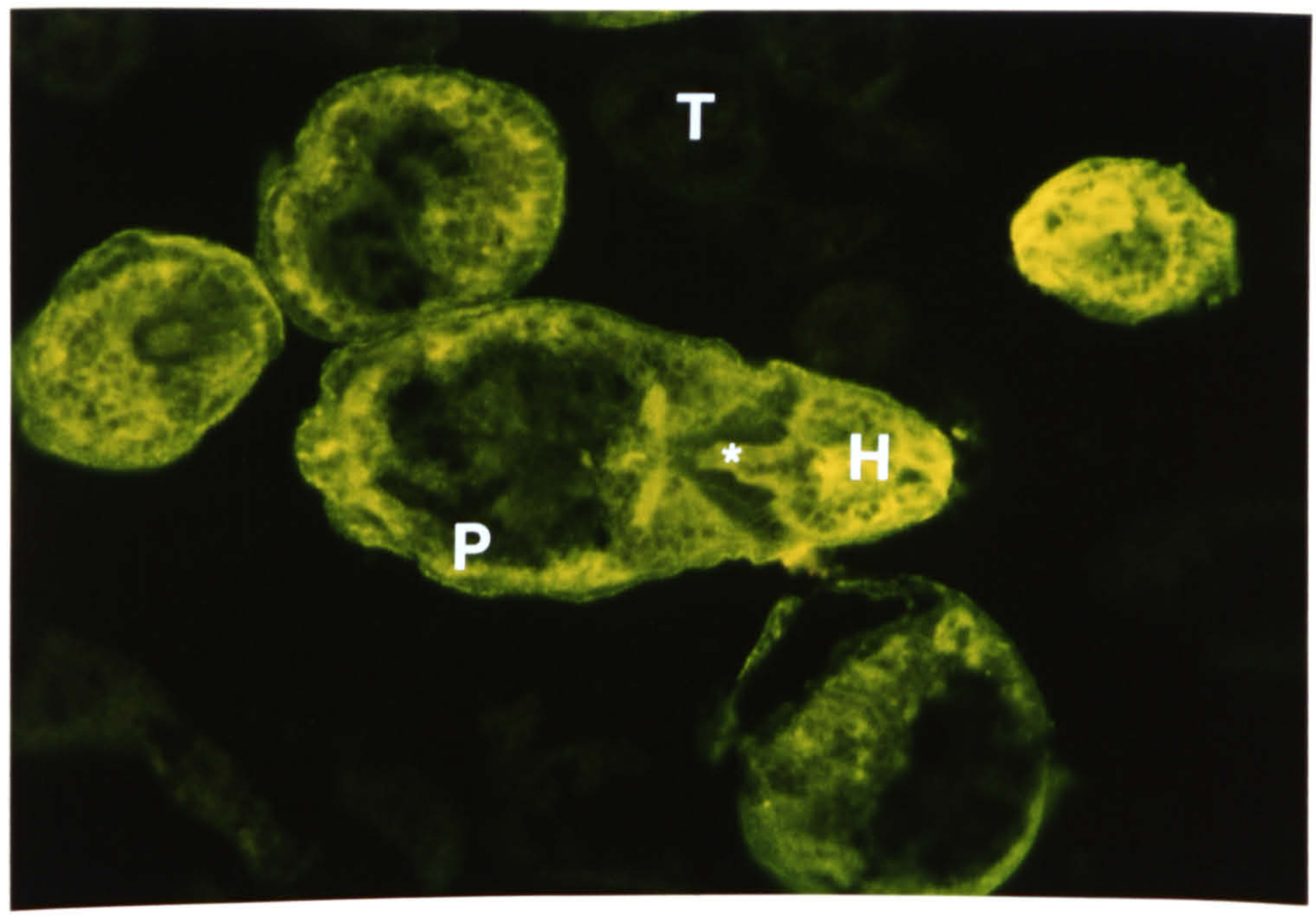
T
*
H
P

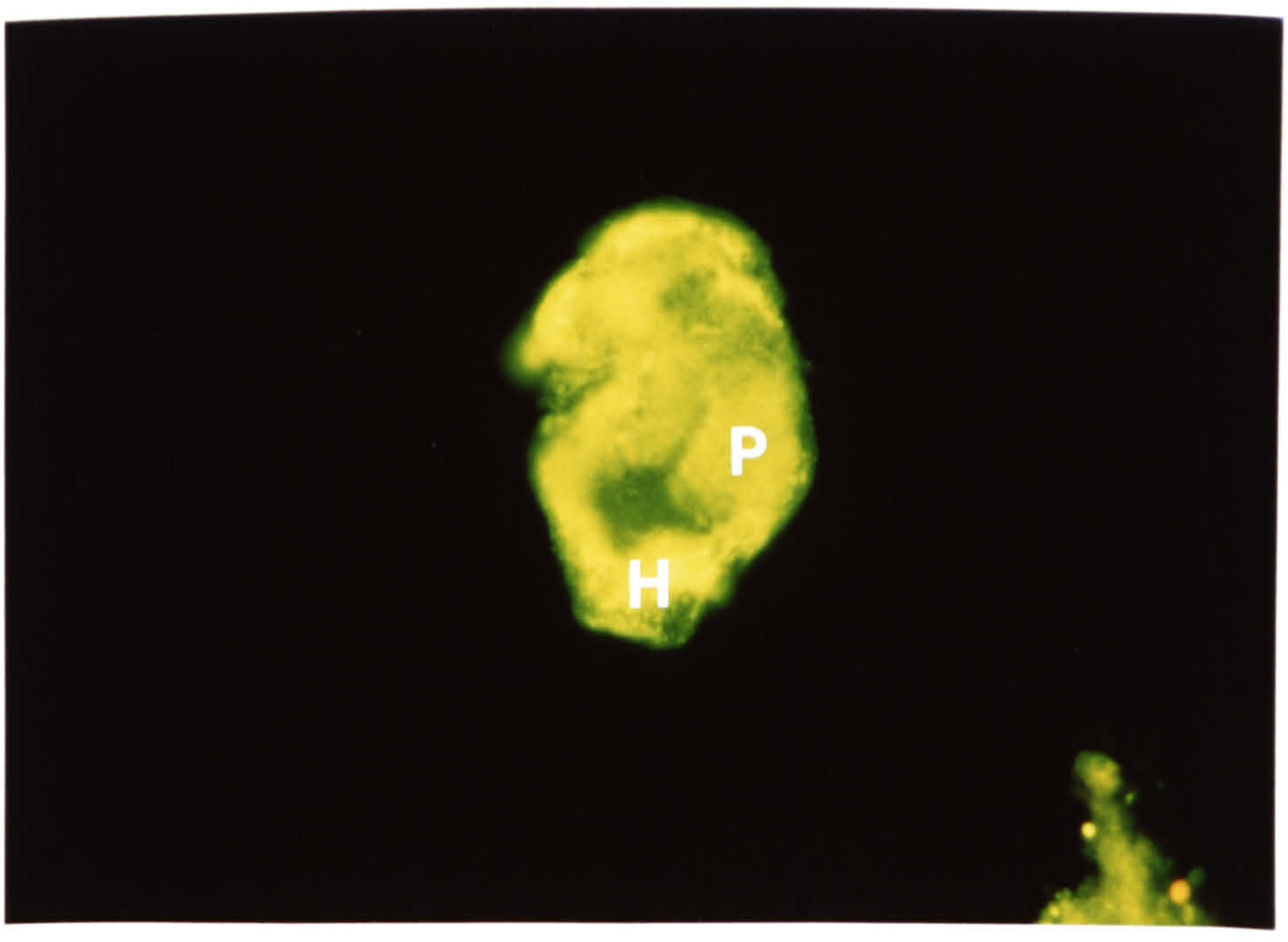
P
H

FIGURES 2.25 & 2.26

Longitudinal sections of PF-fixed cercarial tail (T) stained with MAB G6.7 (1:60) and RAM/Ig/FITC (1:64) shows specific fluorescence on the plasma membranes of the muscle fibres (see " Diagram of the organization of the tail musculature " in Text Figure 3.2 in Chapter 3). In transverse sections the plasma membranes of four lateral muscle blocks are also fluorescently labelled. x 520.

FIGURE 2.27

Acetone-fixed frozen section of 3h skin-transformed schistosomulum reacted with MAB M7.4 and labelled with RAM/Ig/FITC. The tegument and peripheral area of the body are fluorescent. The apical (A) and posterior ends (PE) are strongly labelled. The central fluorescent spiral-structure represents a longitudinal cut of the oesophagus (arrow). Internal structures are weakly positive. Transverse sections of some parasites exhibit fluorescence on the entire section (not shown). x 520.

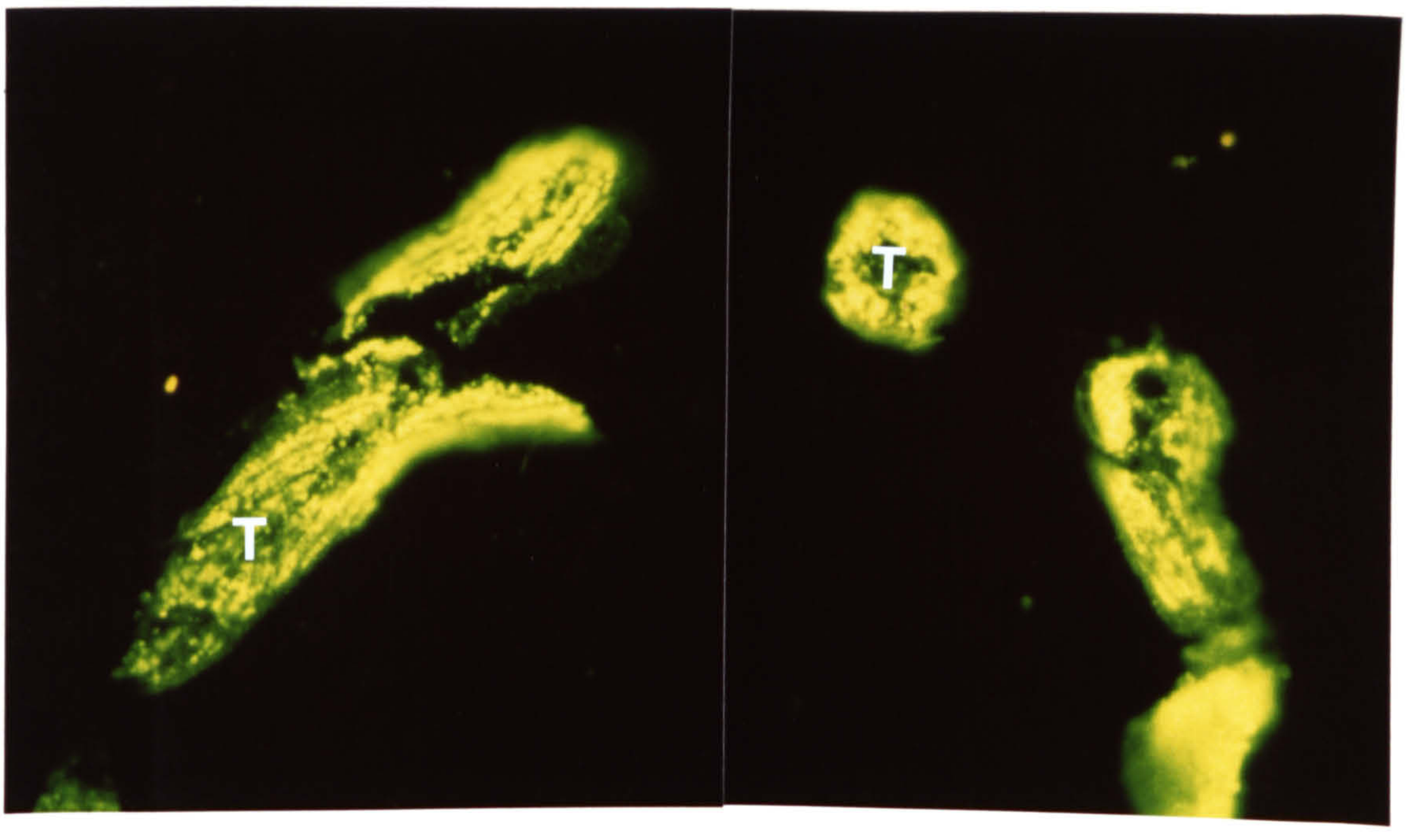
T
T

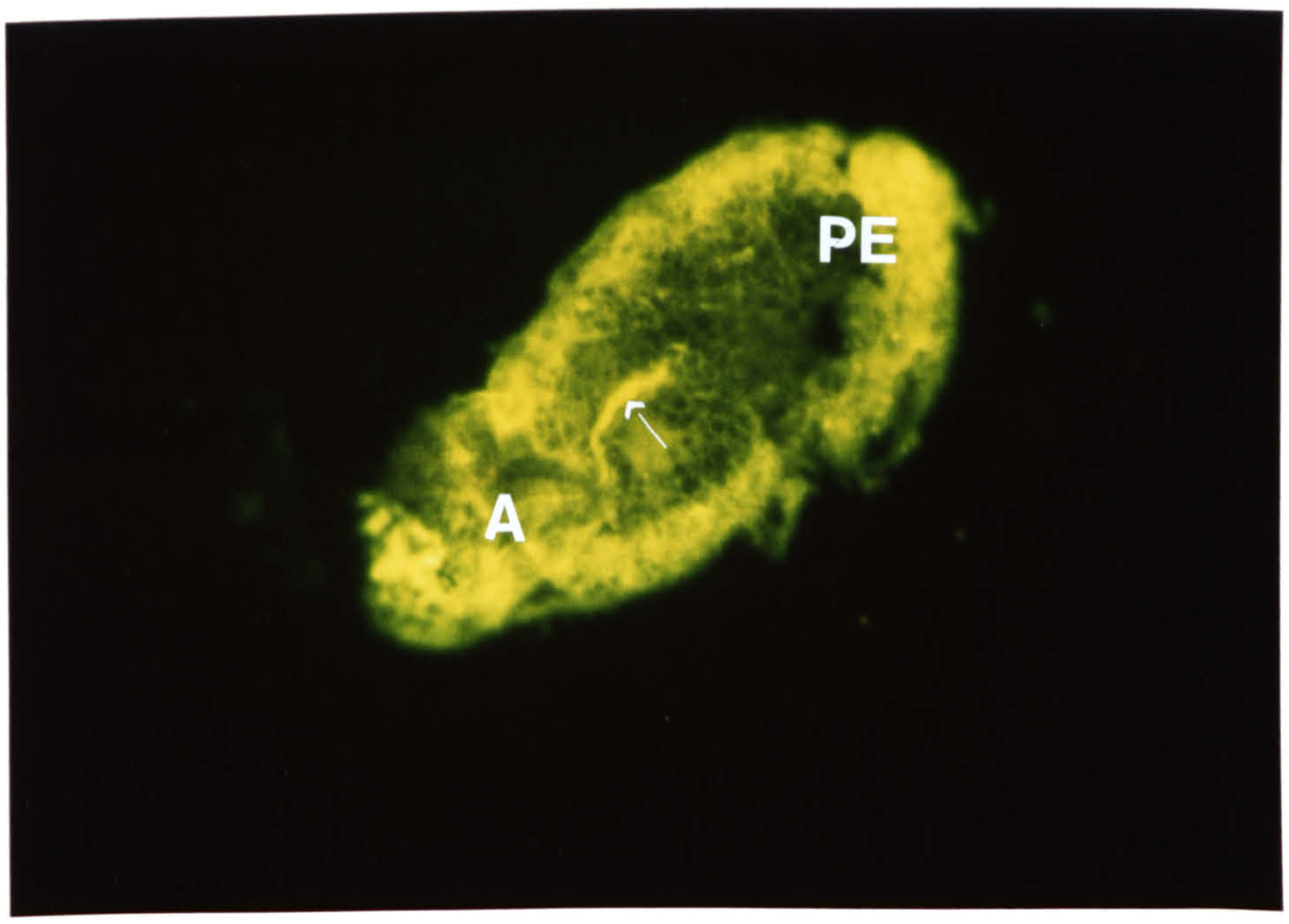
PE
A

FIGURE 2.28

Immunofluorescence micrograph shows the binding of MAB M7.4 (1:60) and RAM/Ig/FITC (1:64) to the entire surface of the intact PF-fixed cercaria. Strong specific fluorescence is seen on the head capsule (H) and at the point (p) where the tail detached from the body. The intensity of fluorescence and the uniformity of binding with MAB M7.4 are not as great as that observed with AMS (Fig. 2.4). The surface of the cercarial tail is unlabelled (not shown). x 520.

FIGURE 2.29

PF-fixed intact 3h skin-transformed schistosomulum reacted with MAB M7.4 (1:60) and RAM/Ig/FITC (1:64). The antibodies bind uniformly to the surface of the parasite and give an intense, diffuse fluorescent pattern. The anterior (A) of the body is brighter than the posterior end. The staining pattern is comparable to that with AMS as shown in Fig. 2.5. The intensity of fluorescence with MAB G6.7 is weaker. x 520.

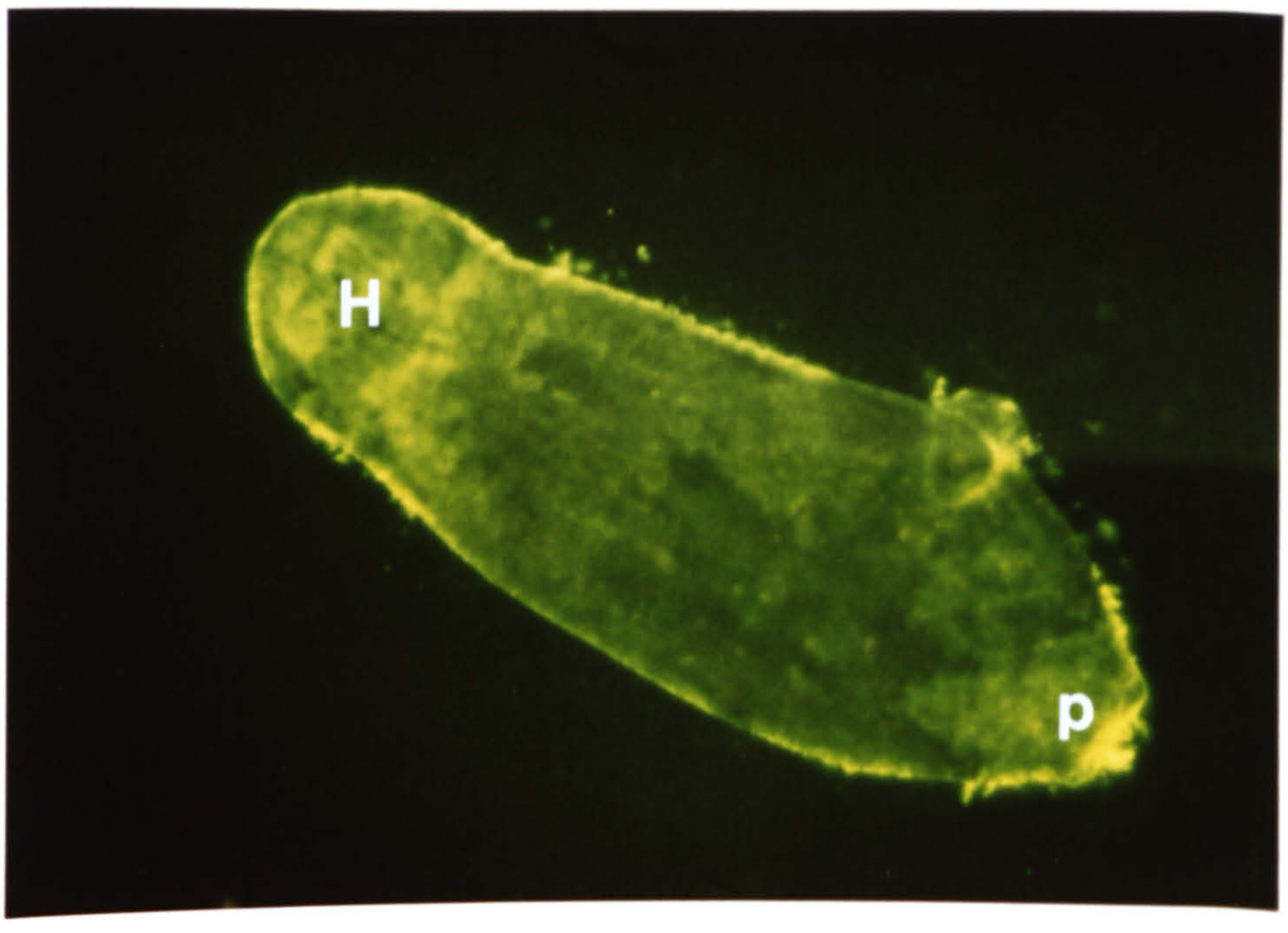
H
p

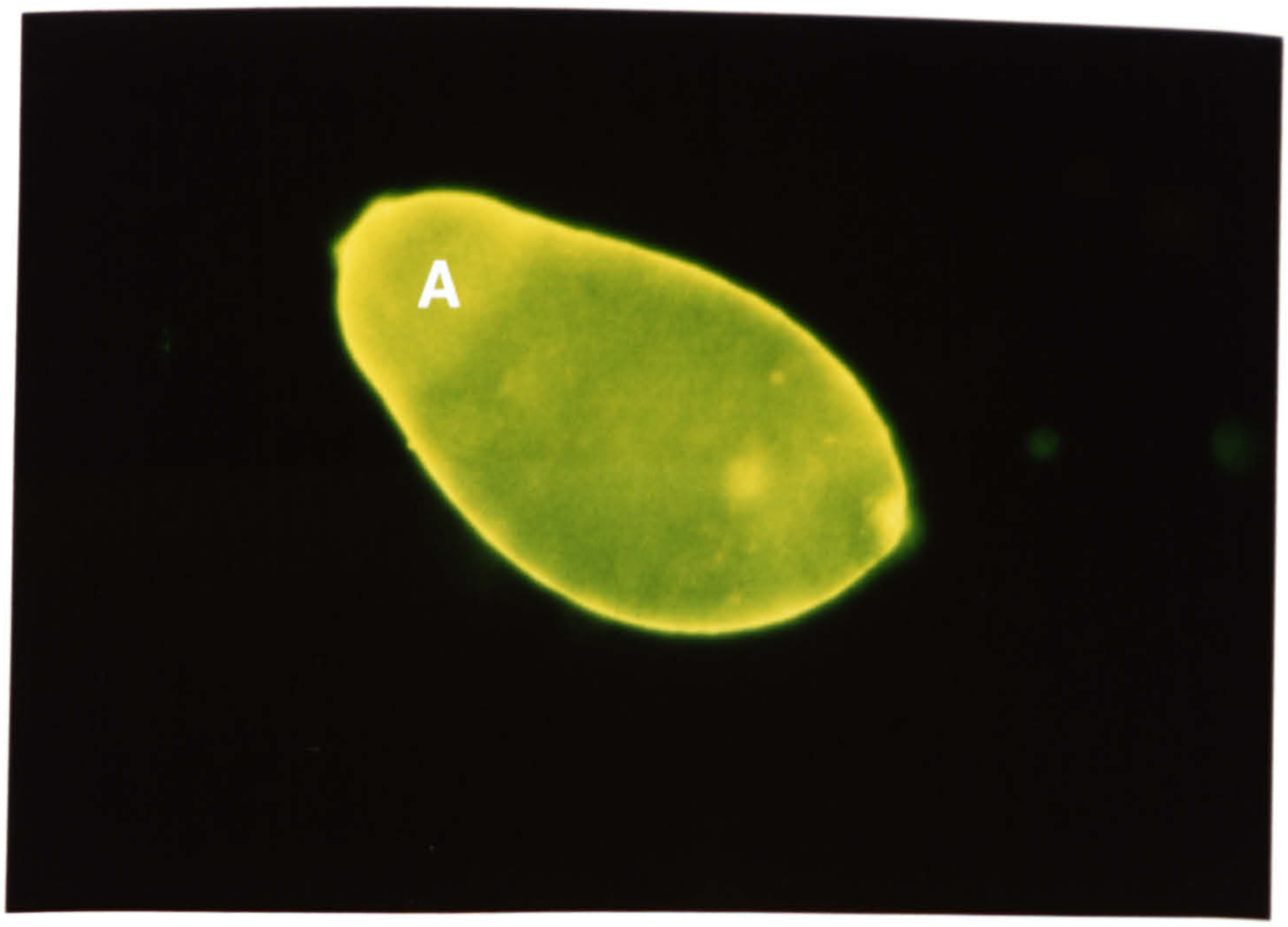
A

FIGURE 2.30

21-day-liver worms after 24 h in culture were reacted with MAB M7.4 (1:40) and GAR/Ig/FITC (1:25). Positive fluorescence is seen on the surface of each parasite where the tegument is damaged. x 130.

FIGURE 2.31

Higher magnification of Fig. 2.30 showing area of false positive fluorescence of the muscle layer (M). x 520.

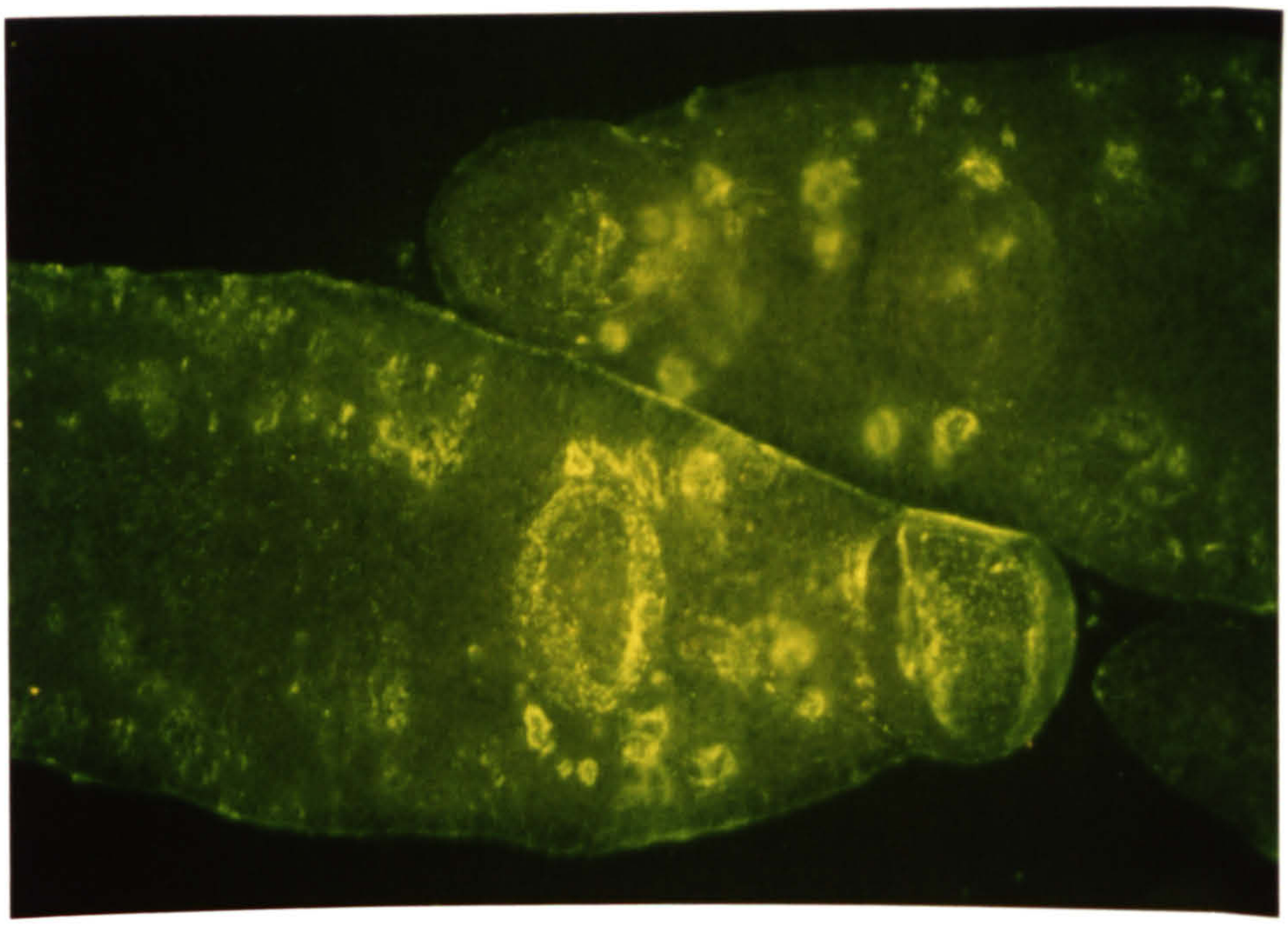

M

FIGURES 2.32 & 2.33

PF-fixed frozen section of cercariae reacted with MAB G6.1 (1:60) and labelled with RAM/Ig/FITC (1:64). Discrete packets of strong specific fluorescence are seen inside the body beneath the muscle layers. Other internal structures are less antigenic. The tegument of the cercarial body is unlabelled. Sections of tail are negative (not shown). The penetration gland cells (g) inside the body are also non-reactive. x 520.

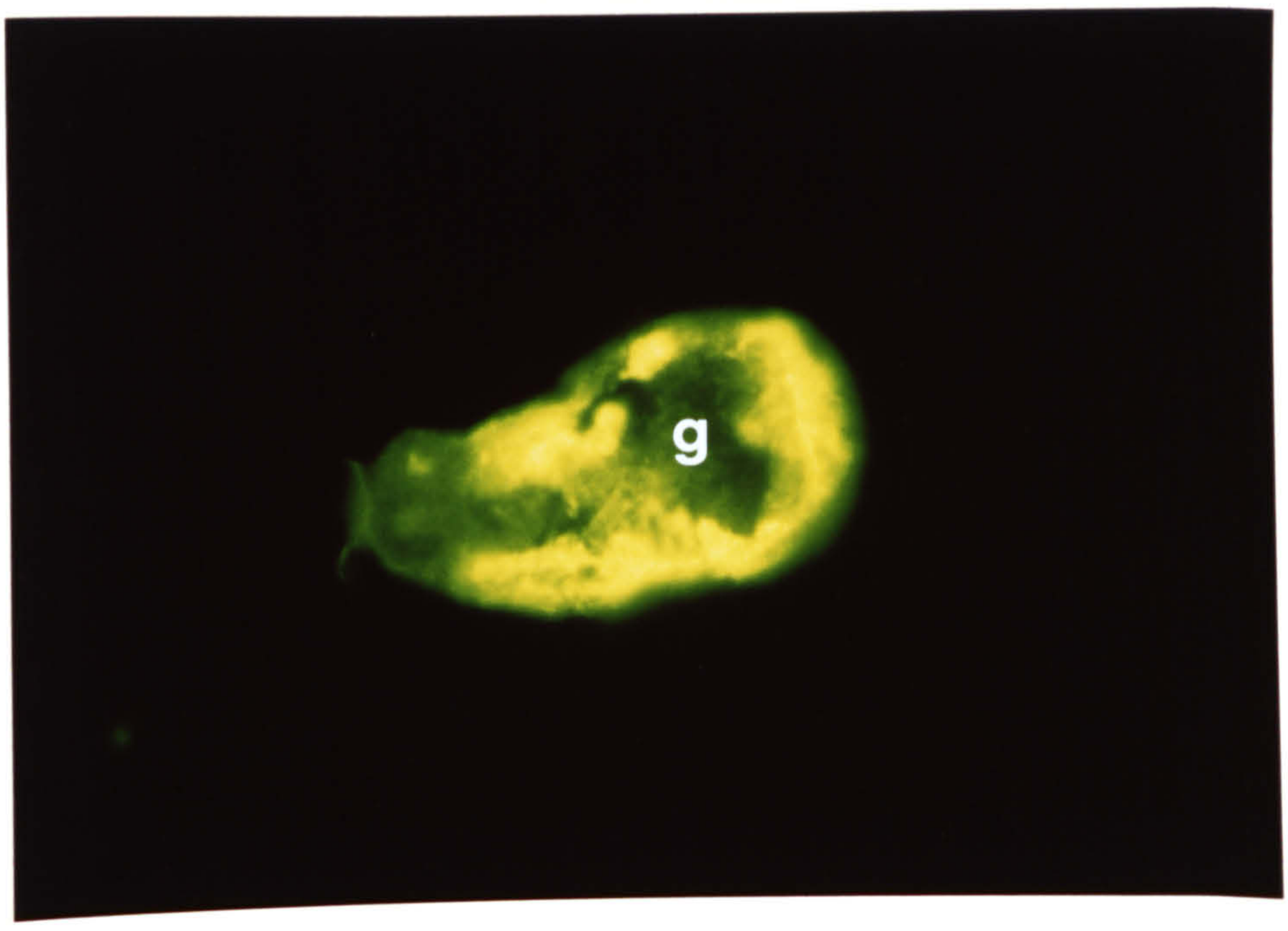
g

FIGURE 2.34

Acetone-fixed frozen sections of 3h skin-transformed schistosomula were incubated with MAB D7.2 (1:60) and RAM/Ig/FITC (1:64). The tegument of the parasites shows bright fluorescence. Peripheral areas beneath the tegument are also labelled. Other internal structures are less reactive except the digestive tract (D) which is fluorescently labelled and is seen as a wavy-structure in the centre. Packets are no longer present inside the body. x 520.

FIGURE 2.35

PF-fixed intact cercariae did not react with MABs G6.1 and D7.2. The surface of the parasite is unlabelled. Some cercariae exhibit weak fluorescent labelling at the apical end (A) and at the point (PE, posterior end) where the tail has detached from the body. The anterior end of the cercarial tail (the point of attachment between the body and the tail) is also positive and appears as a fluorescent dot (not shown). x 520.

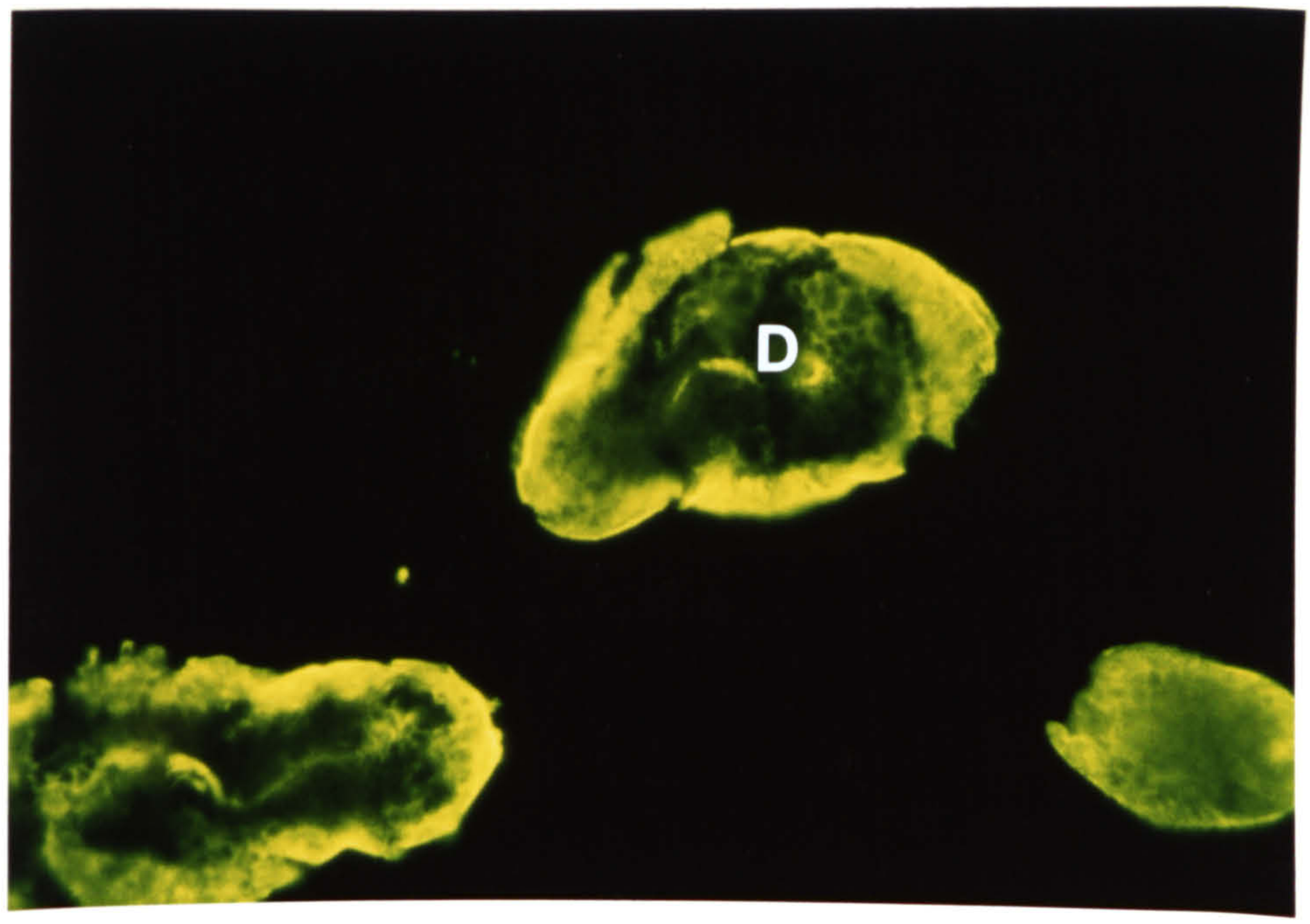
D

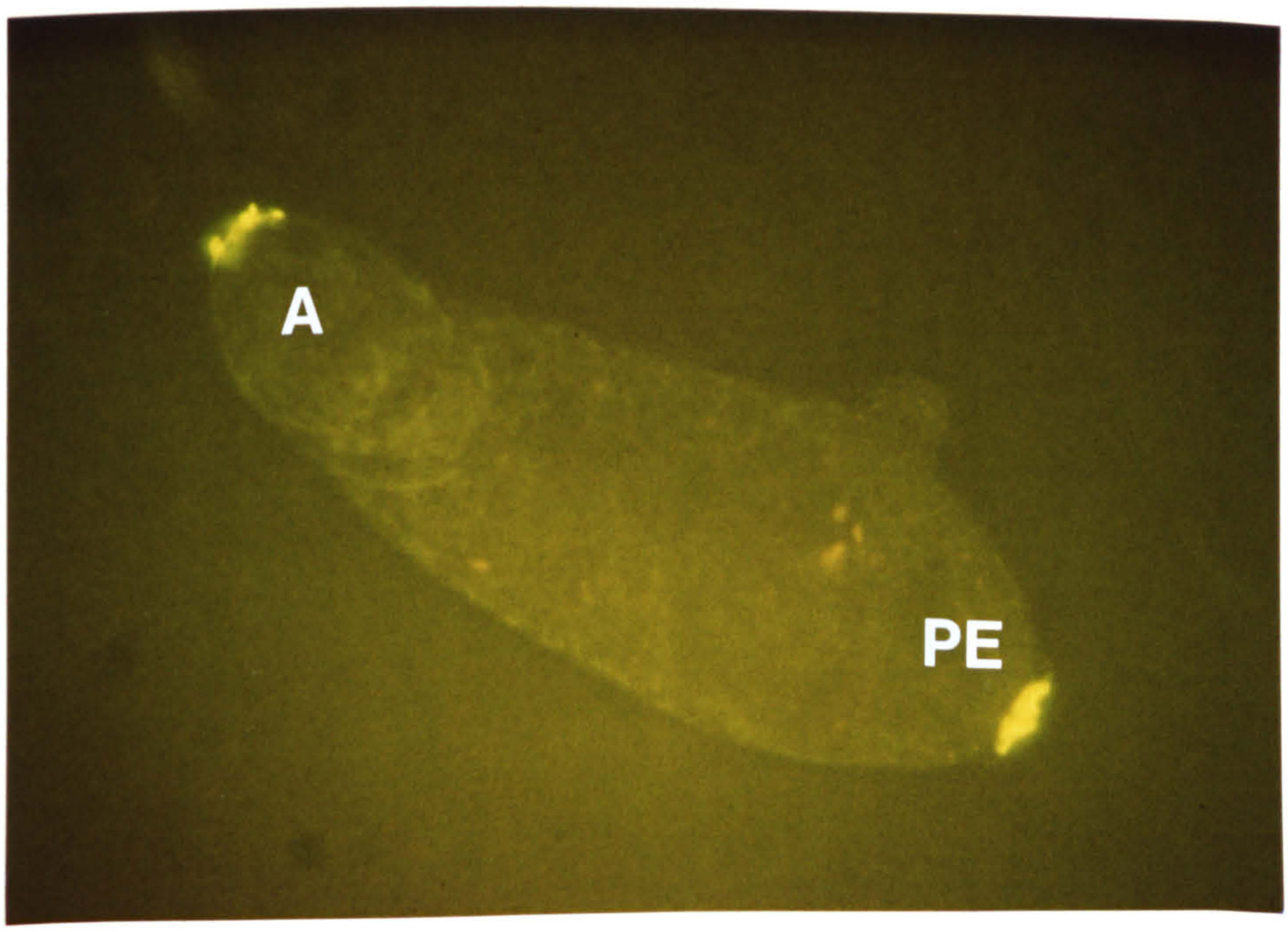
A
PE

FIGURE 2.36

Acetone-fixed frozen section of cercaria stained with MAB D7.4 (1:60) and RAM/Ig/FITC (1:64). Fluorescent label is present predominantly in the tegument and the periphery of the body. Internal tissues are unlabelled. Sections of tail (T) are also negative. x 520.

FIGURE 2.37

Acetone-fixed frozen sections of 3h skin-transformed schistosomula reacted with MAB G6.2 (1:60) and RAM/Ig/FITC (1:64). The tegument which invests the outer aspect of the parasite is strongly antigenic. Internal tissues are mostly unlabelled; some react positively, but more weakly than the tegument. x 520.

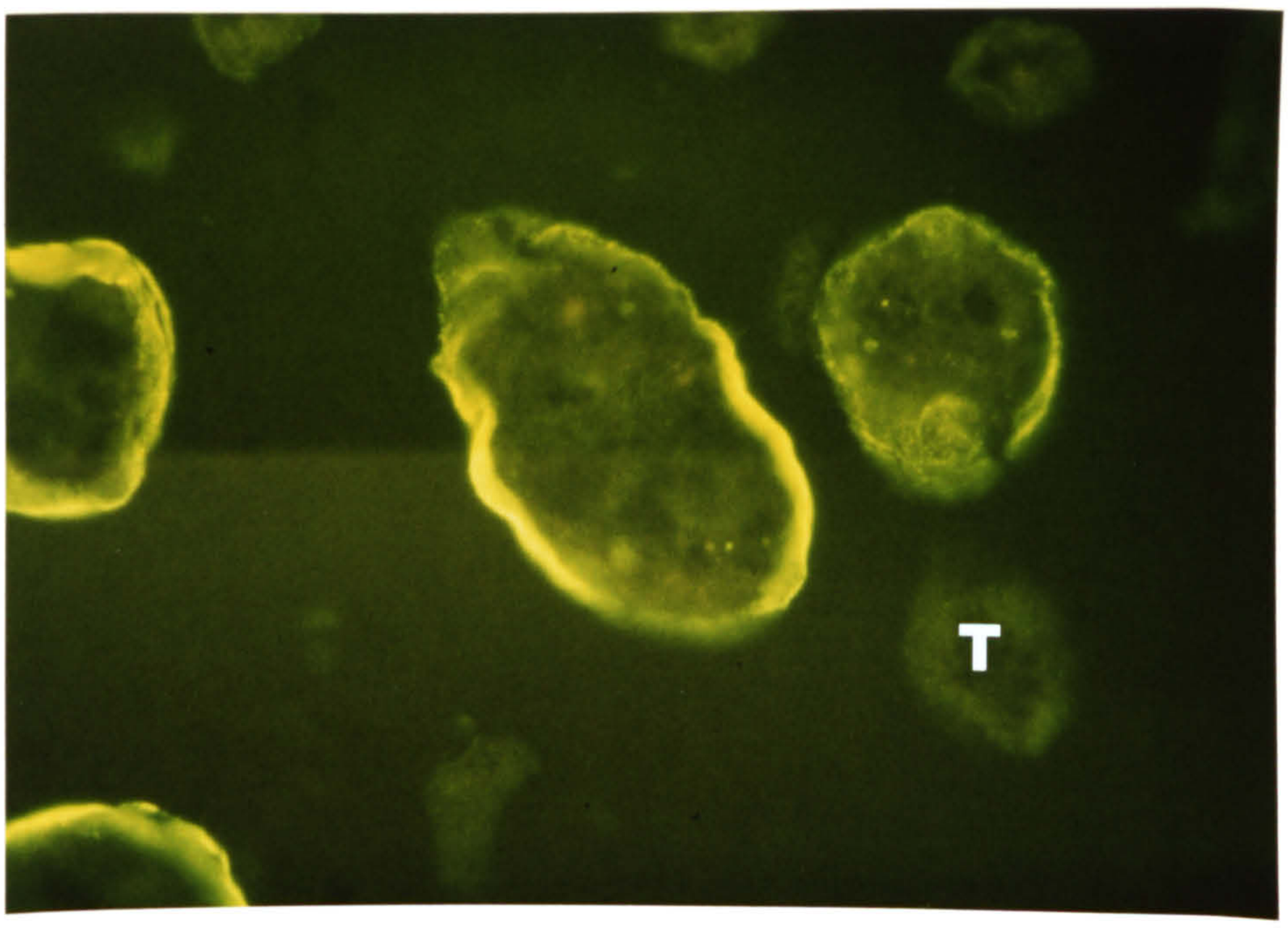
T

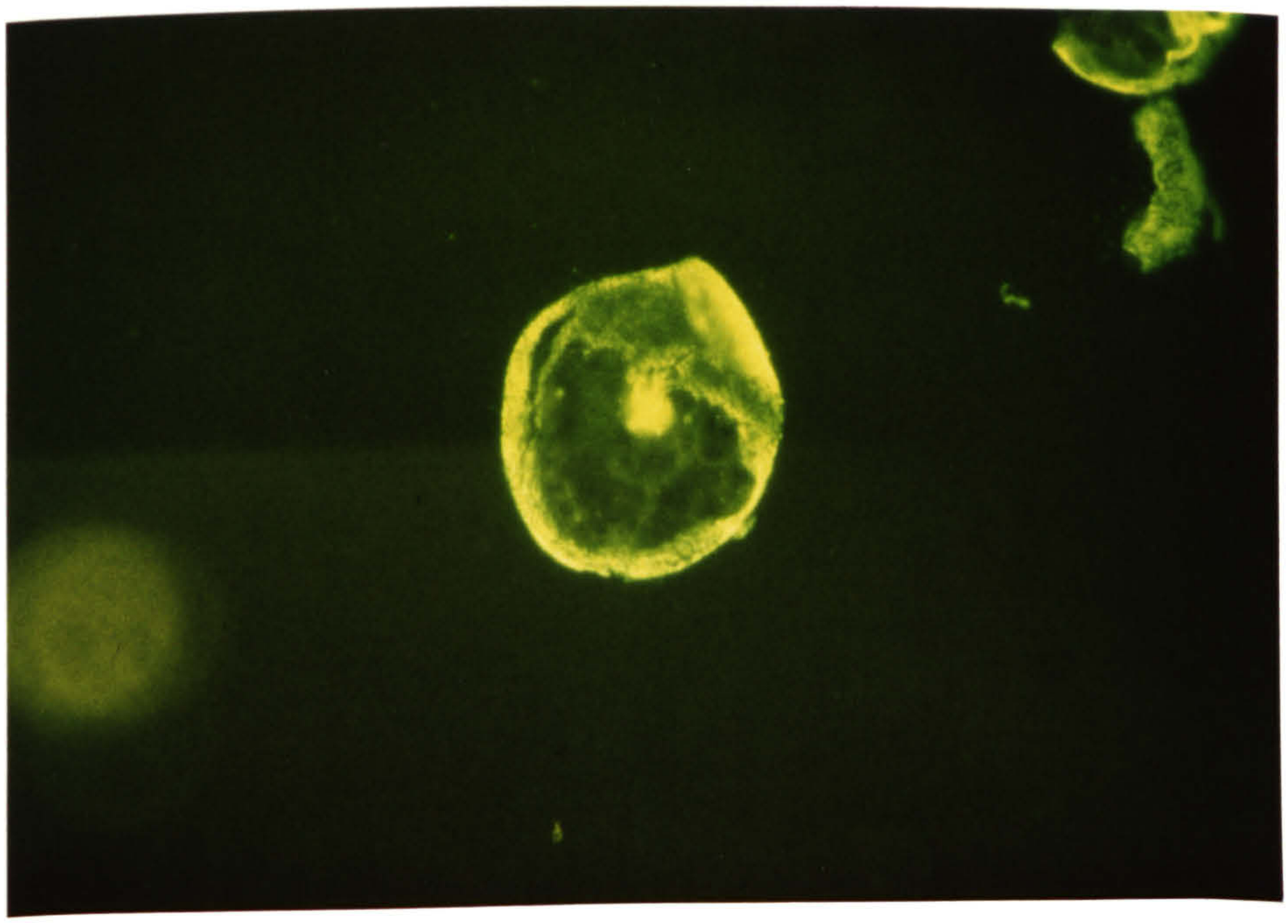

FIGURE 2.38

PF-fixed frozen section of adult male worm stained with MAB G6.6 (1:60) and RAM/Ig/FITC (1:64). Positive fluorescence is seen in the tegument and in all internal membranes. Membranes of parenchymal cells are brighter than their cytoplasm. The muscle layers are very weakly stained. The gut epithelium is also positive. PF-fixed sections give brighter fluorescent staining than acetone-fixed worms (see Figs. 2.15 & 2.16). x 130.

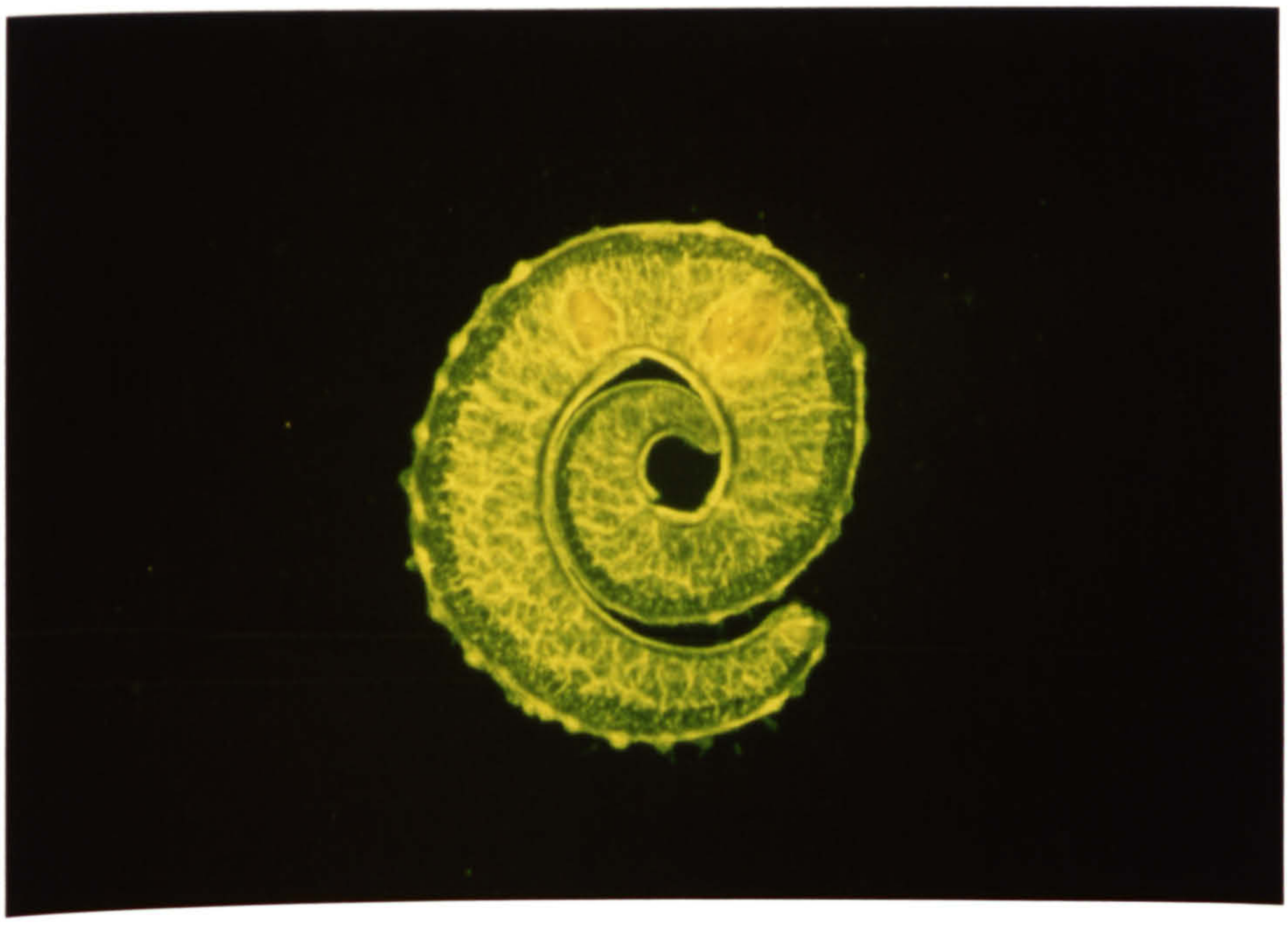

FIGURES 2.39 & 2.40

Higher magnification of Fig. 2.31 shows strong specific fluorescence on tubercles of the tegument and membranes of parenchymal tissues (PT). Fluorescent staining of the plasma membranes of parenchymal cells is stronger than that of their cytoplasm. The cytoplasm of muscle cells beneath the tegument is unlabelled, but membranes of muscle fibres (M) are weakly positive. x 520.

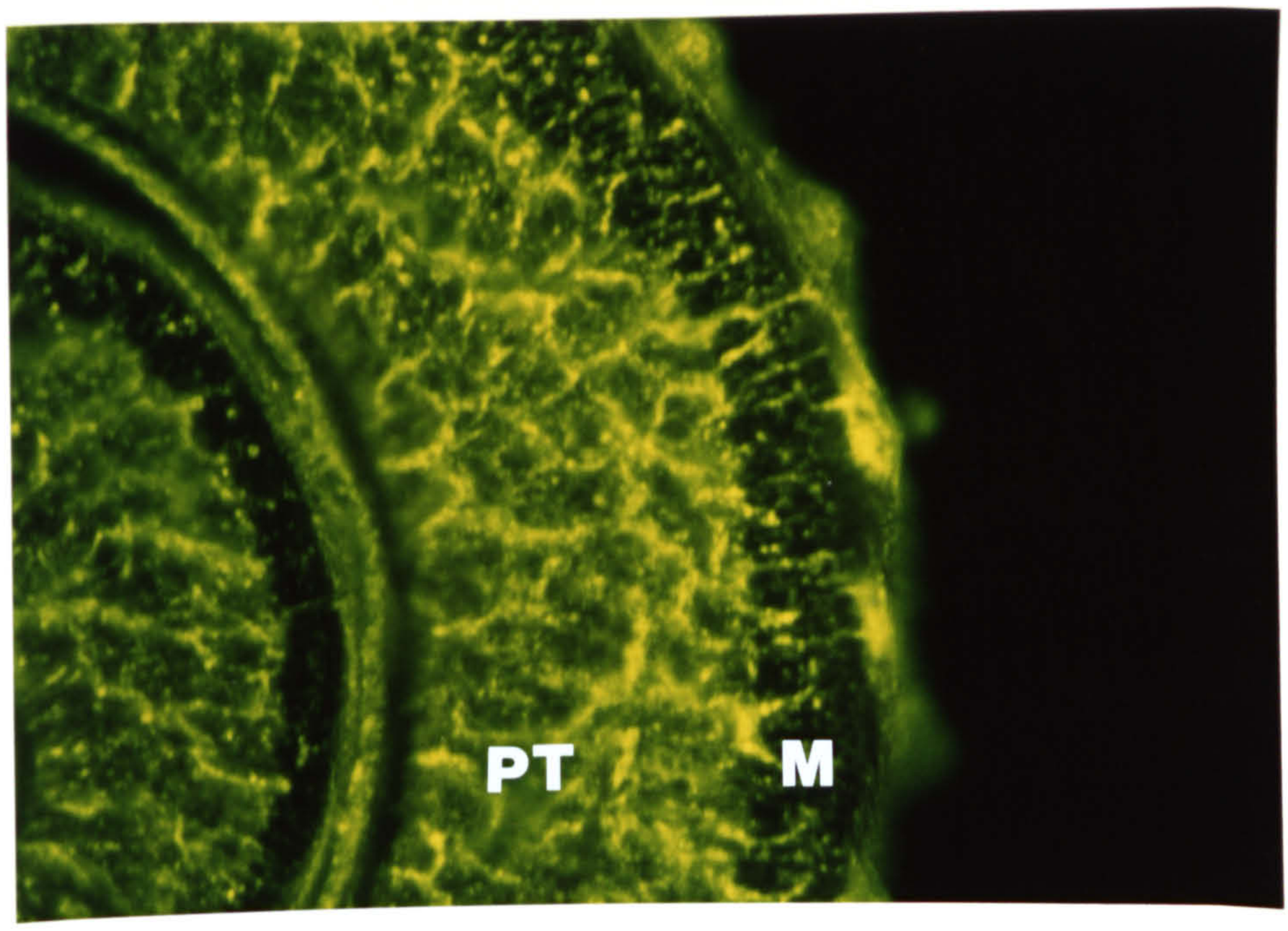
PT
M

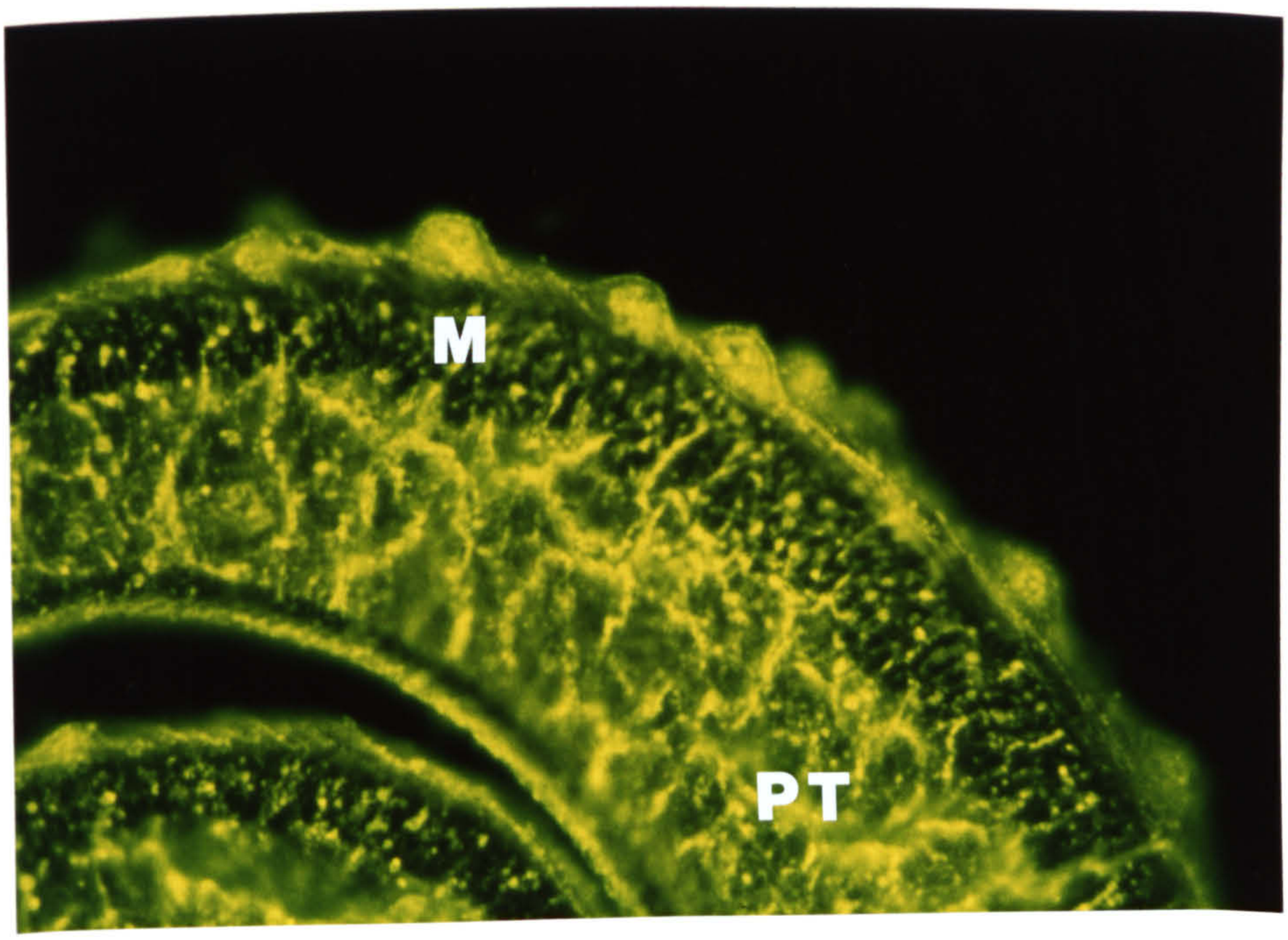
M
PT

FIGURE 2.41

Acetone-fixed frozen sections of cercariae immunostained with MAB G6.6 (1:60) and RAM/Ig/FITC (1:64). Fluorescent label is seen on the entire section of most parasites. Some sections show very bright fluorescence at the periphery. The gland cells (G) within the body are unlabelled. Sections of tail are weakly labelled, some are negative. Two fluorescent dots are seen opposite to each other at the periphery on the transverse section of tail (*). x 520.

FIGURE 2.42

PF-fixed frozen section of 3h skin-transformed schistosomulum reacted with MAB G6.6 (1:60) and RAM/Ig/FITC (1:64). The entire section is brightly fluorescent. x 520.

FIGURE 2.43

Acetone-fixed frozen section of 3h skin-transformed schistosomulum prepared as described in FIG. 2.42 showing the entire section is fluorescently labelled with the strongest reactivity in some internal structures. The nuclei of internal tissues are unstained (arrow). x 520.

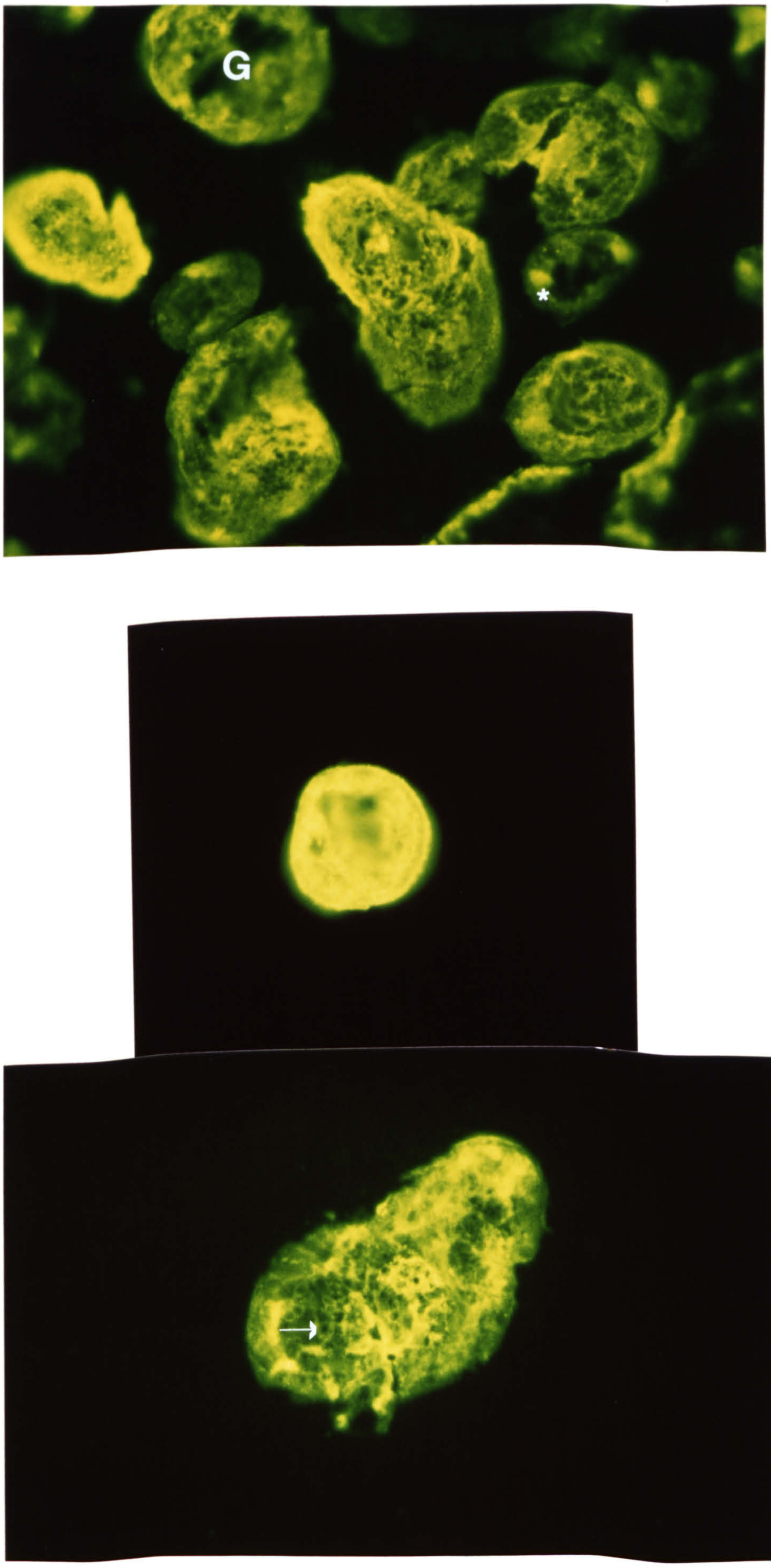
G
*

FIGURE 2.44

PF-fixed frozen section of adult male worm reacted with MAB D7.3 (1:60) and RAM/Ig/FITC (1:64). The tegument and tubercles are both intensely fluorescent labelled. Membranes of internal tissues are also positive but weaker than the tegument. The muscle cytoplasm and the gut are unstained. The nuclei of parenchymal cells are negative. The membranes of muscle fibres are also positive. The membranes of the tegument (*) are stained but not the cytoplasm. x 520.

FIGURE 2.45

PF-fixed frozen section of cercaria immunostained with MAB D7.3 (1:60) and RAM/Ig/FITC (1:64). Tegument fluorescence is especially strong with MAB D7.3. The tegument appears as a very thin line covering the cercarial body. Internal tissues are weakly labelled. x 520.

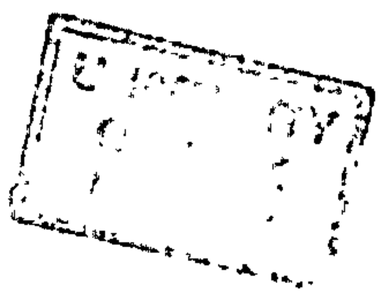

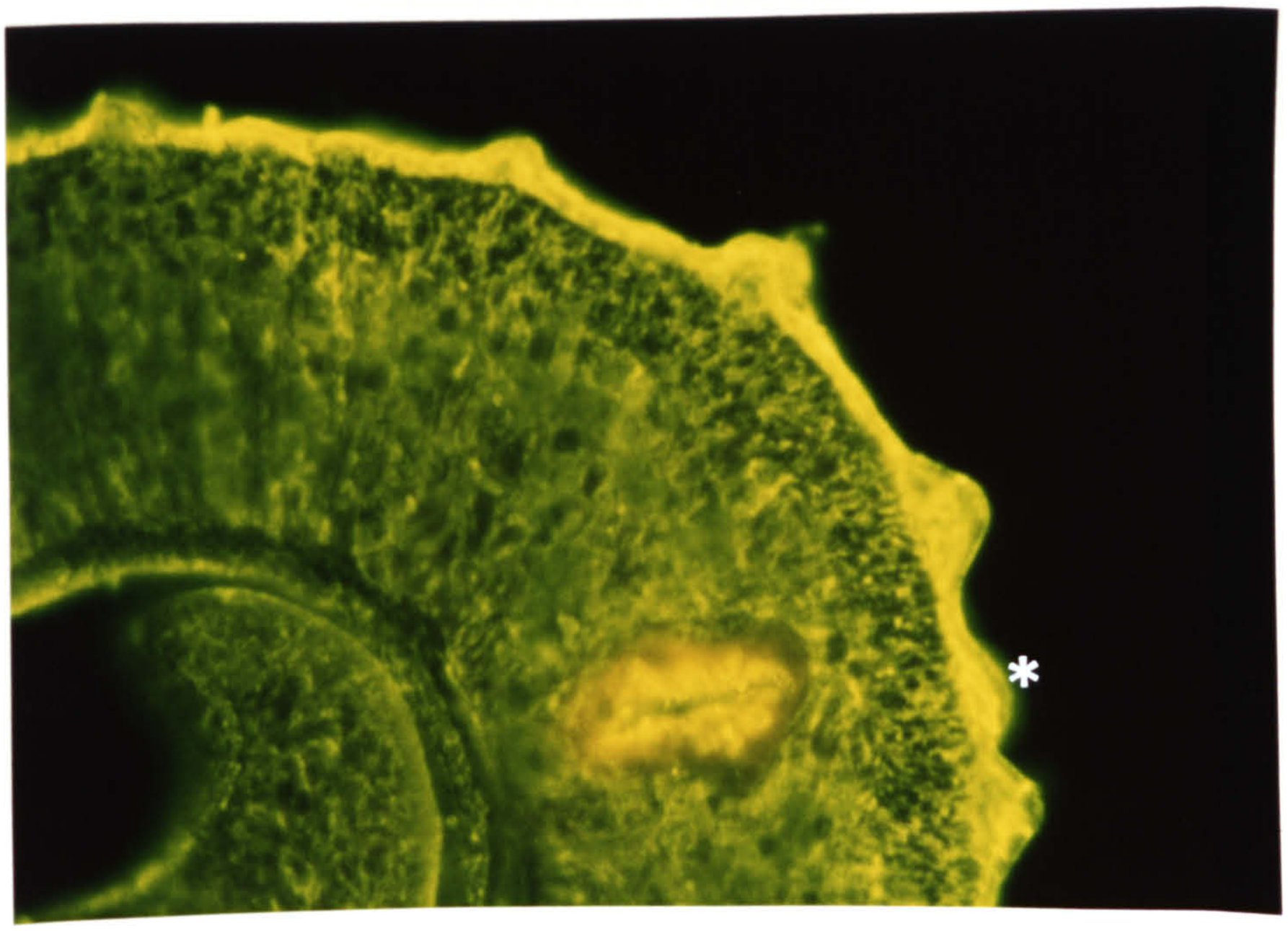

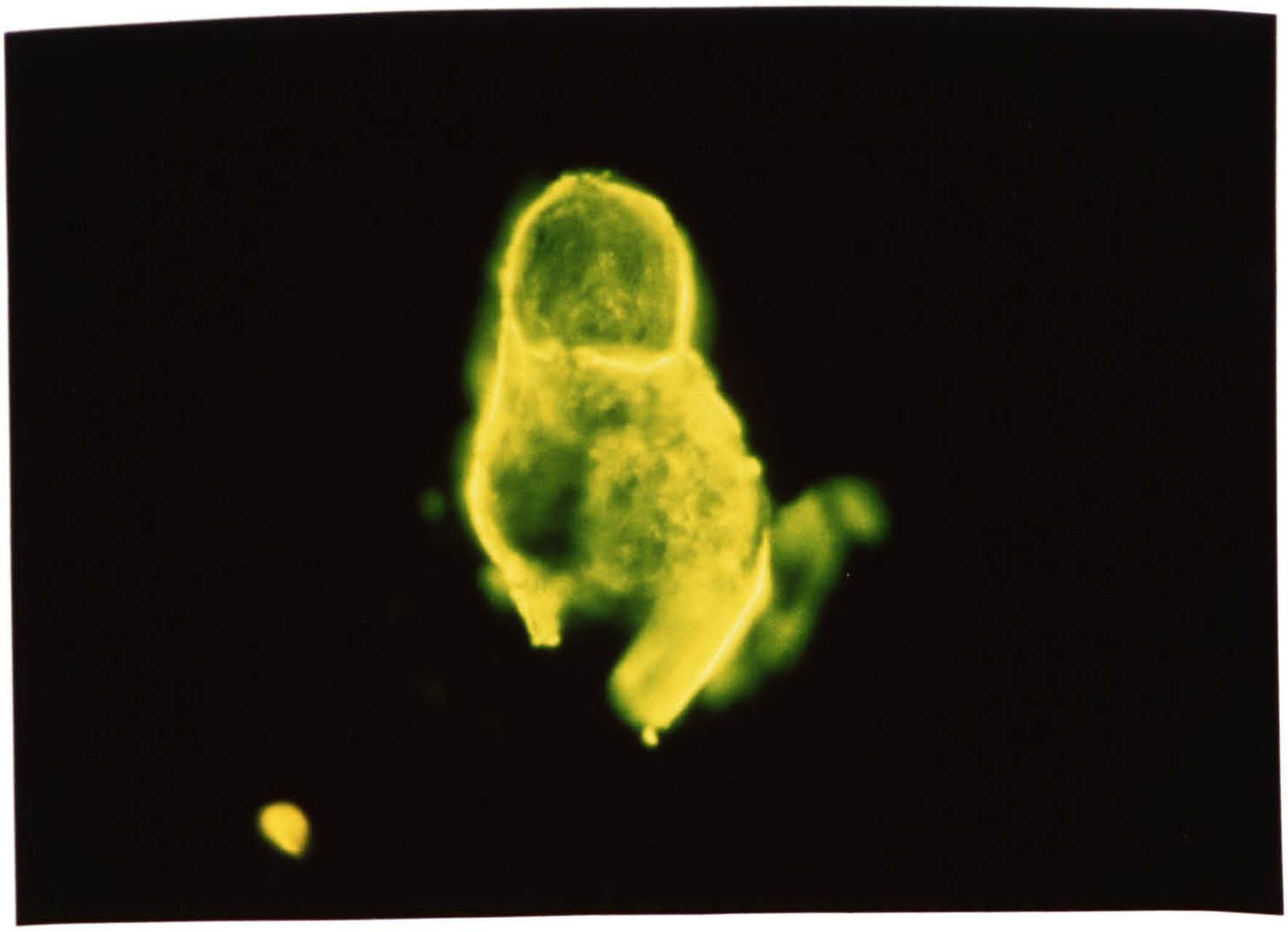

FIGURES 2.46 & 2.47

PF-fixed frozen section of cercaria reacted with MAB G5.3 (1:60) and RAM/Ig/FITC (1:64). The tegument and the oesophagus are both brightly fluorescent. The diaphragm fibres (arrow) of the head capsule are also positive. Internal structures are unlabelled. x 520.

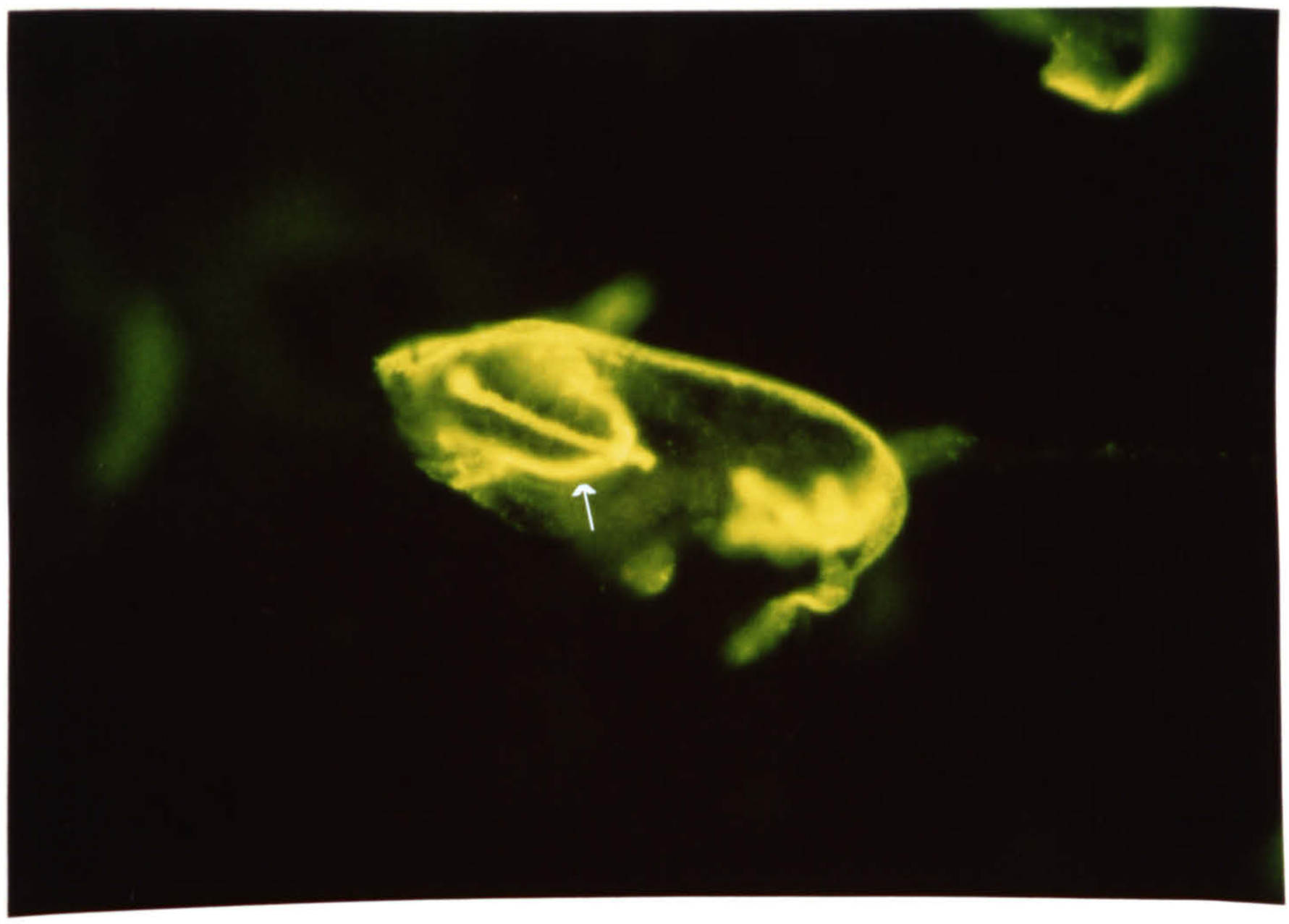

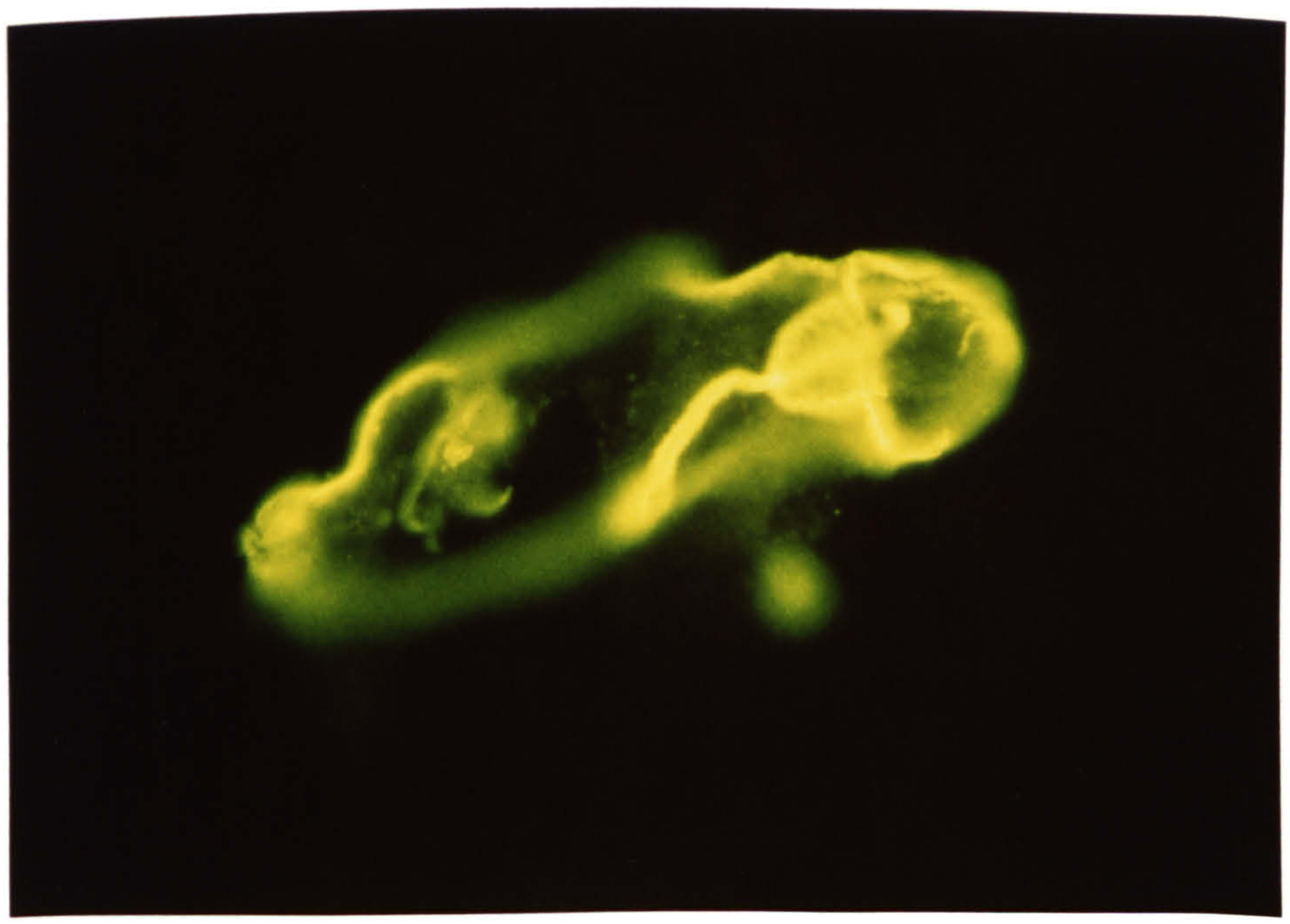

FIGURE 2.48

PF-fixed frozen section of 3h skin-transformed schistosomulum reacted with MAB C5.3 (1:60) and RAM/Ig/FITC (1:64). The tegument is brightly fluorescent. Strong specific fluorescence is also seen in the membrane of the head capsule. Fluorescent label in the centre of the section represents the oesophagus (*). The membrane (arrow) of the ventral sucker which lies posteriorly on the body is also labelled. The membranes of muscle fibres beneath the tegument are less antigenic than the tegument, but other internal tissues are negative. x 520.

FIGURE 2.49

PF-fixed frozen section of cercaria reacted with MAB M7.5 (1:60) and RAM/Ig/FITC (1:64). The epitopes recognized by MAB M7.5 are in the body muscle which lies beneath the tegument, muscle in the head capsule and in the internal organs. In the head capsule the muscular ensheathment of the acetabular glands (arrow) is markedly sparse around the ducts as they near the pores. The fluorescent labelled muscle cells are seen running parallel to each other towards the duct openings. Postacetabular gland (g) contents appear autofluorescent at the posterior end of the body. x 520.

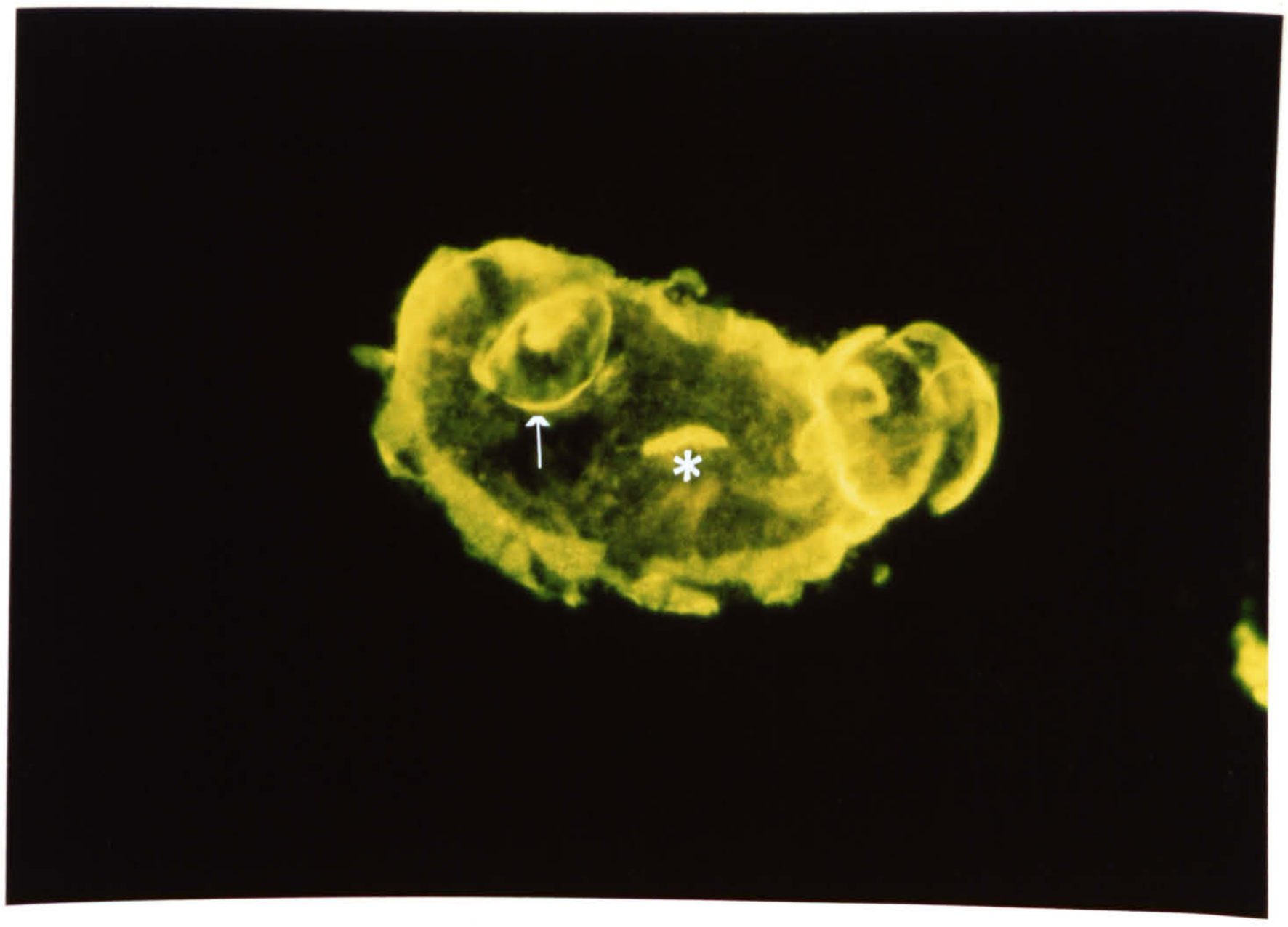
*

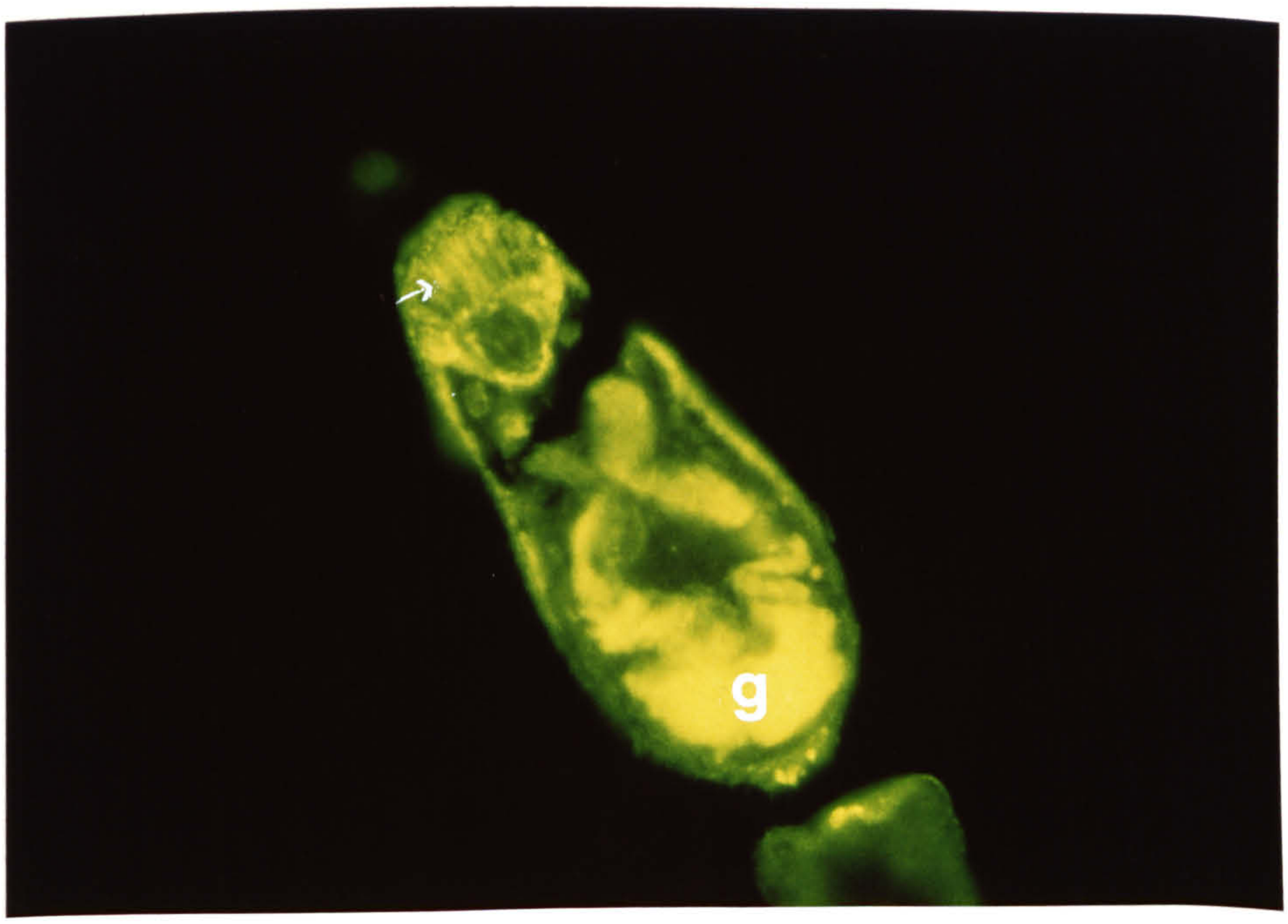
g

FIGURE 2.50

PF-fixed section of the cercarial tail (T) treated in the same way as that in Fig. 2.49 shows striations (arrow) of myofibres in longitudinal muscle. x 520.

FIGURE 2.51

PF-fixed frozen section of 3h schistosomulum reacted with MAB M7.5 (1:60) and RAM/Ig/FITC (1:64). An individual muscle block (arrow) of the body wall is fluorescently labelled. x 520.

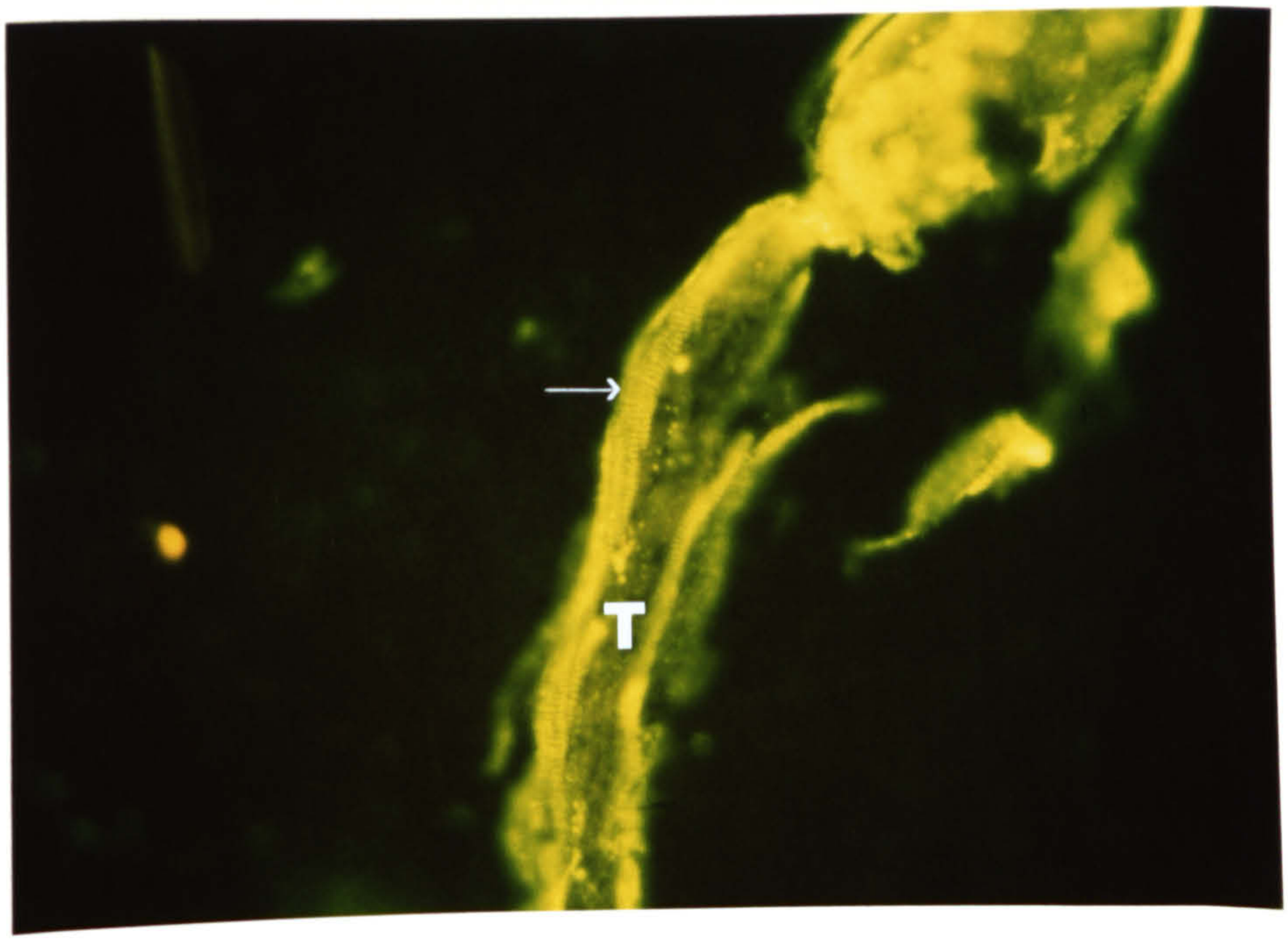
T

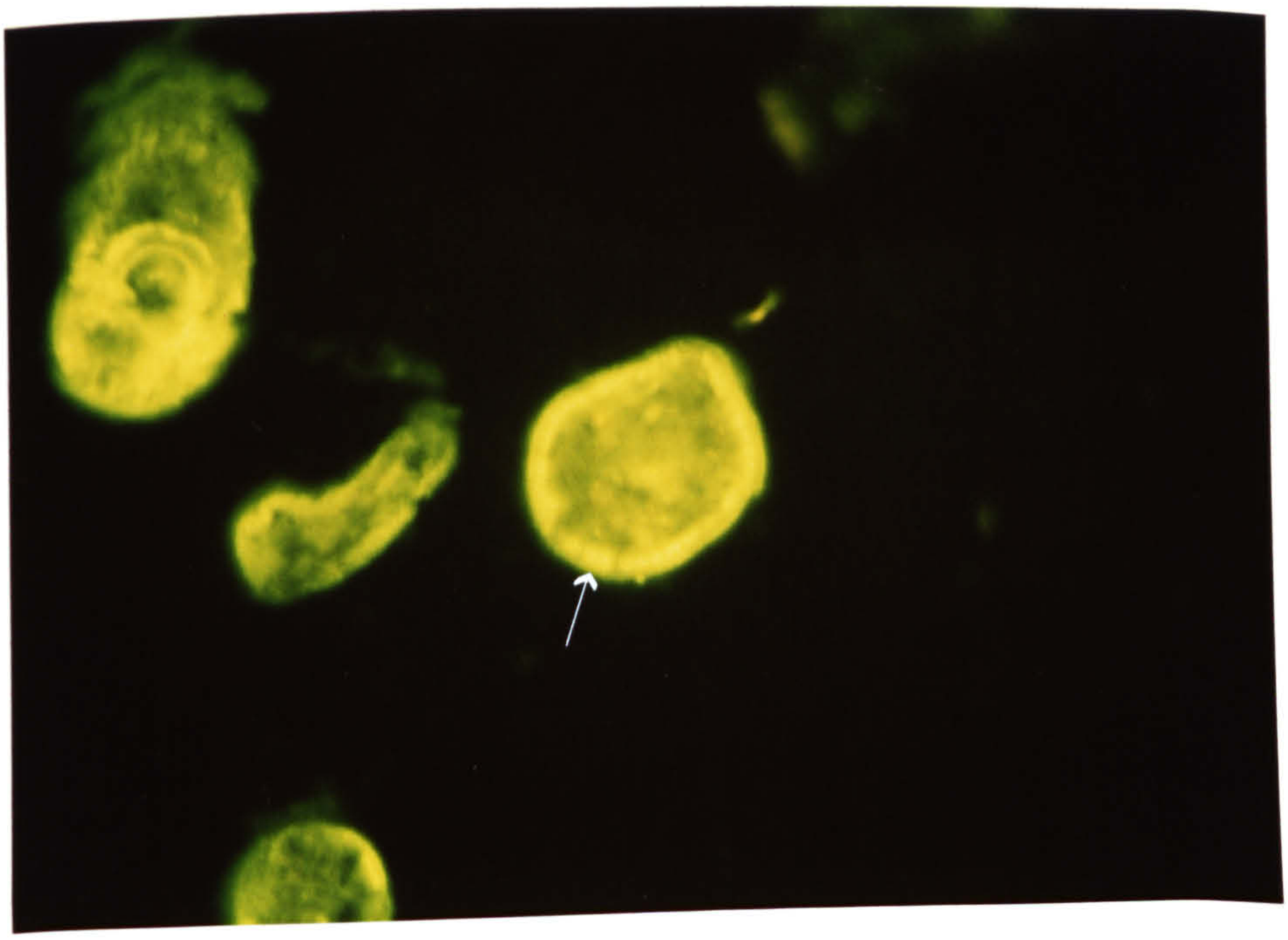

FIGURE 2.52

PF-fixed frozen section of 3h skin-transformed schistosomulum immunostained with MAB G6.4 (1:30) and RAM/Ig/FITC (1:64). The tegument is brightly fluorescent. Nephridia (arrow) are also fluorescently labelled but the reactivity is weaker. Nephridia are spiral-like structures lying internally and posteriorly in the body. Other internal structures are unlabelled. Tegument fluorescence at the posterior end (PE) is stronger than that observed at the apical area (A). x 520.

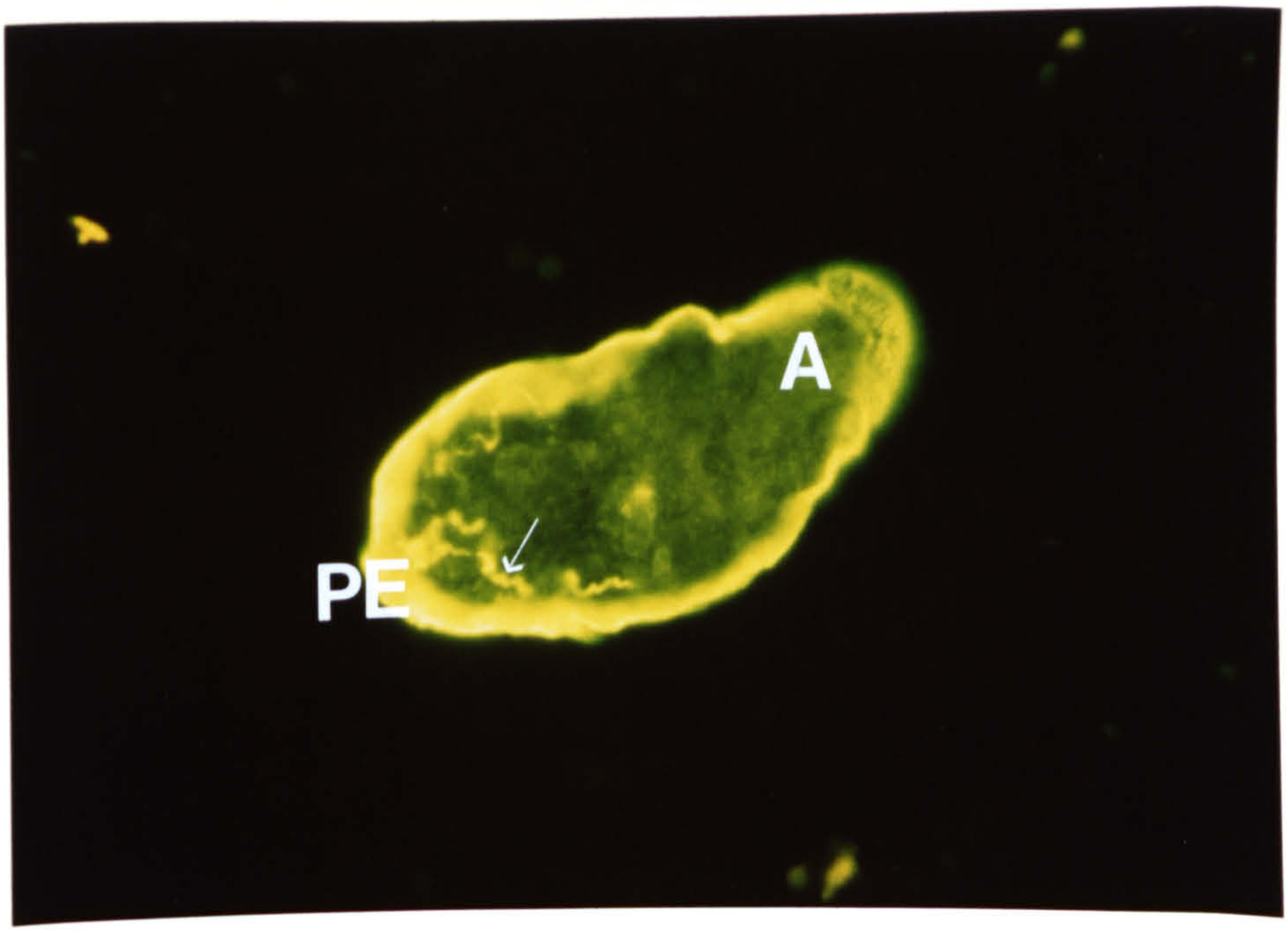
A
PE

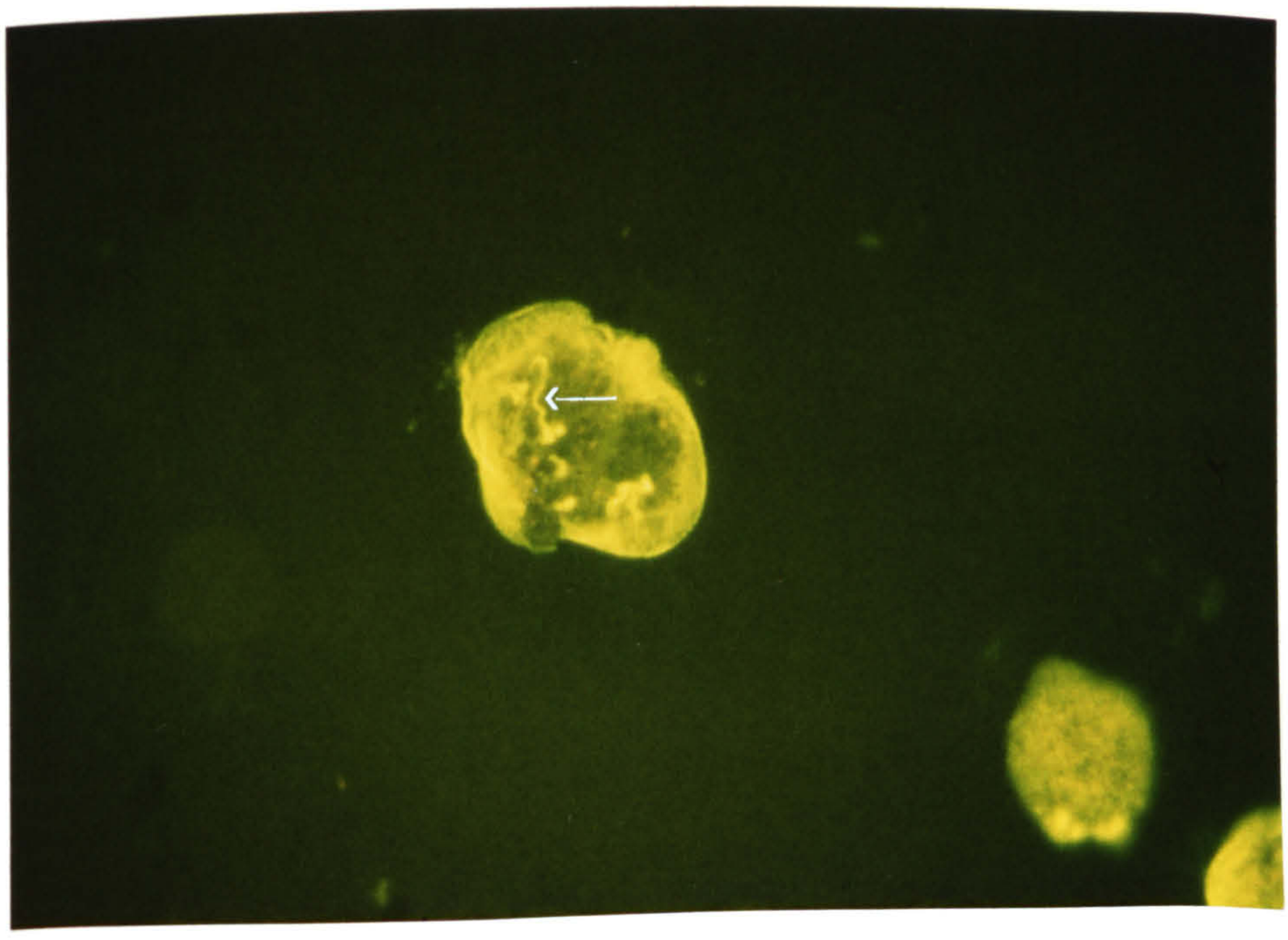

FIGURES 2.53 & 2.54

PF-fixed frozen section of cercaria reacted with MAB M7.6 (1:30) and RAM/Ig/FITC (1:64). The antibody is bound to the tegument of the cercarial body (B) and tail (T), and the nephridia. Nephridia (arrow) are long, thin structures, seen running along the entire length of the tail (T). Other internal tissues are also weakly labelled. x 520.

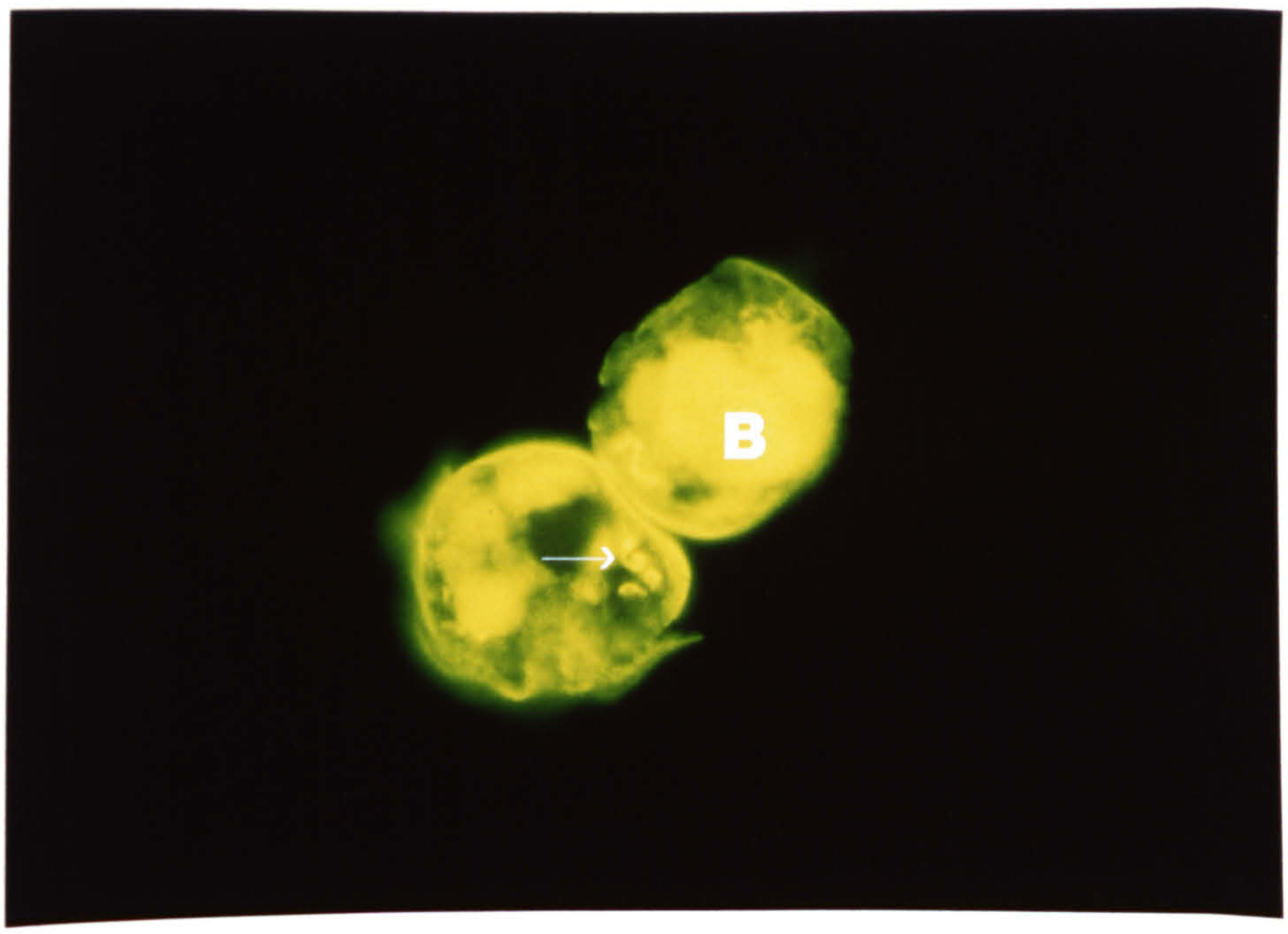
B

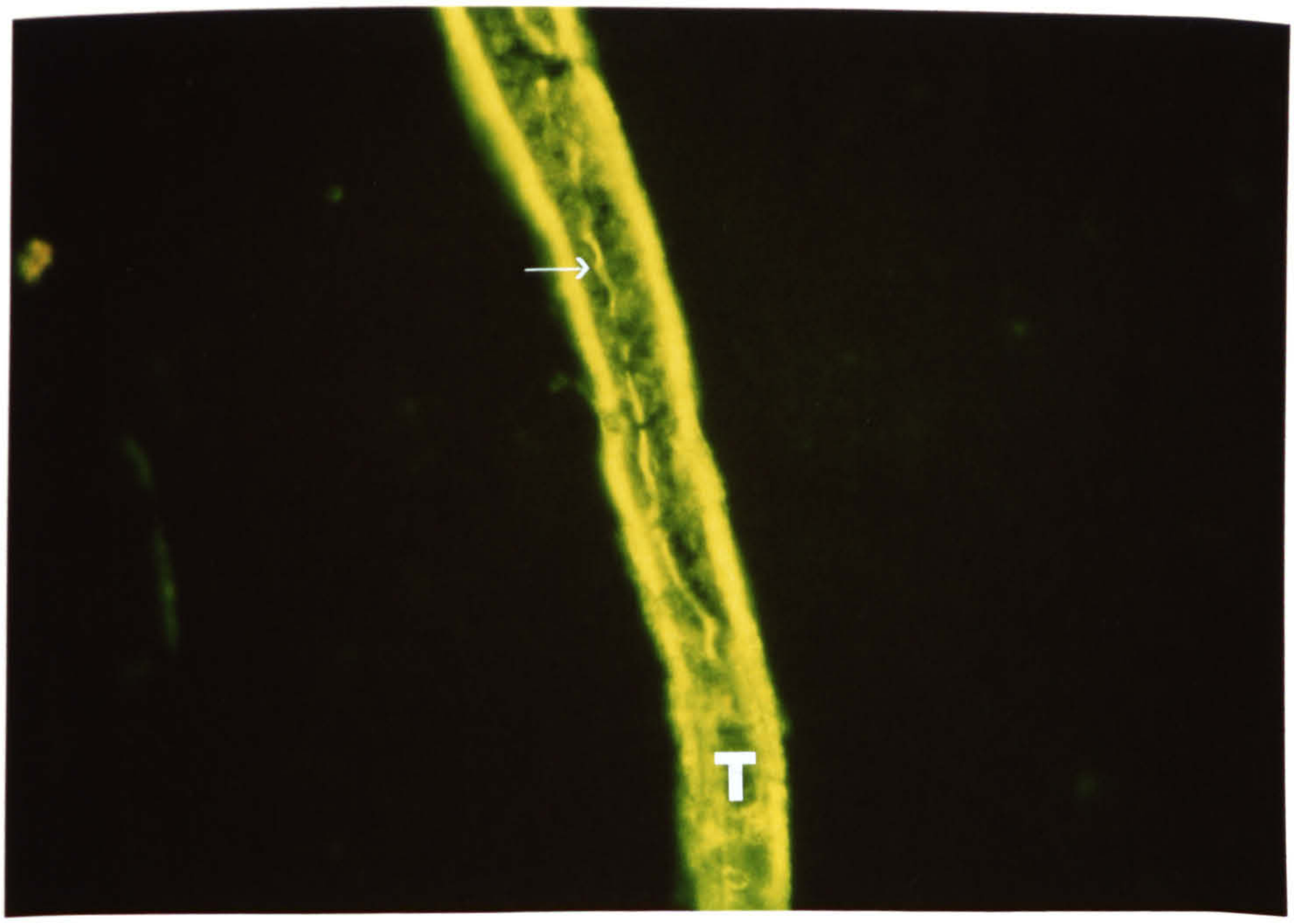
T

FIGURE 2.55

PF-fixed frozen section of S. japonicum adult male worm reacted with MAB G6.6 (1:60) and RAM/Ig/FITC (1:64). Fluorescent label is seen in the parenchyma of the worm. Most of the tegument and the muscle layers are unlabelled. Regions of tegument (arrow) are false positive. x 520.

FIGURE 2.56

A 5-day-old schistosomulum recovered from the lungs of a S. mansoni-infected mouse was fixed in PF and reacted with rabbit anti-mouse erythrocyte ghost serum (1:40) and GAR/Ig/FITC (1:25). The fluorescent antibodies bind to the entire surface of the parasite. x 520.

FIGURE 2.57

PF-fixed intact 5-day-lung worm immunostained with vaccinated rabbit serum (1:40) and GAR/Ig/FITC (1:25). The parasite surface exhibits fluorescent label. The binding is weaker than that in Fig. 2.56. x 520.

FIGURE 2.58

A 21-day-old worm recovered from the liver of a S. mansoni infected mouse was fixed in PF and reacted with rabbit anti-mouse erythrocyte ghost antibody (1:40) and GAR/Ig/FITC (1:25). Strong specific fluorescence is seen over the parasite surface. The worm feeds on blood, and haemoglobin pigment in the digestive tract of the parasite, gives it a brown colouration. x 520.

FIGURE 2.59

A 21-day-liver worm cultured in MEM for 24 h at 37°C was fixed in PF and reacted with rabbit anti-mouse erythrocyte ghost antibody (1:40) and GAR/Ig/FITC (1:25). Positive fluorescence is seen covering the entire parasite surface. Note negligible loss of host antigen after 24 h in culture as judged by fluorescent staining using rabbit anti-mouse erythrocyte ghost serum as primary antibody. x 520.

FIGURE 2.60

A 21-day-liver worms cultured in MEM for 24 h at 37°C was fixed in PF and reacted with AMS (1:40) and RAM/Ig/FITC (1:25). Positive fluorescence is seen on the surface of each parasite where the tegument is damaged (*). x 520.

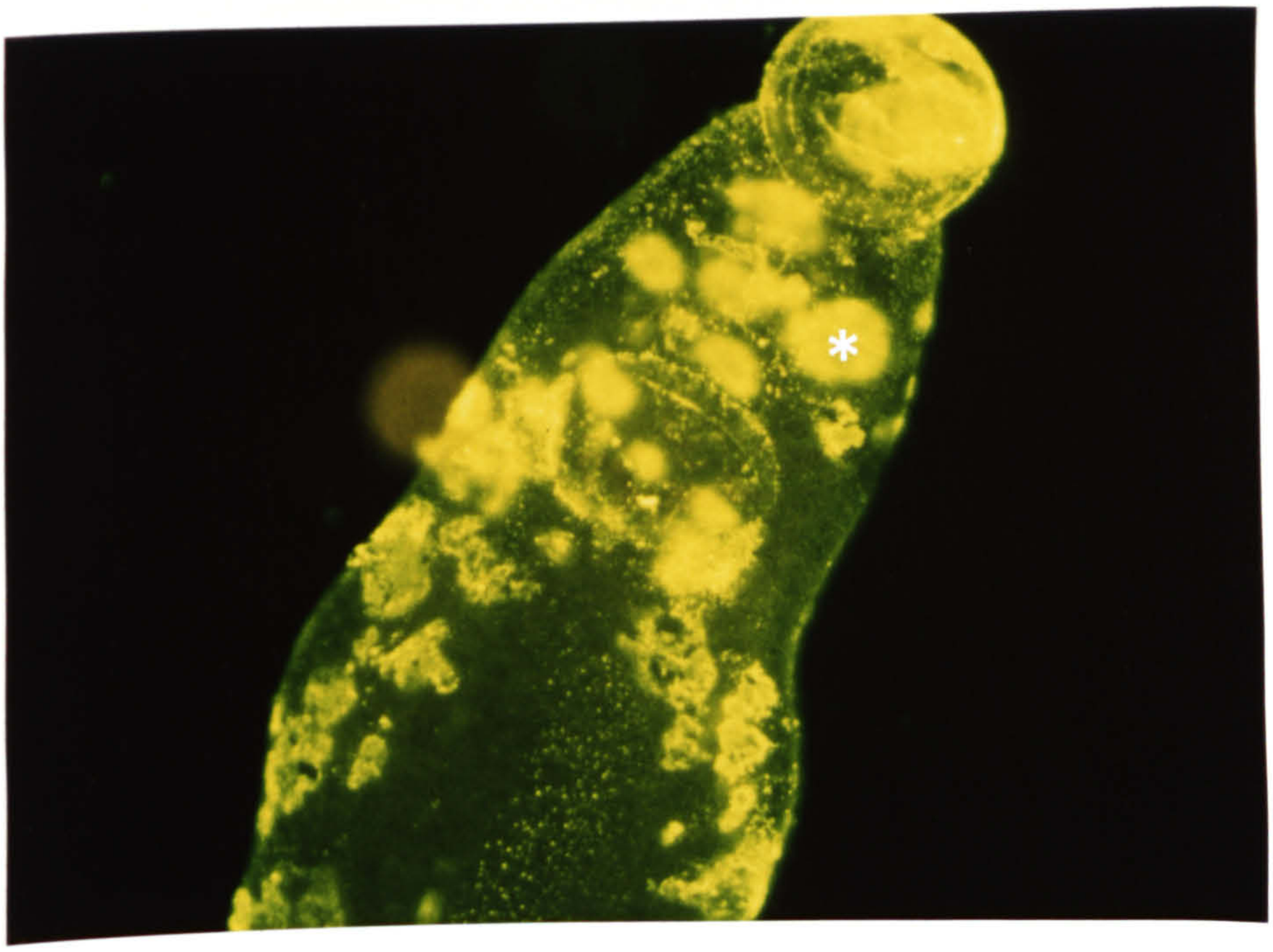

FIGURE 3.1

Acetone-fixed frozen section of adult male S. mansoni were incubated in a 1:60 dilution of MAB G3.1 followed by RAM/Ig/FITC (1:64) as described in detail in the Materials & Methods. Transverse section showing positive fluorescence in the muscle fibres throughout the body. In the section of the female worm (F), the thin layers of muscle beneath the tegument and the muscle inside the body are fluorescently labelled. The vitelline cells in the female autofluoresce bright yellow. x 130.

FIGURE 3.2

High magnification of Fig. 3.1 showing the MAB G3.1 reacts with the muscle fibres of the adult worm. The outer circular and inner longitudinal muscle (M) layers beneath the tegument are fluorescently labelled. The muscle fibres in the parenchyma (PT) are also positive. The layer of muscles beneath the ventral surface is thinner than that beneath the dorsal. x 520.

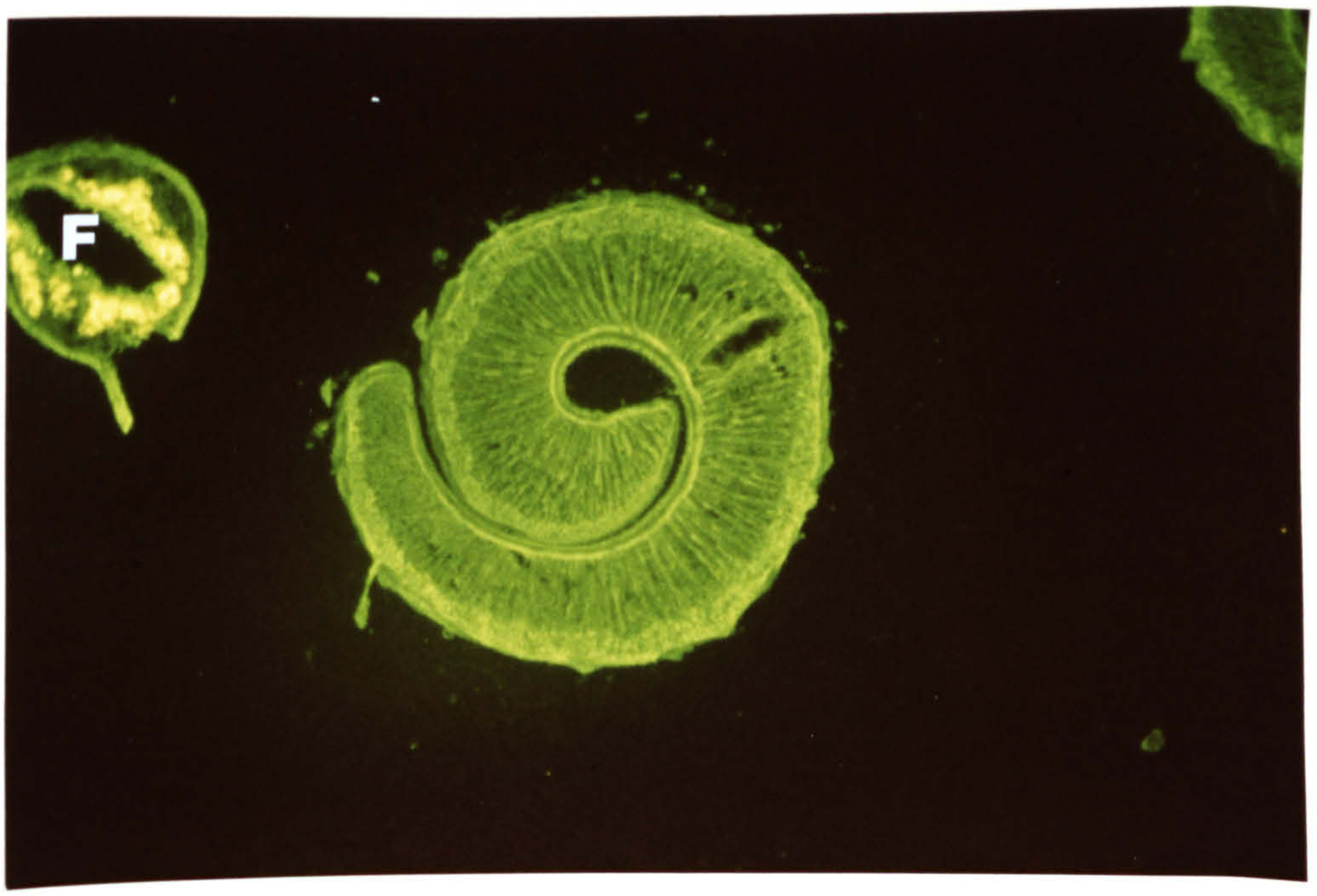
F

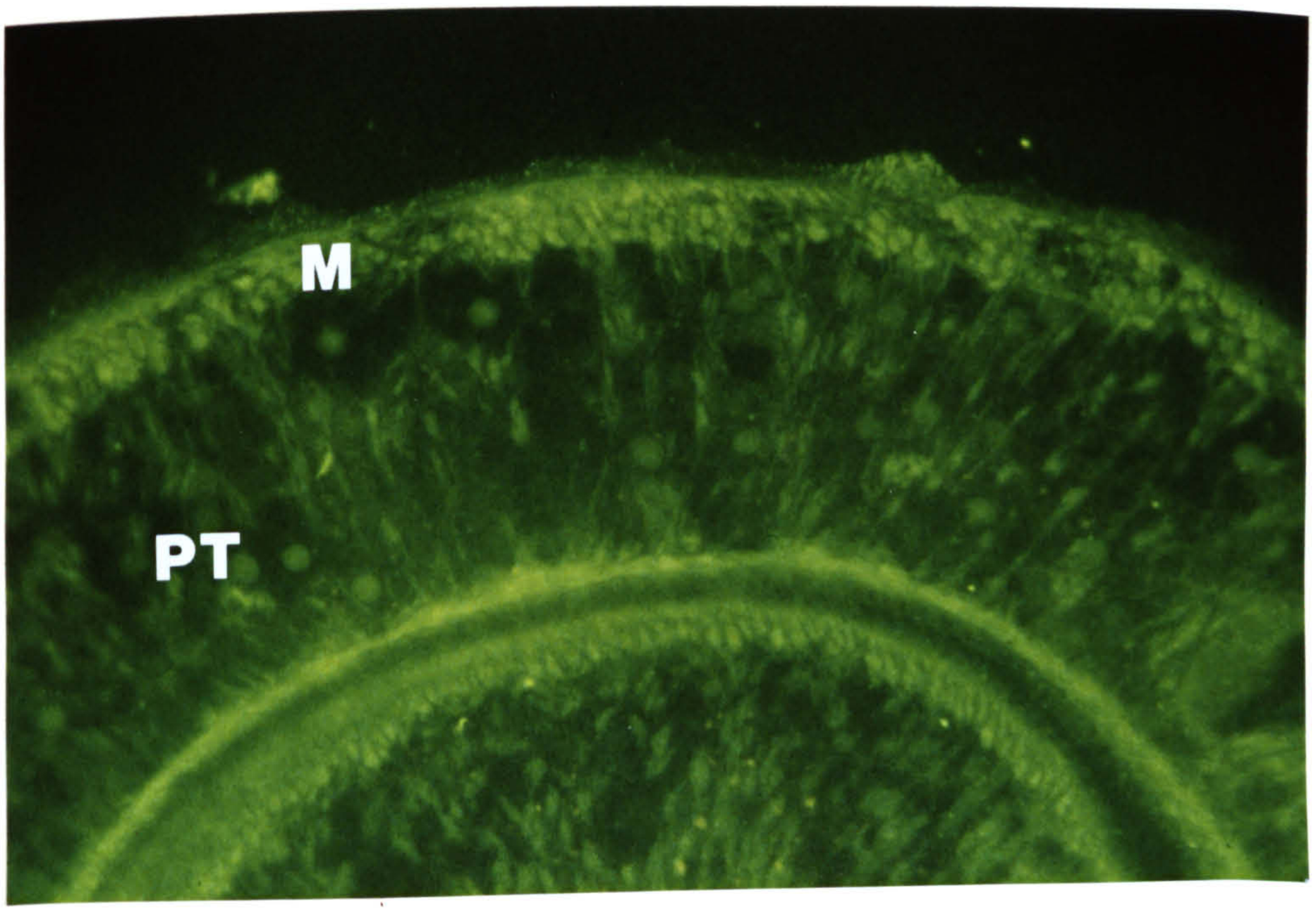
M
PT

FIGURE 3.3

Acetone-fixed frozen section of adult male worm immunostained with MAB M7.8 (1:60) and RAM/Ig/FITC (1:64). The muscle cells in the entire body are fluorescently labelled. The muscle layers of the body wall appear as a thick band; the muscle fibres in the parenchymal tissues are fine dots. x 130.

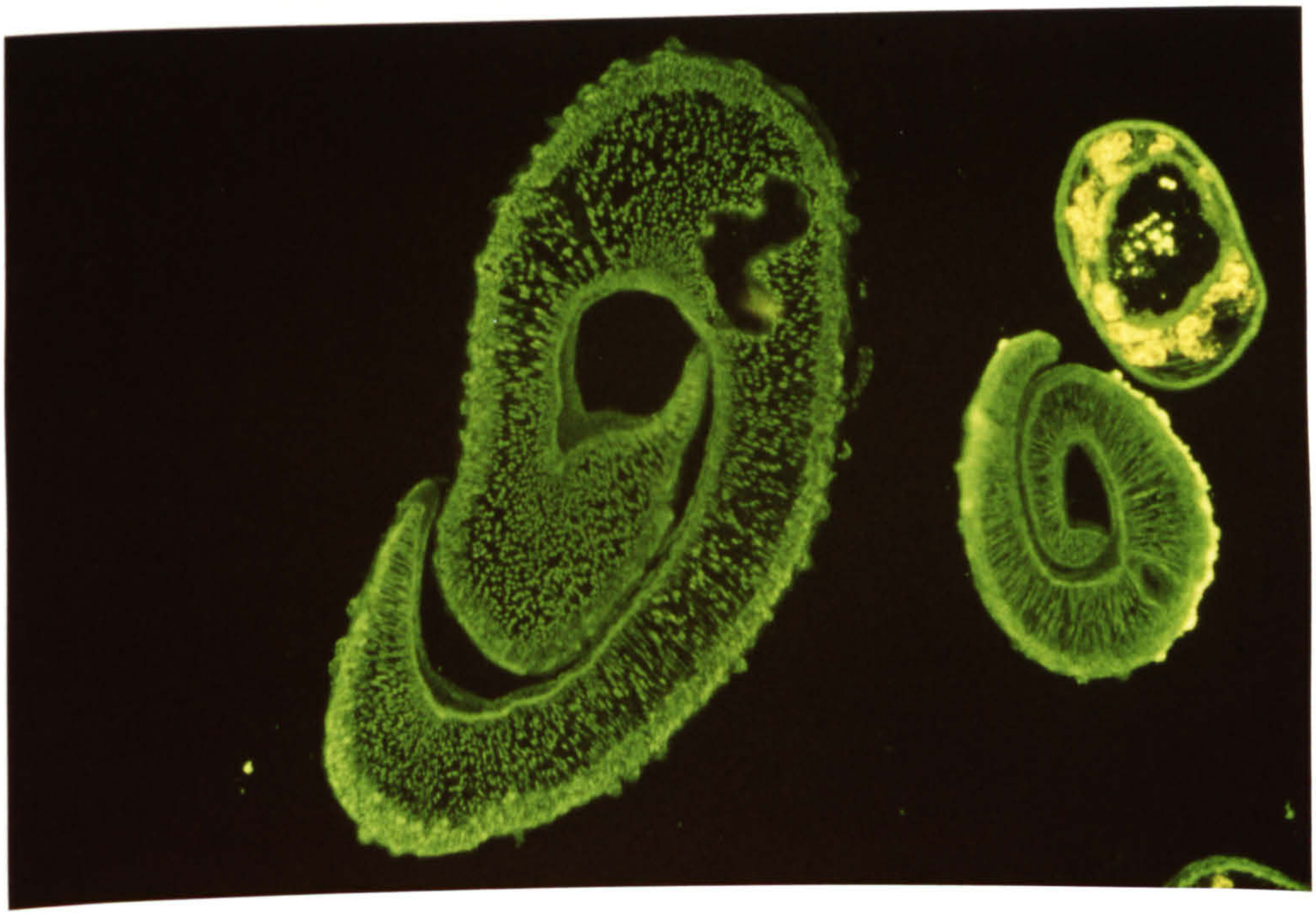

FIGURES 3.4 & 3.5

Higher magnification of Fig. 3.3 shows positive fluorescence in the individual muscle fibres (MF) in the subtegumental muscle of the body wall, and also in the parenchymal tissues (PT). x 520.

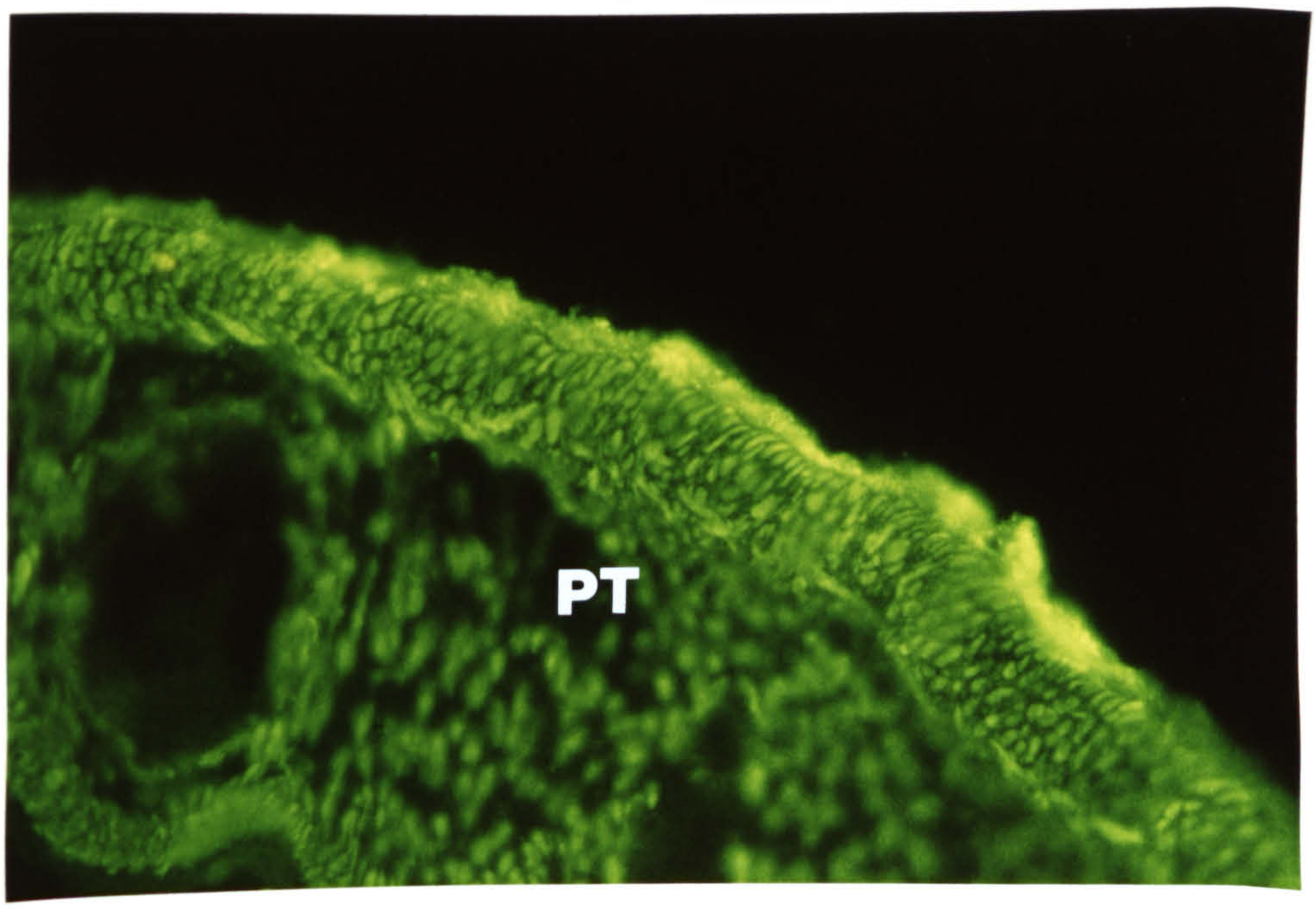
PT

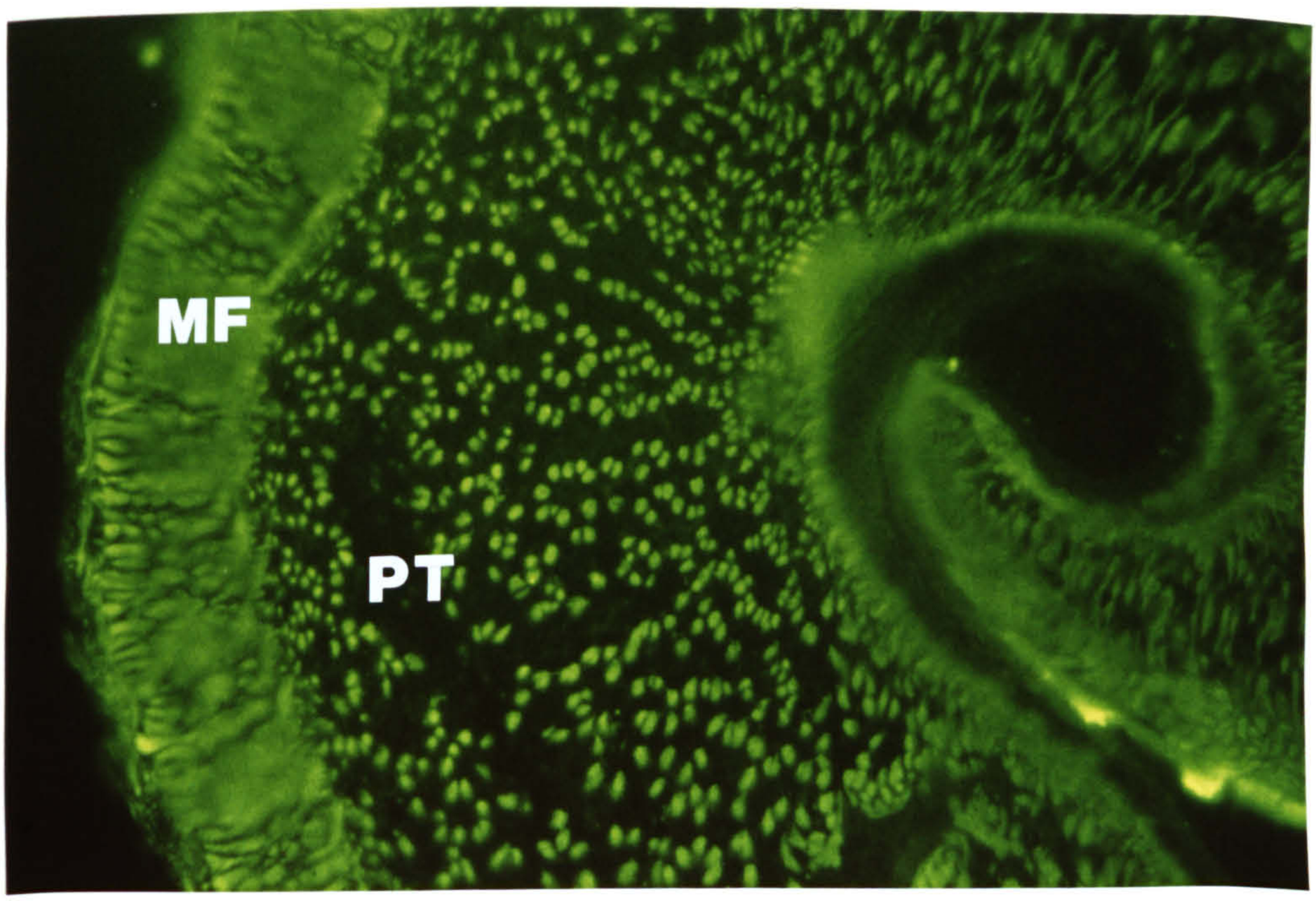
MF
PT

FIGURE 3.6

Acetone-fixed frozen section of adult male worm reacted with MAB M7.9 (1:60) followed by RAM/Ig/FITC (1:64). The antibody binds to the membrane of the myofibres; the muscle cytoplasm is unlabelled. x 520.

FIGURE 3.7

Similar treatment to that described in Fig.3.3. A section of female adult worm shows positive fluorescence in the body muscle. The female musculature is not as well developed as that of the male, the outer circular and the inner longitudinal layers are also thinner. Note the muscle cells surrounding the digestive tract which are clearly labelled. The vitelline cells in the parenchyma autofluoresce bright yellow. x 520.

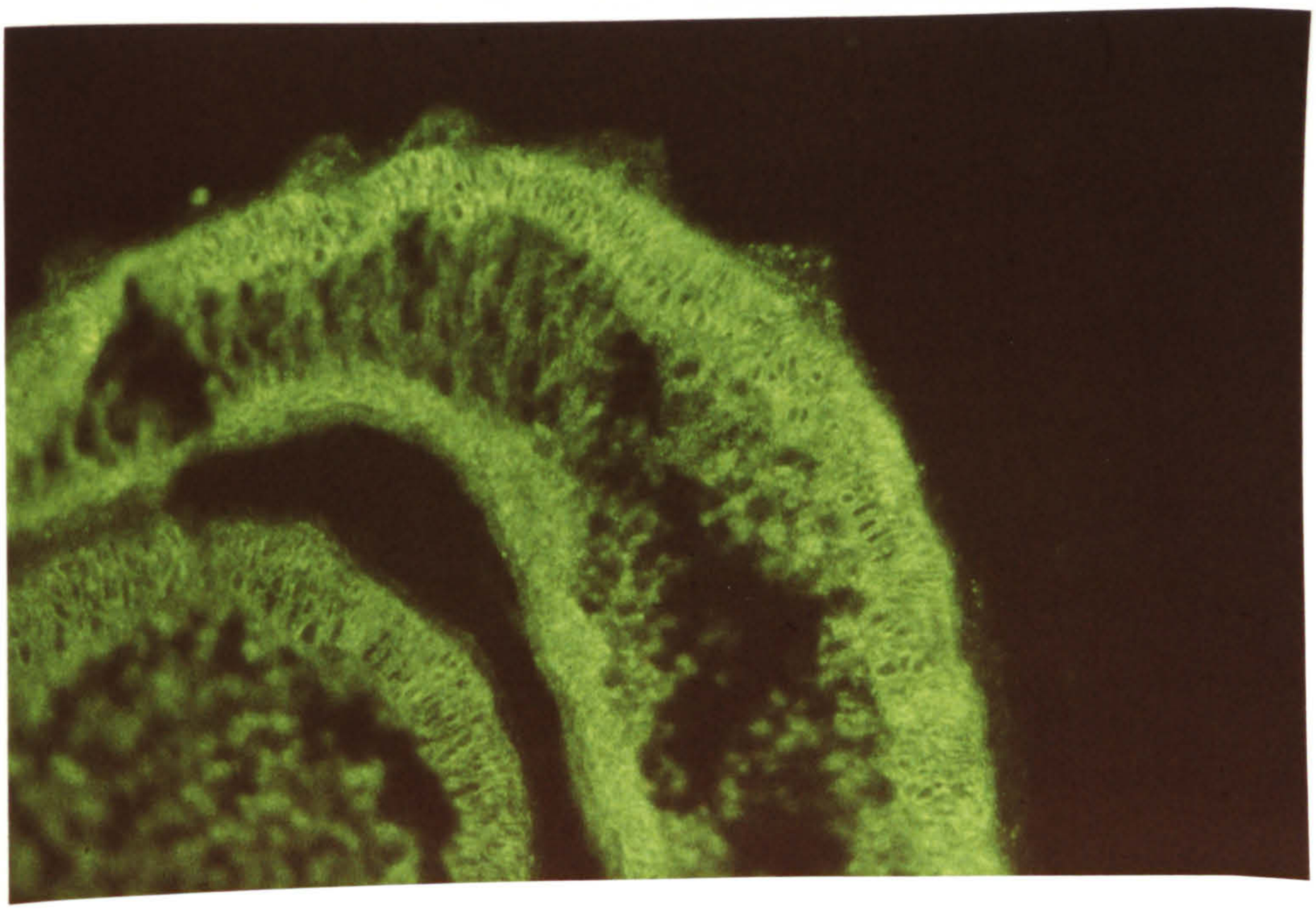

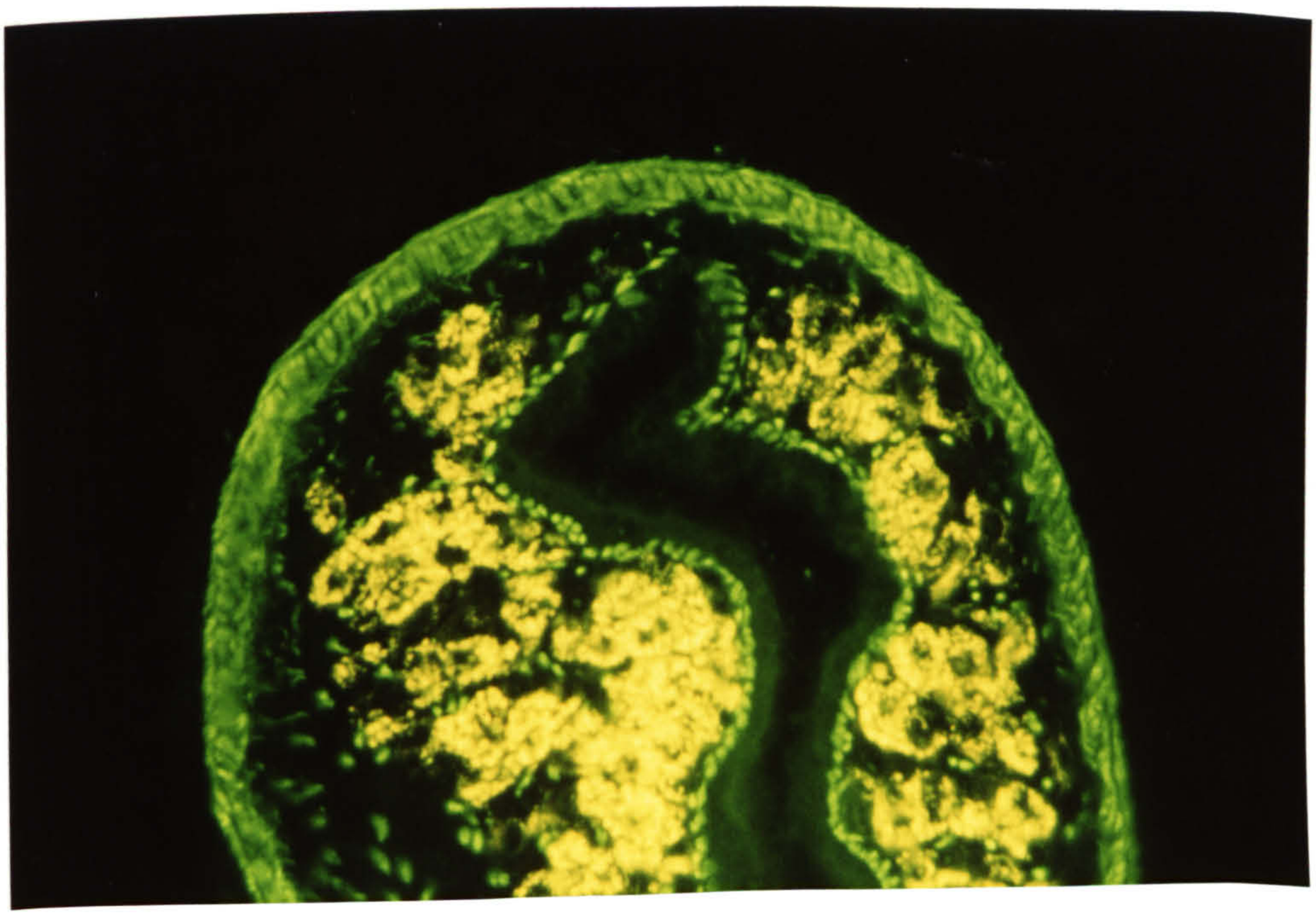

FIGURE 3.8

Acetone-fixed frozen section of adult male worm treated with MAB G5.2 (1:60) and subsequently labelled with RAM/Ig/FITC (1:64). Fluorescent label is seen in the muscle fibres of the body wall (M). The small muscle fibres which traverse the parenchymal tissue are also positive. The parenchymal nuclei (arrow) appear as distinct open circles. The junction between the muscle layers and parenchyma is strongly positive. The spines within the tegument are also fluorescently labelled. x 520.

FIGURE 3.9

Acetone-fixed frozen section of cercaria reacted with MAB G5.1 (1:60) and labelled with RAM/Ig/FITC (1:64). The subtegumental muscle layers (outer circular and subjacent longitudinal layers of muscle fibres) are fluorescently labelled. The conical and diagonal head capsule (H) musculature is also positive. The small discrete muscle cells of the parenchymal tissue are weakly labelled. x 520.

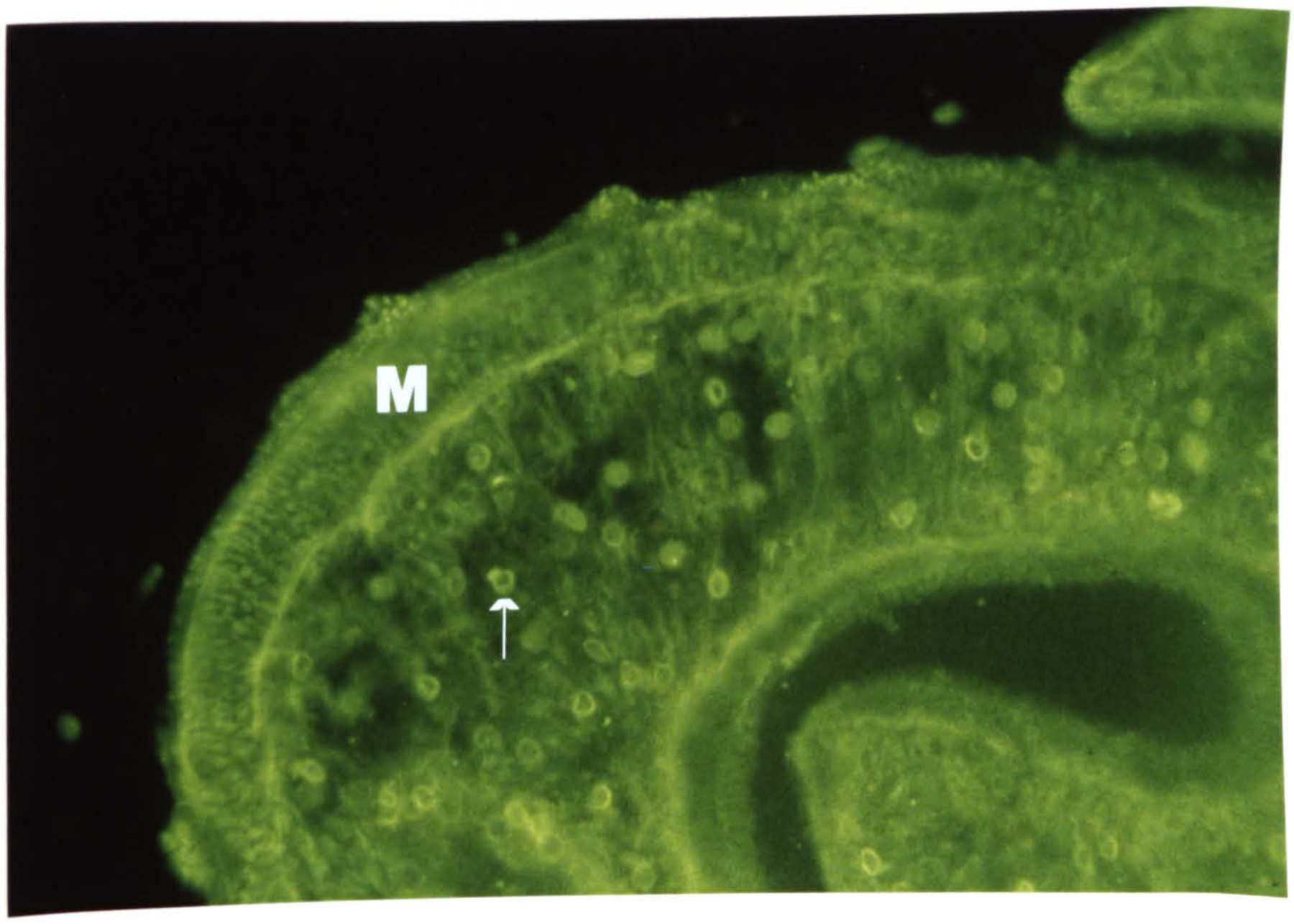
M

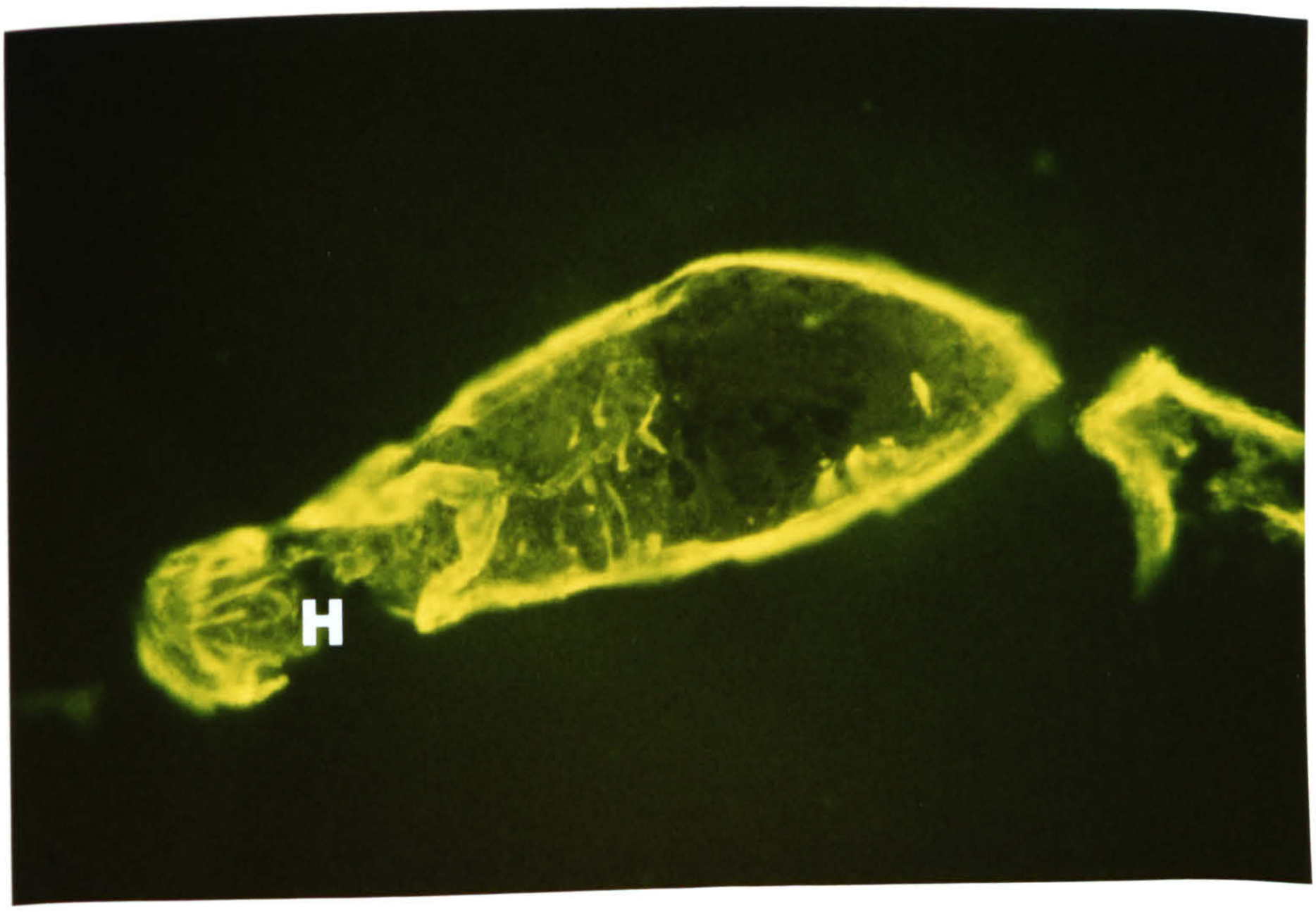
H

FIGURE 3.10

Similar treatment as described in Fig. 3.9 showing fluorescent label in the four lateral longitudinal muscle blocks in sections of tail (T). x 520.

FIGURE 3.11

Acetone-fixed frozen sections of cercariae reacted with MAB G5.12 (1:60) and RAM/Ig/FITC (1:64) showing specific fluorescence in the peripheral muscle of the body (B). In transverse sections of tail (T), the four lateral longitudinal muscle blocks are fluorescently labelled. Distinct striations can be observed in the longitudinal sections of tail. x 520.

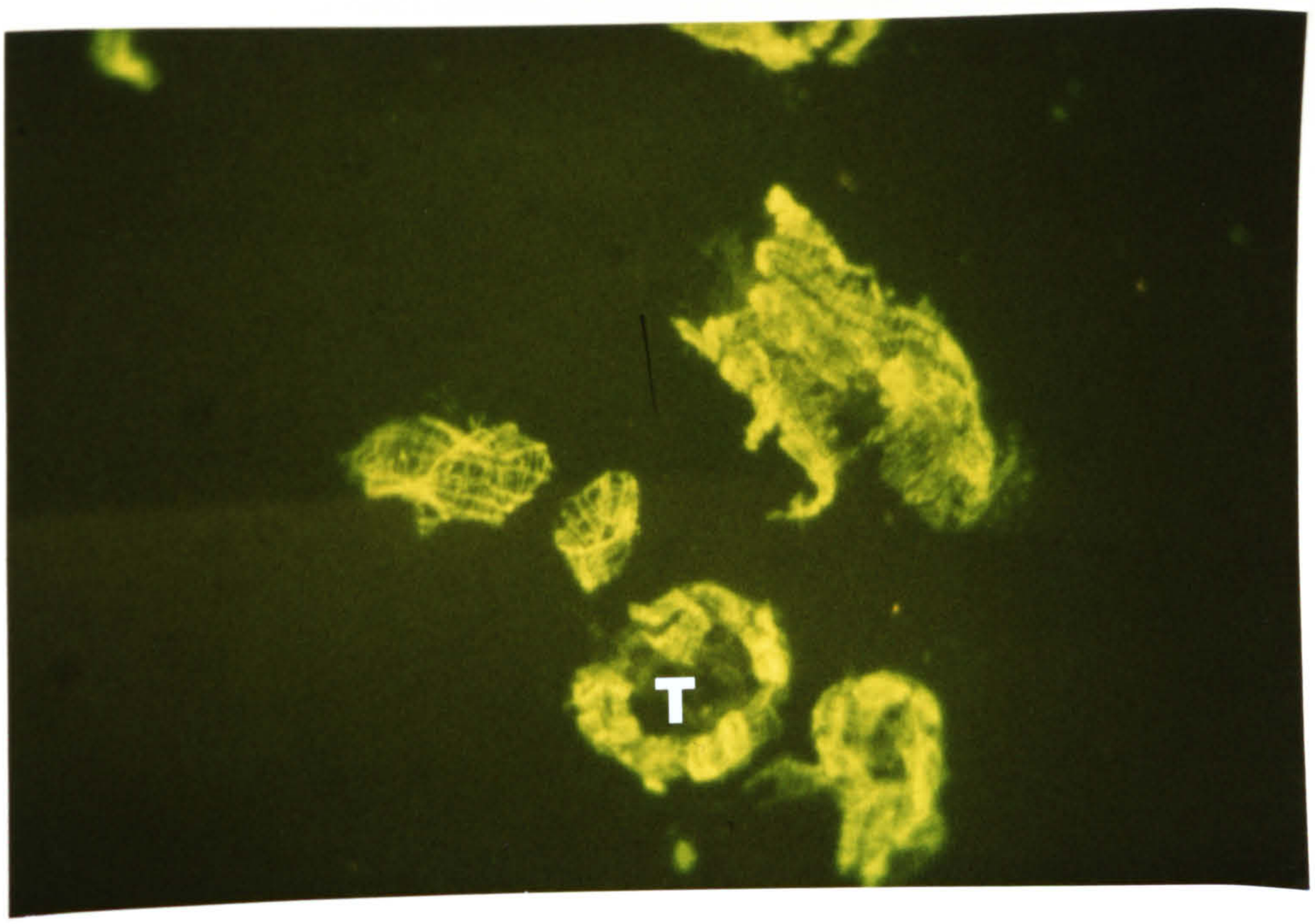
T

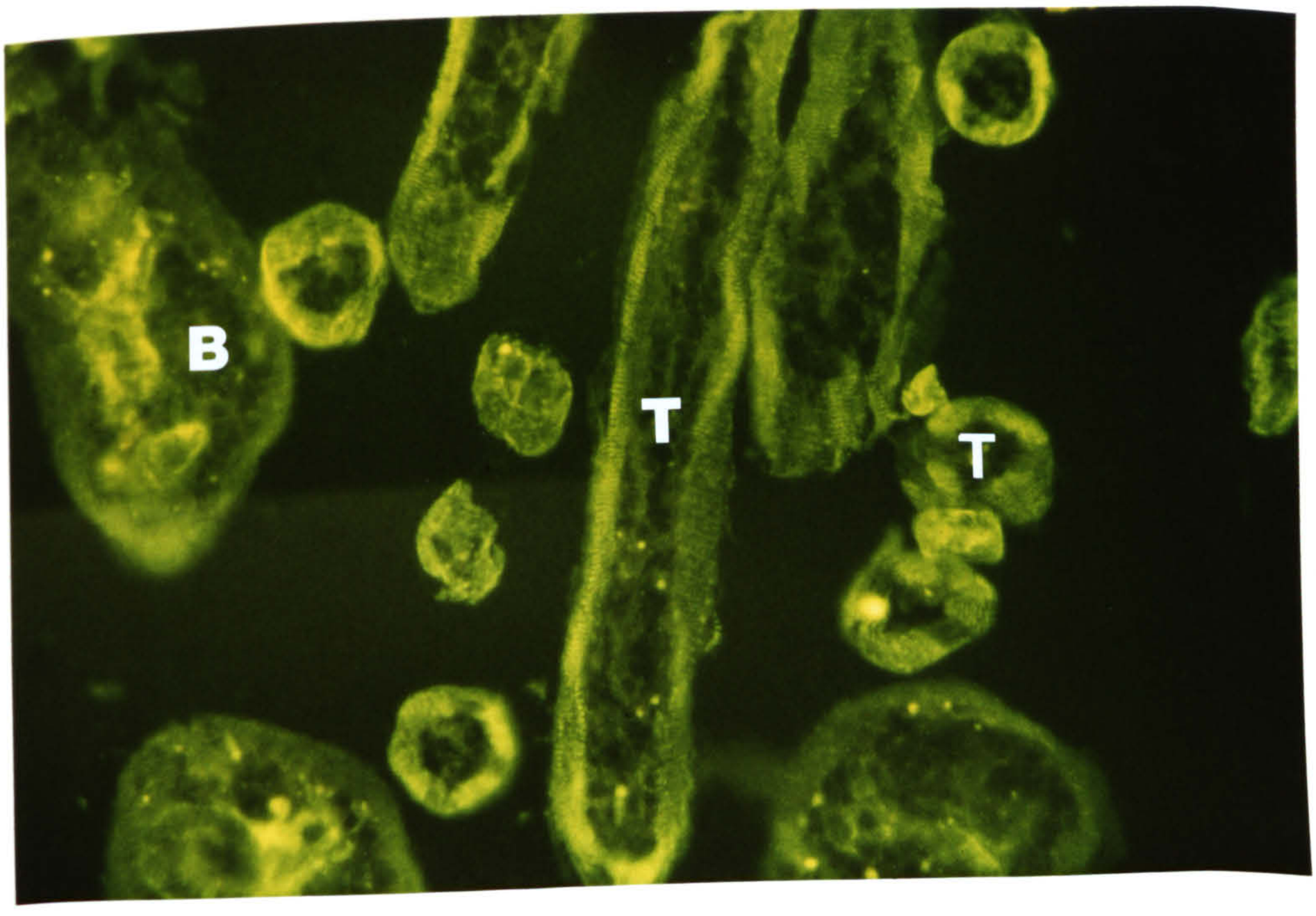
B
T
T

FIGURE 3.12

Acetone-fixed frozen sections of cercariae immunostained with MAB G3.8 (1:60) and RAM/Ig/FITC (1:64). The myofibres (arrow) of the body (B) wall are fluorescently labelled and appear as individual muscle blocks. The muscle in the head capsule (H) is also positive. x 520.

FIGURE 3.13

Acetone-fixed cryostat sections of cercariae were incubated in a 1:60 dilution of MAB M7.8 followed by RAM/Ig/FITC (1:64). Myofibres of the body (B) wall are fluorescently labelled and appear as a filamentous structure (arrow). The myofibres of the head capsule (H) are also brightly labelled. x 520.

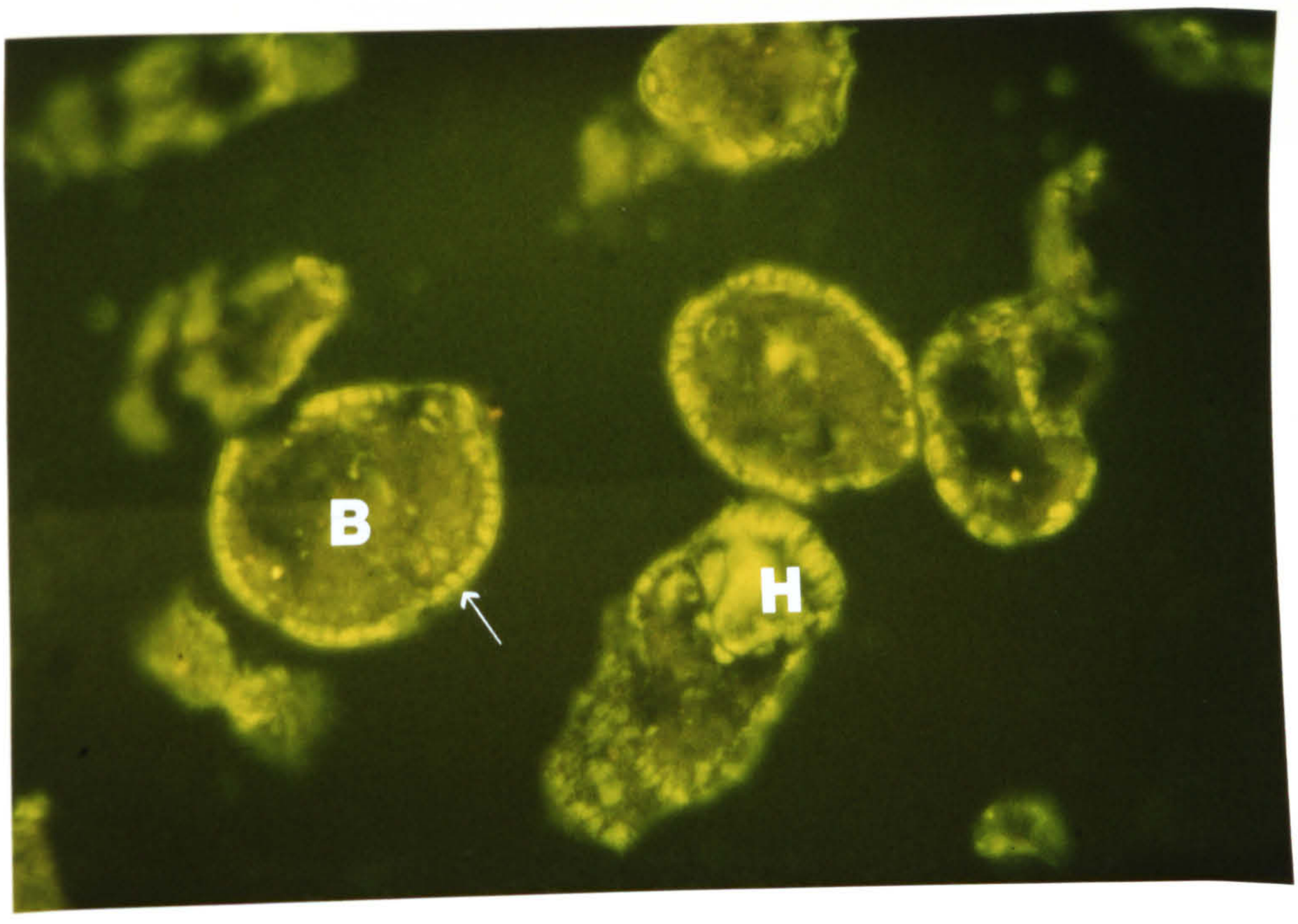
B
H

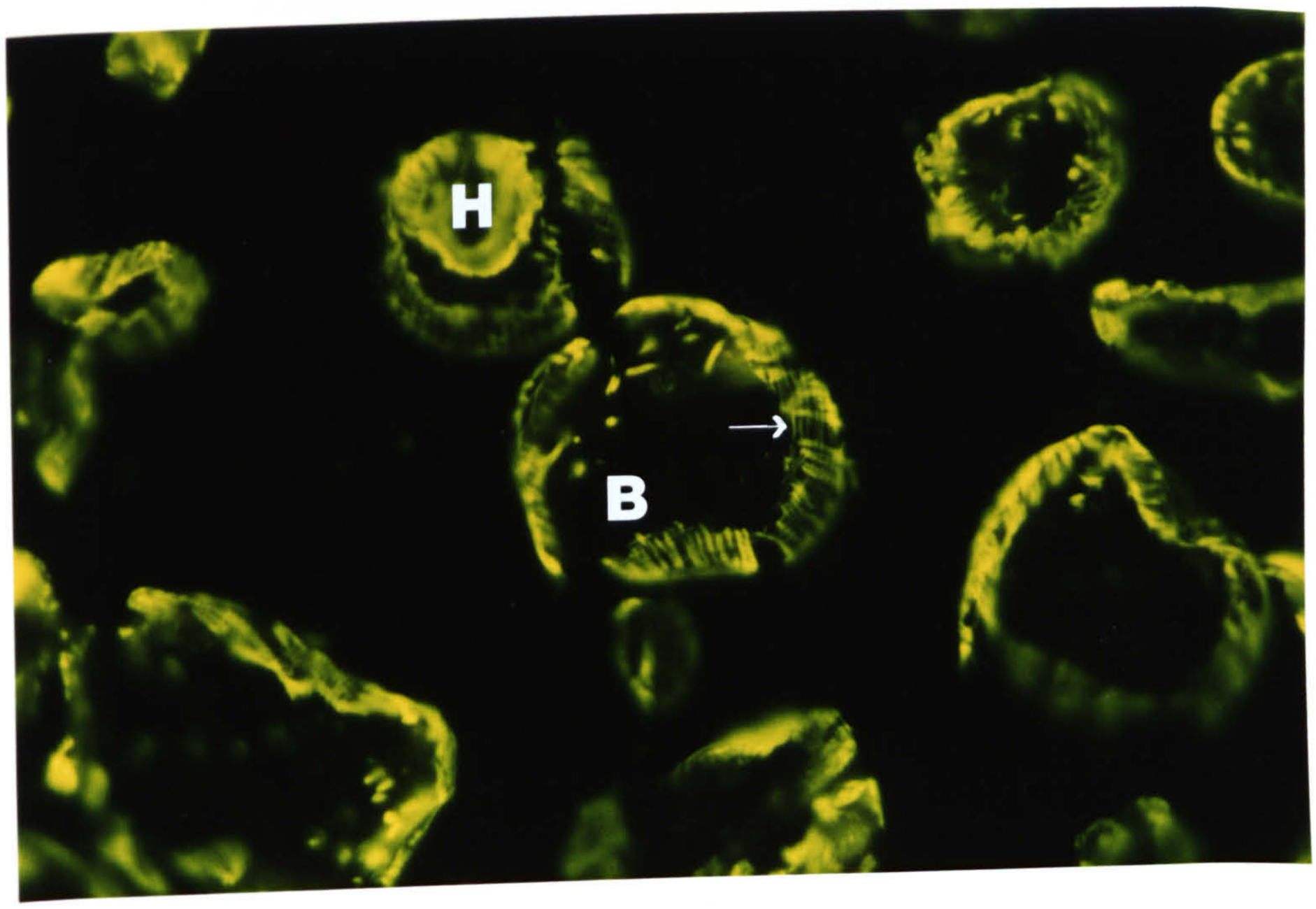
H
B

FIGURE 3.14

Sections of the cercarial tail (T) treated as described in Fig. 3.13 show specific fluorescence in the muscle cells (the muscle fibres present along the entire length of the cercarial tail are arranged in outer circular and inner longitudinal layers as in the body). Note the longitudinal, cross-striated muscle. x 520.

FIGURE 3.15

Acetone-fixed frozen sections of cercariae reacted with MAB M7.9 (1:60) and RAM/Ig/FITC (1:64). Peripheral muscle of the body (B) appears as fine dots. The small discrete muscle cells of the parenchymal network are fluorescently labelled. In transverse sections of the cercarial tail (T) the four lateral longitudinal muscle blocks are brightly fluorescent. x 520.

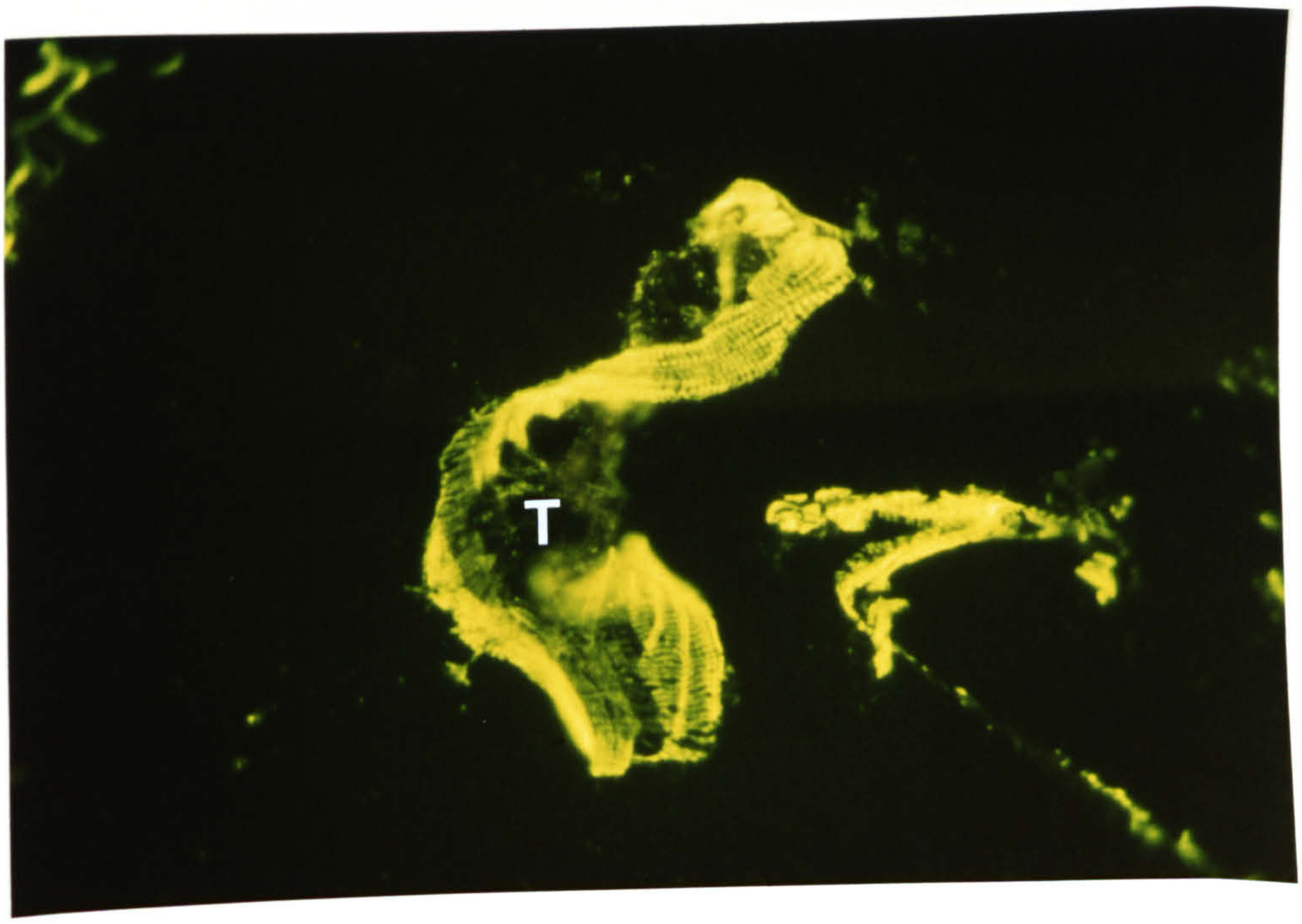
T

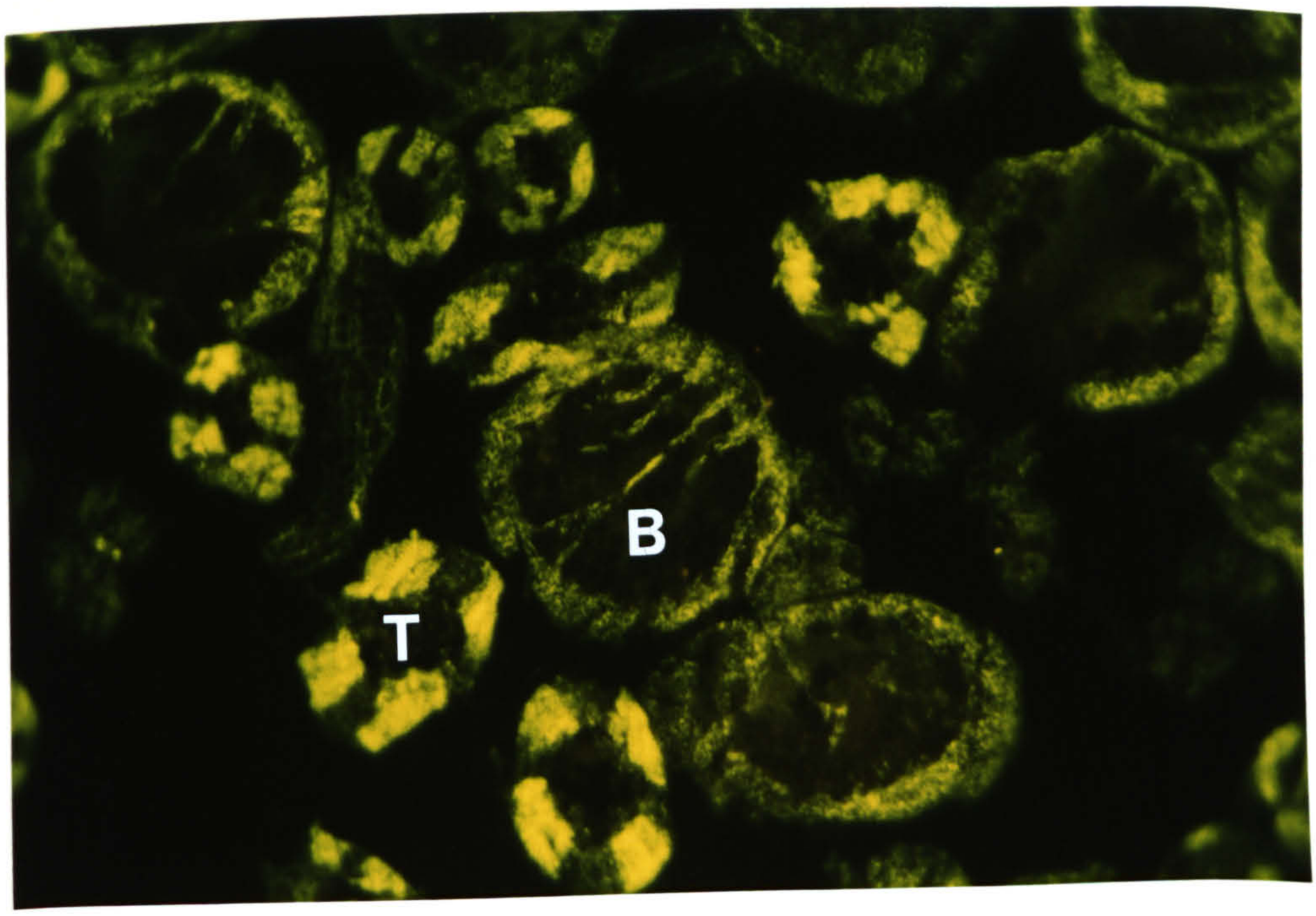
B
T

FIGURE 3.16

Acetone-fixed frozen sections of 3h schistosomula were incubated with MAB G5.7 (1:60) and RAM/Ig/FITC (1:64). The muscle cells at the periphery and in the internal tissues are brightly fluorescent (longitudinal section). x 520.

FIGURE 3.17

Transverse sections of 3h schistosomula were treated as described in Fig. 3.16. MAB G5.1 bound to individual muscle fibres of the parasite. Especially at the periphery of the body the muscle cells appear as a thick band. x 520.

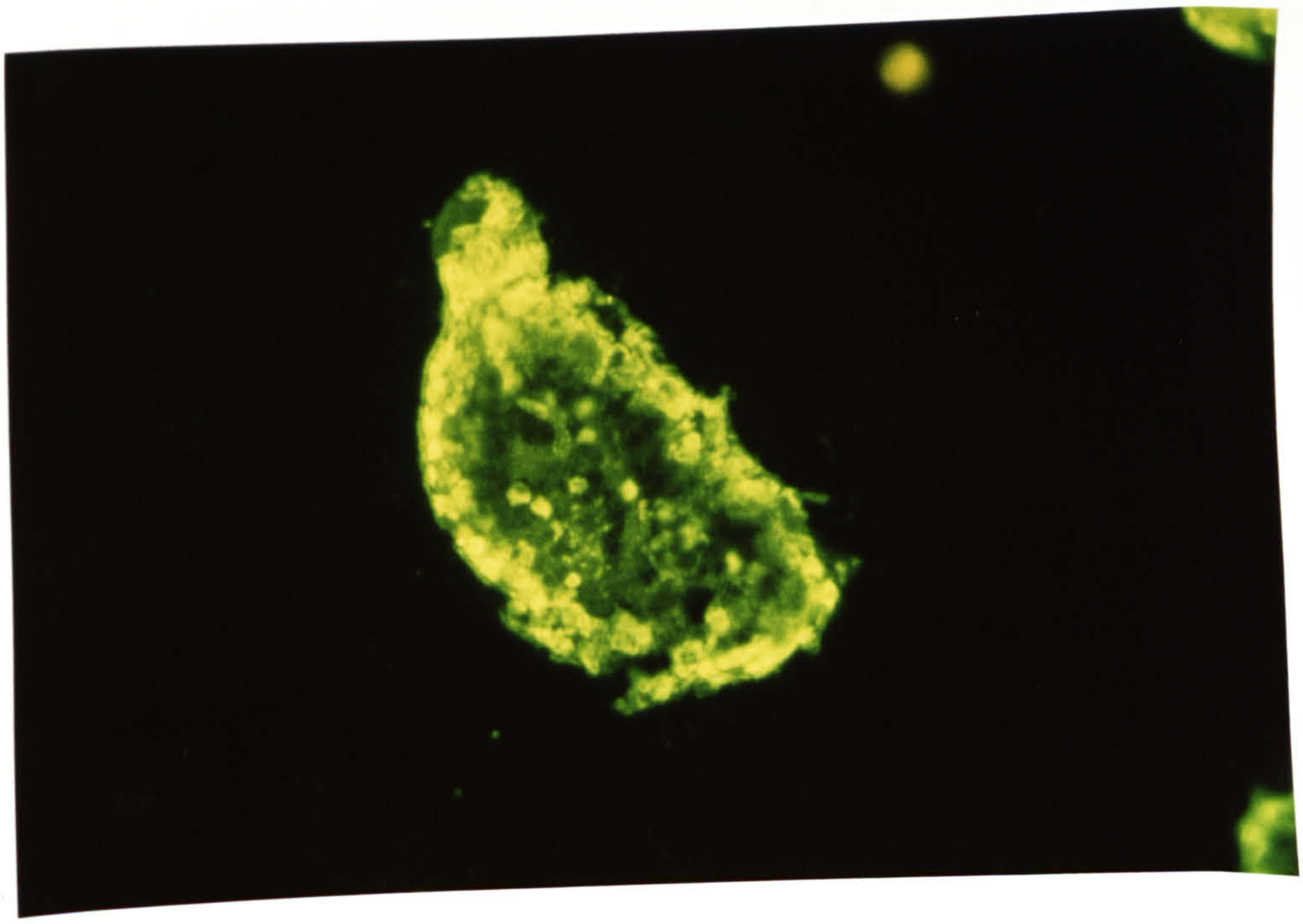

FIGURE 3.18

Transverse sections of 3h schistosomula as described in Fig. 3.16 showing positive fluorescence in the muscle sheath around the digestive tract (*) of the parasite and the muscle layers at the periphery. x 520.

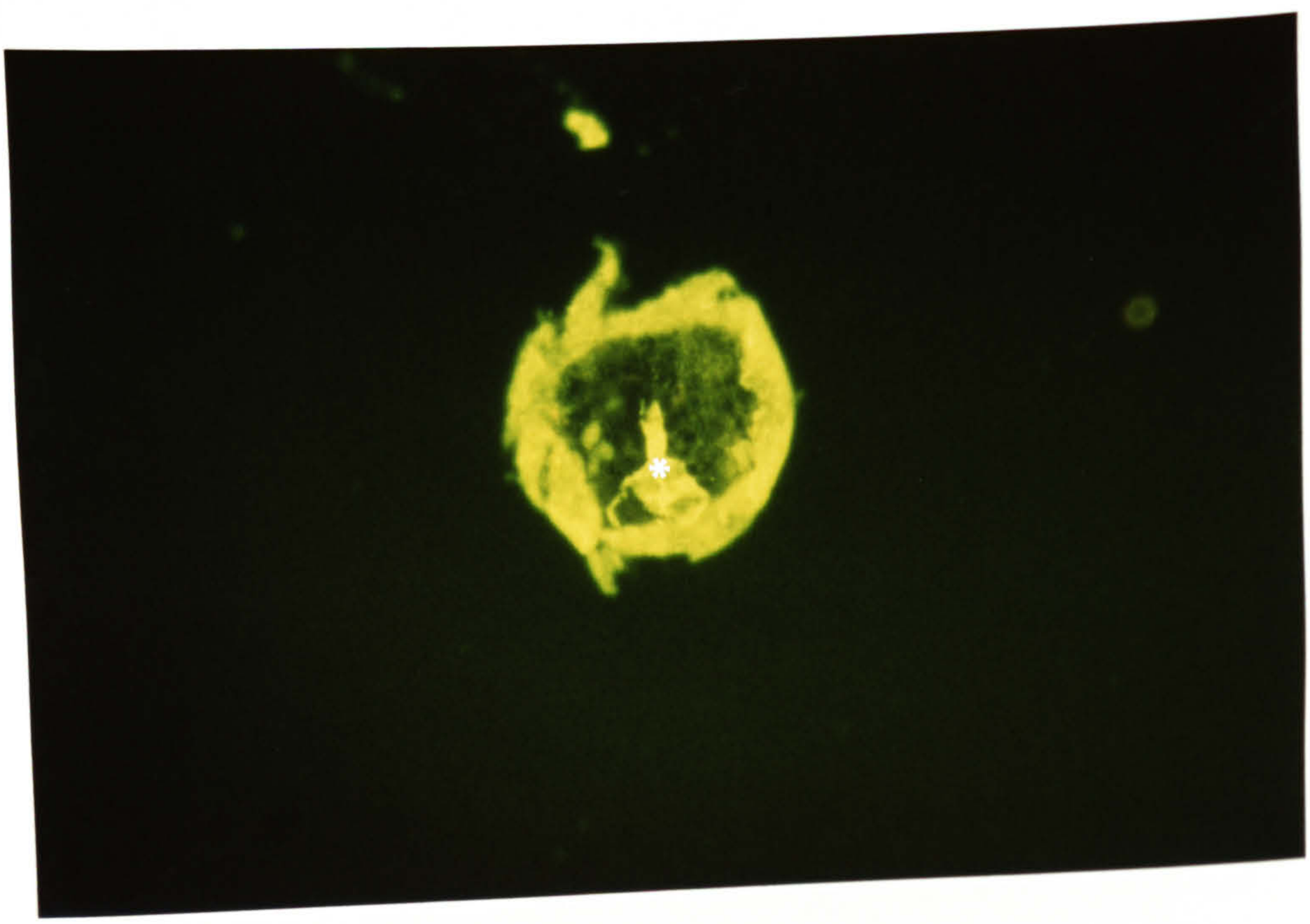

FIGURE 3.19

Acetone-fixed frozen sections of 3h schistosomula stained with MAB M7.8 (1:60) and RAM/Ig/FITC (1:64). Myofibres in the body (B) and the head capsule (H) are fluorescent. x 520.

FIGURE 3.20

Acetone-fixed frozen sections of 3h schistosomula were incubated with MAB M7.9 (1:60) and RAM/Ig/FITC (1:64). Myofibres of the parasite are positive and have a dotted and filamentous appearance. x 520.

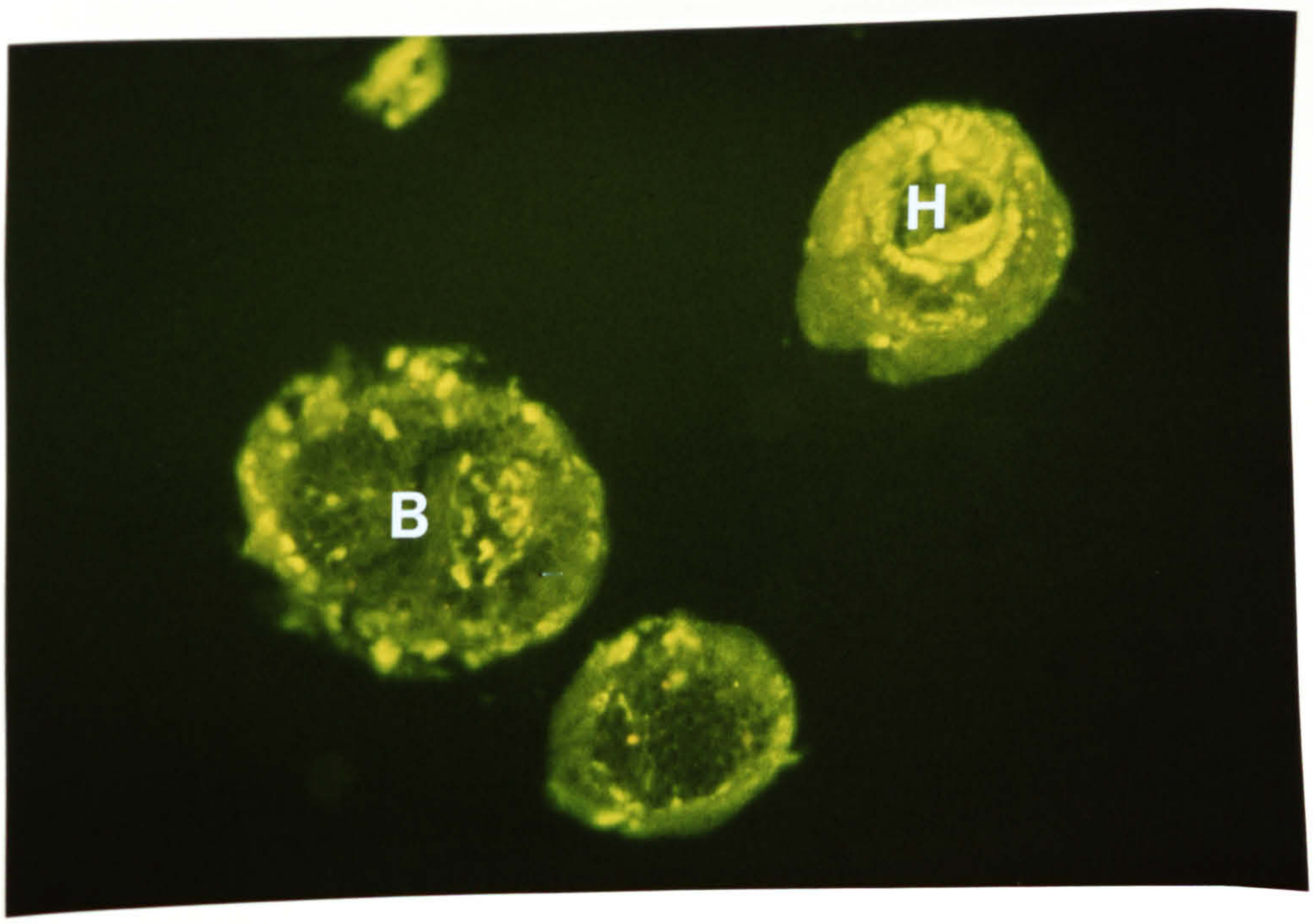
H
B

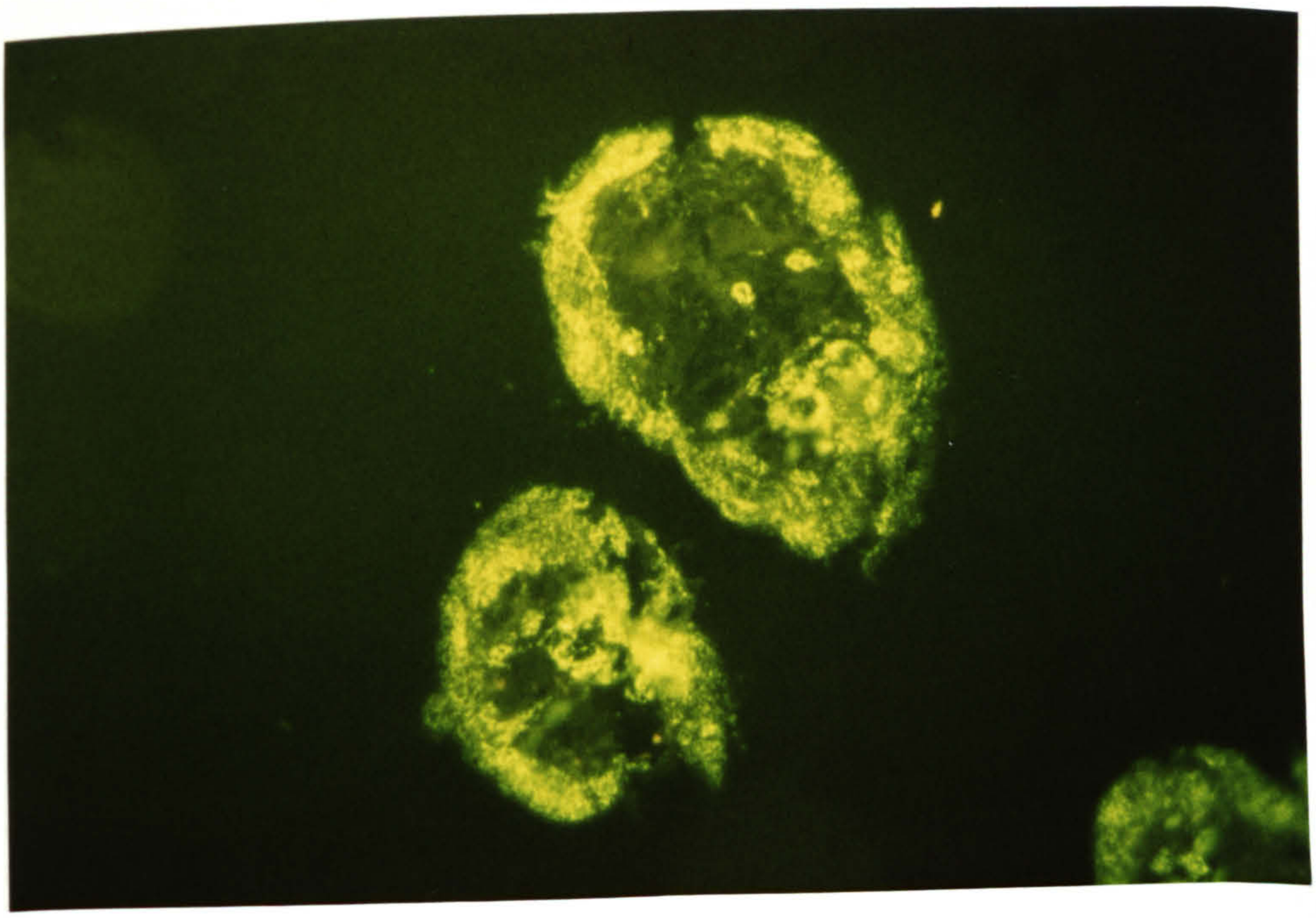

FIGURE 3.21

Fibrillar flight muscle of blowfly (Calliphora erythrocephala) reacted with MAB G5.7 (1:40) followed by RAM/Ig/FITC (1:60). The protein in the myofibril is fluorescently labelled giving a cross-striated pattern (arrow). x 520.

FIGURE 3.22

Fibrillar flight muscle of blowfly (Calliphora erythrocephala) reacted with MAB M7.9 (1:40) followed by RAM/Ig/FITC (1:60). The protein in the myofibril is fluorescently labelled giving a cross-striated pattern (arrow). The distance between bands is wider than those shown in Fig. 3.21. x 520.

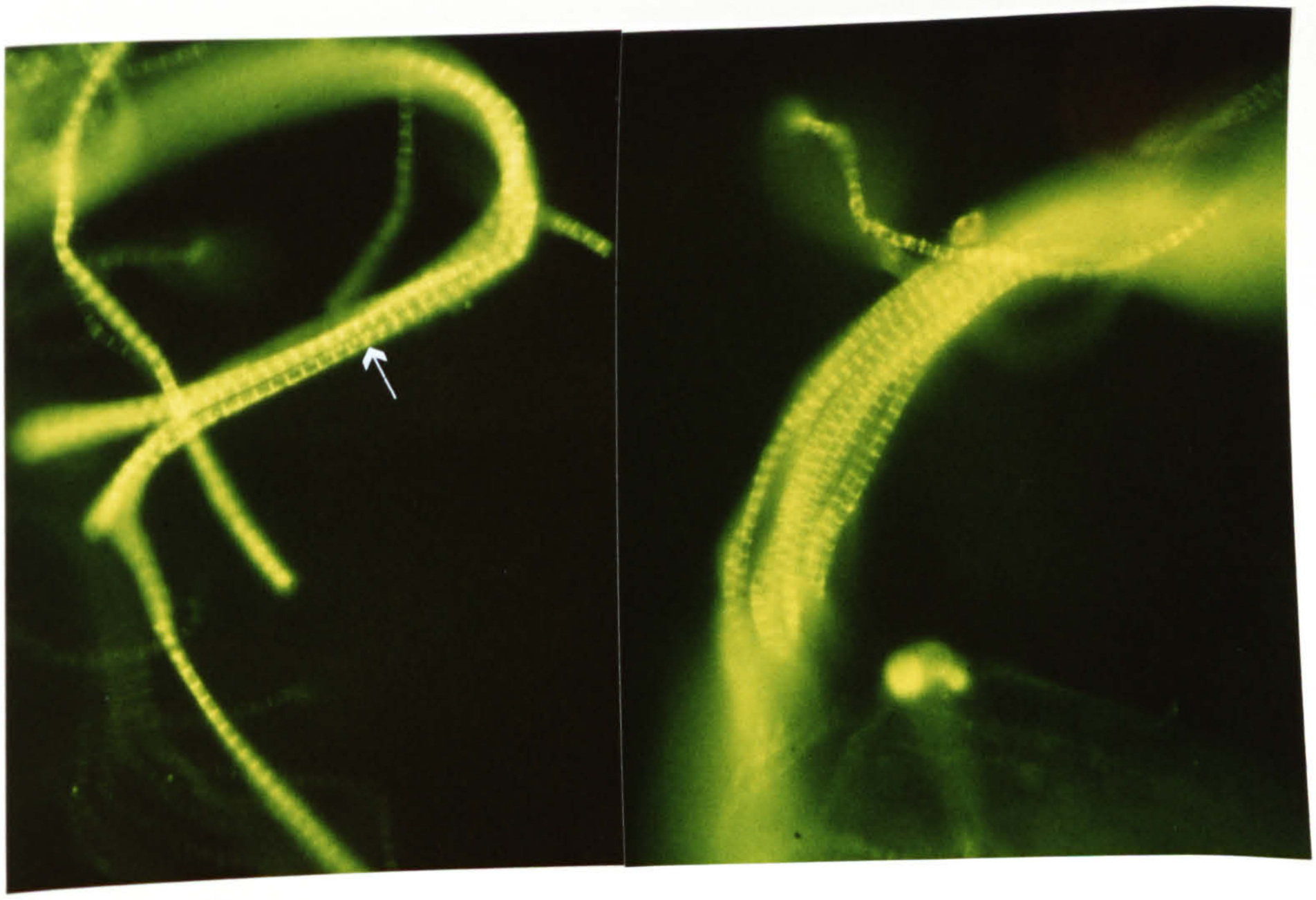

FIGURE 3.23

Acetone-fixed frozen section of dorso-longitudinal flight muscle of Bumble bee (Bombus terrestris) reacted with MAB G5.7 (1:40) and labelled with RAM/Ig/FITC (1:64). Specific fluorescence was seen in the myofibrils which were striated. x 520.

FIGURE 3.24

Acetone-fixed frozen section of dorso-longitudinal flight muscle of Bumble bee reacted with MAB G3.5 (1:40) and labelled with RAM/Ig/FITC (1:64). Membranes of the myofibres (MF) are fluorescently labelled. A pattern of cross-striation is not observed. The peripheral regions of each fibre are usually divided into sectors by deep longitudinally running clefts (arrow) formed by the invagination of the sarcolemma (as described by Smith, 1965; Ashhurst, 1967; Smith & Sacktor, 1970). x 520.

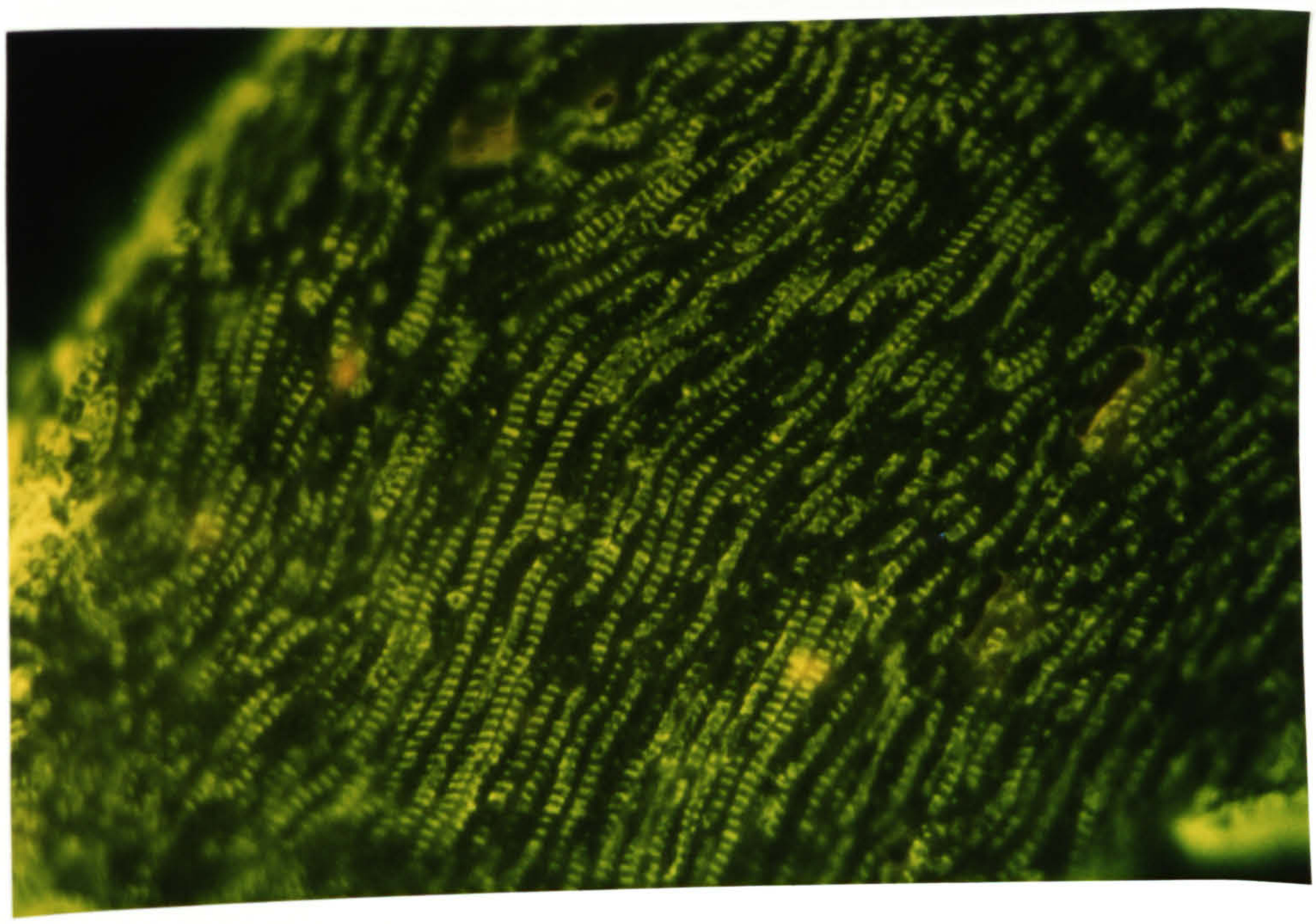

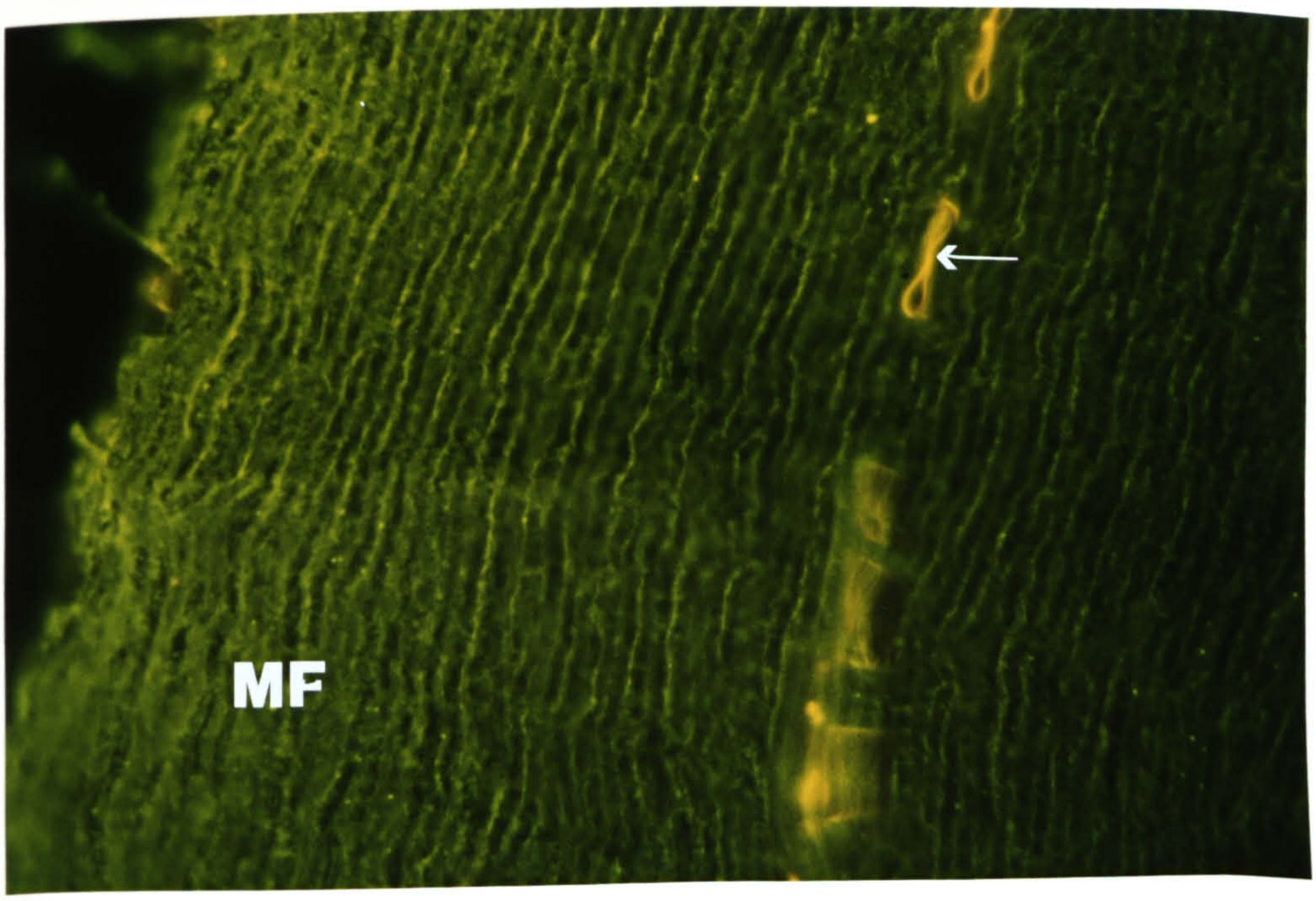
MF

FIGURE 3.25

Acetone-fixed frozen section of rabbit utorus reacted with MAB G5.1 (1:60) and RAM/Ig/FITC (1:64) showing specific fluorescence in the smooth muscle fibres (MF). x 520.

FIGURE 3.26

Acetone-fixed frozen section of rabbit uterus reacted with MAB G5.12 (1:60) and RAM/Ig/FITC (1:64) showing strong specific fluorescence in the epithelium of the uterine gland duct (GD). The myofibres (MF) are also weakly stained. x 520.

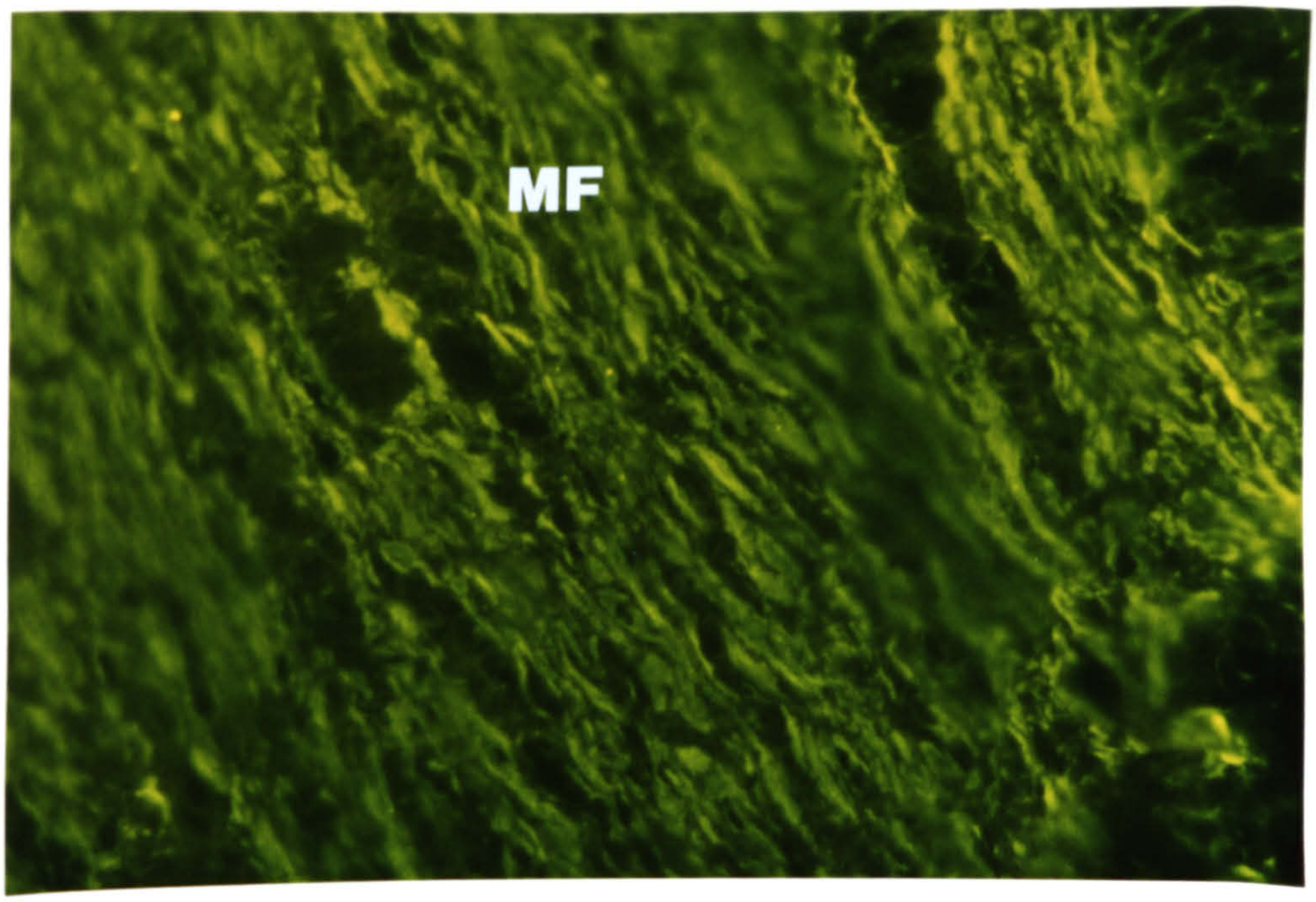
MF

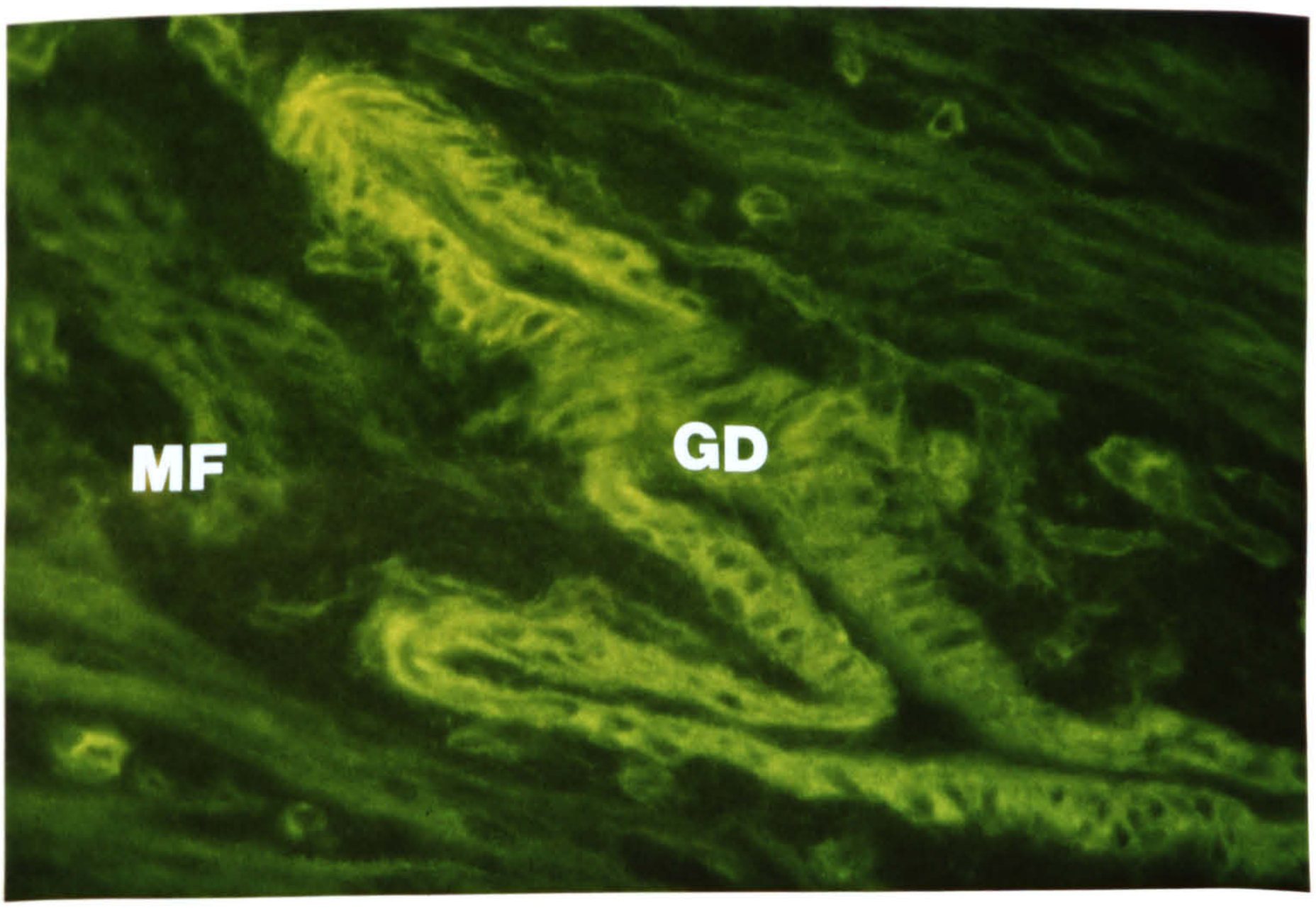
MF
GD

FIGURES 3.27 & 3.28

PF-fixed frozen sections of cercariae immunostained with MAB G3.3 (1:60) and RAM/Ig/FITC (1:64). The tegument (arrow) appears as a very thin line covering the cercarial body and the tail (T). Internal tissues (I) are also positive. x 520.

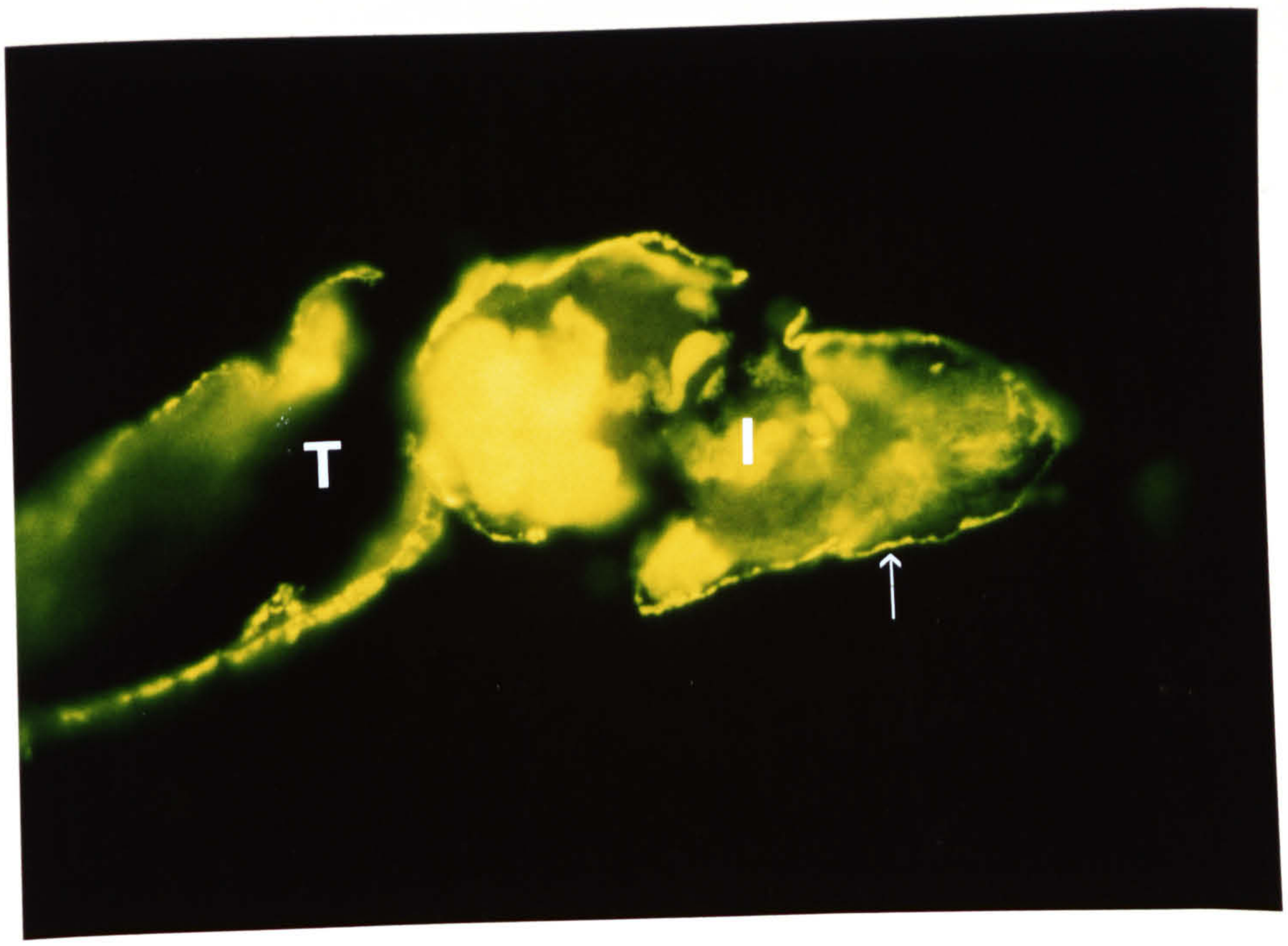
T
I

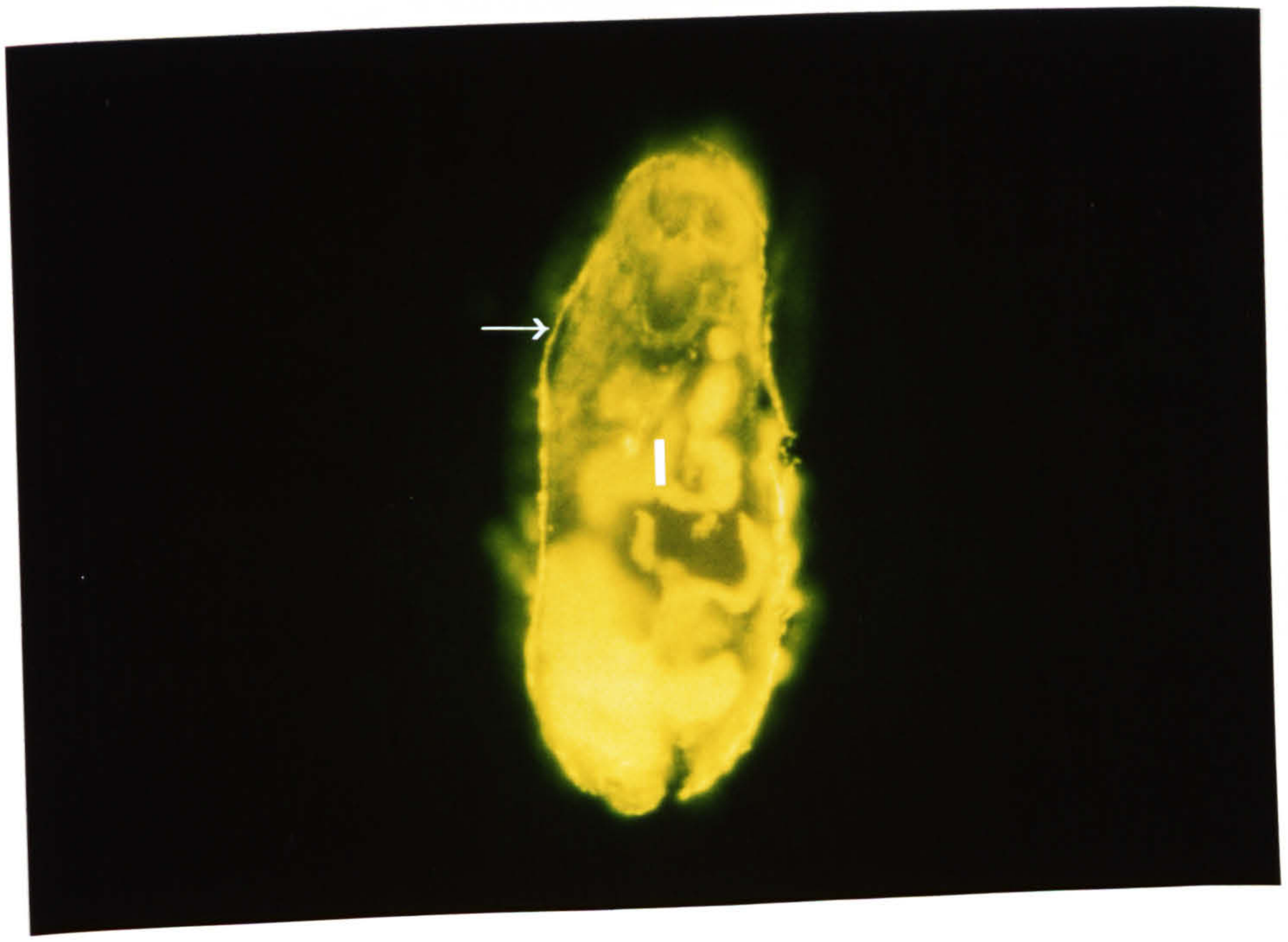
I

CHAPTER 4

LOCALISATION OF SCHISTOSOME ANTIGENS AT THE ULTRASTRUCTURAL LEVEL

FIGURE 4.1

Cryosection of adult male S. mansoni fixed in 4% PF, 3.5 h, at room temperature. The tegument is invaginated to form surface pits (sp), circular muscle fibres (CM) and longitudinal muscle fibres (LM) occur beneath the basal membrane. Parenchymal cells (PT) are seen underneath the muscle layers. x 3,600.

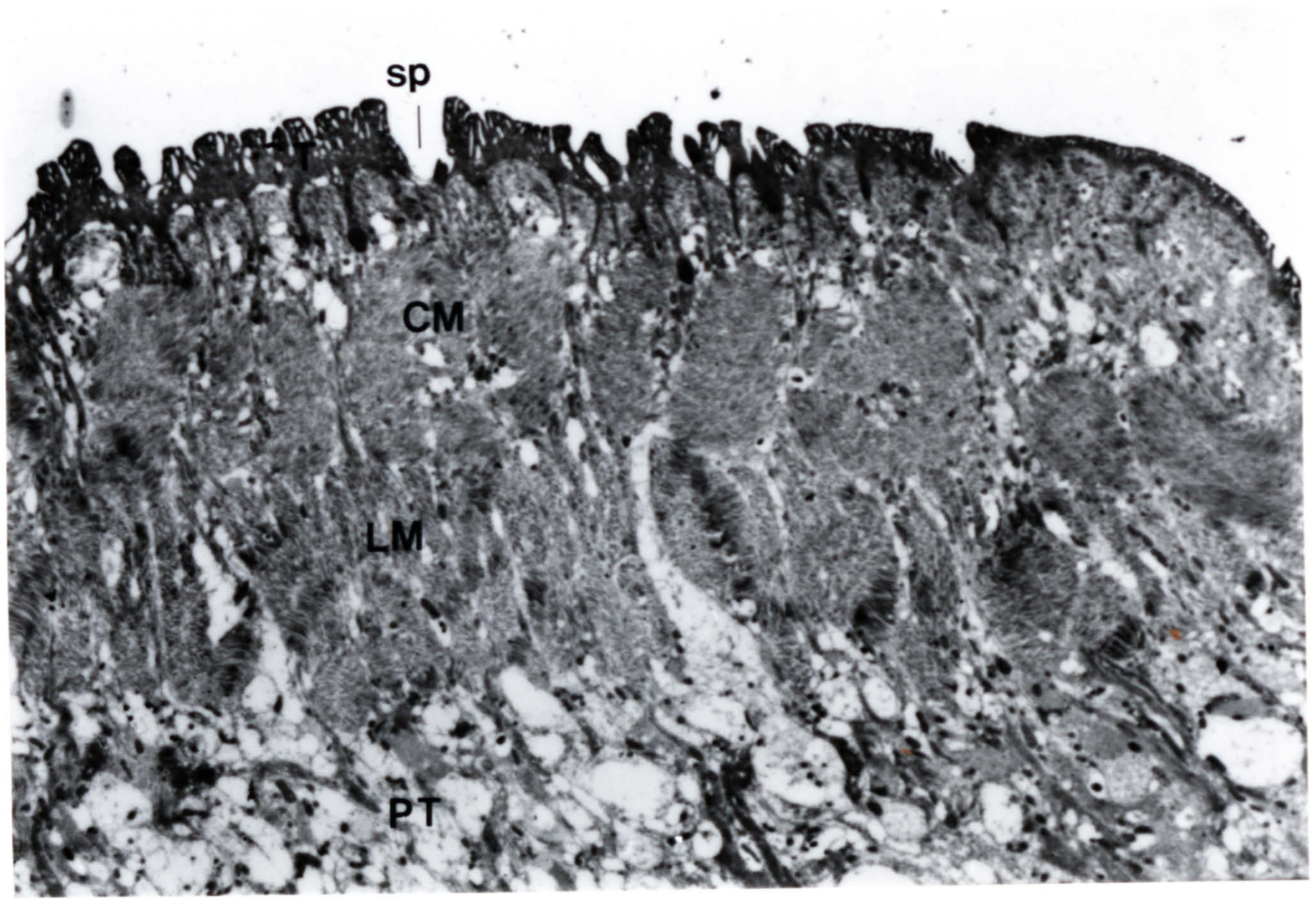
sp
CM
LM
PT

FIGURE 4.2

A similar electron micrograph to that shown in Fig. 4.1, at higher magnification. The section is rather thick, the tegument (TM) is darkly stained, the myofilaments (MF) of the subtegumental musculature are clearly seen as dense bands. The spaces within the basal invaginations have expanded to form large extracellular vacuoles (V). Numerous mitochondria (MT) of parenchymal cells are identifiable. x 6,000.

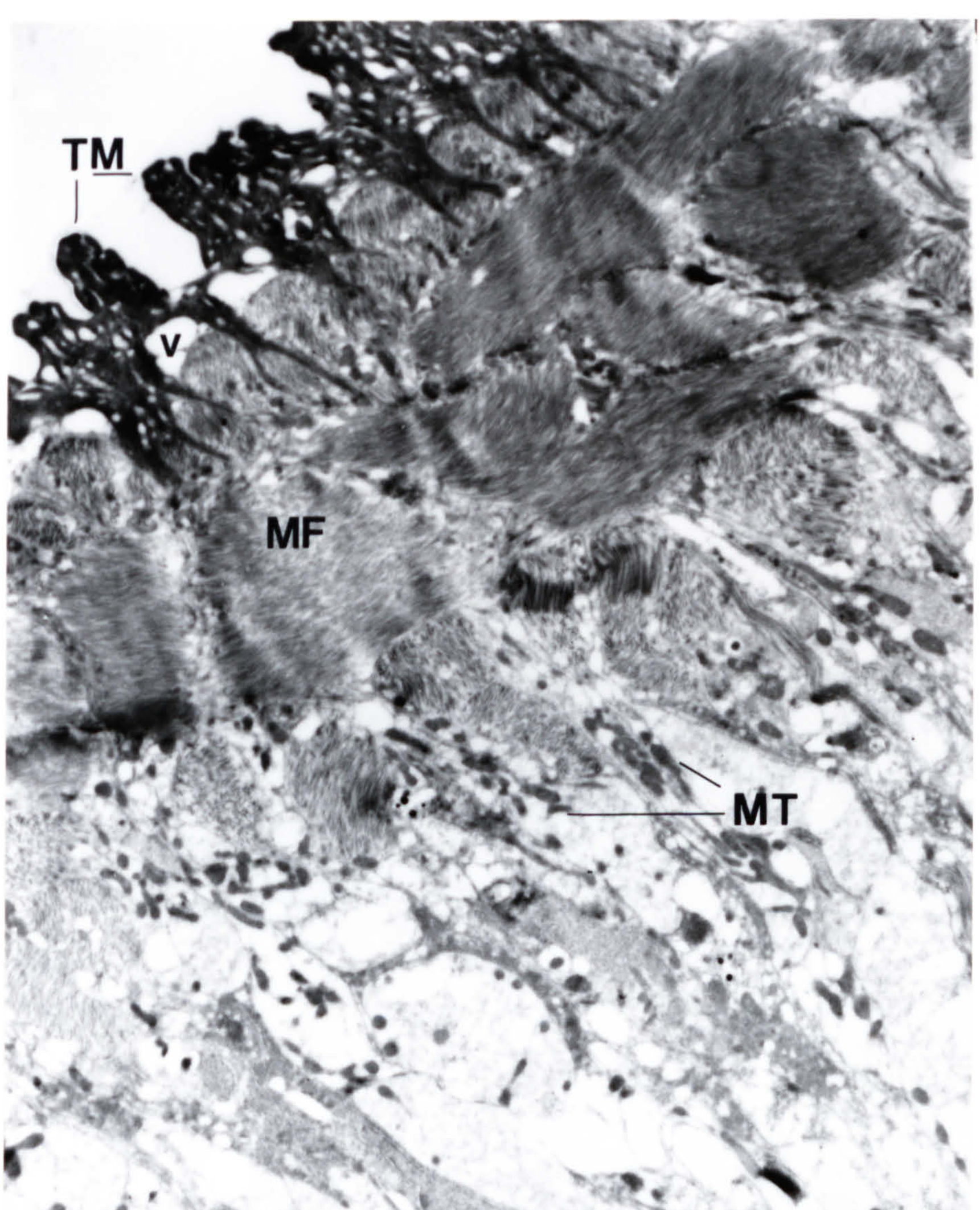
TM
V
MF
MT

FIGURE 4.3

Tegument cell bodies are situated beneath the muscle fibres (MF); they contain a nucleus (N), rough endoplasmic reticulum, Golgi bodies and inclusion bodies (not shown). The subtegumental cells are joined to the tegument by cytoplasmic connections (C). Due to its nature, the continuity between the cells and the tegument is difficult to see in sections. x 4,700.

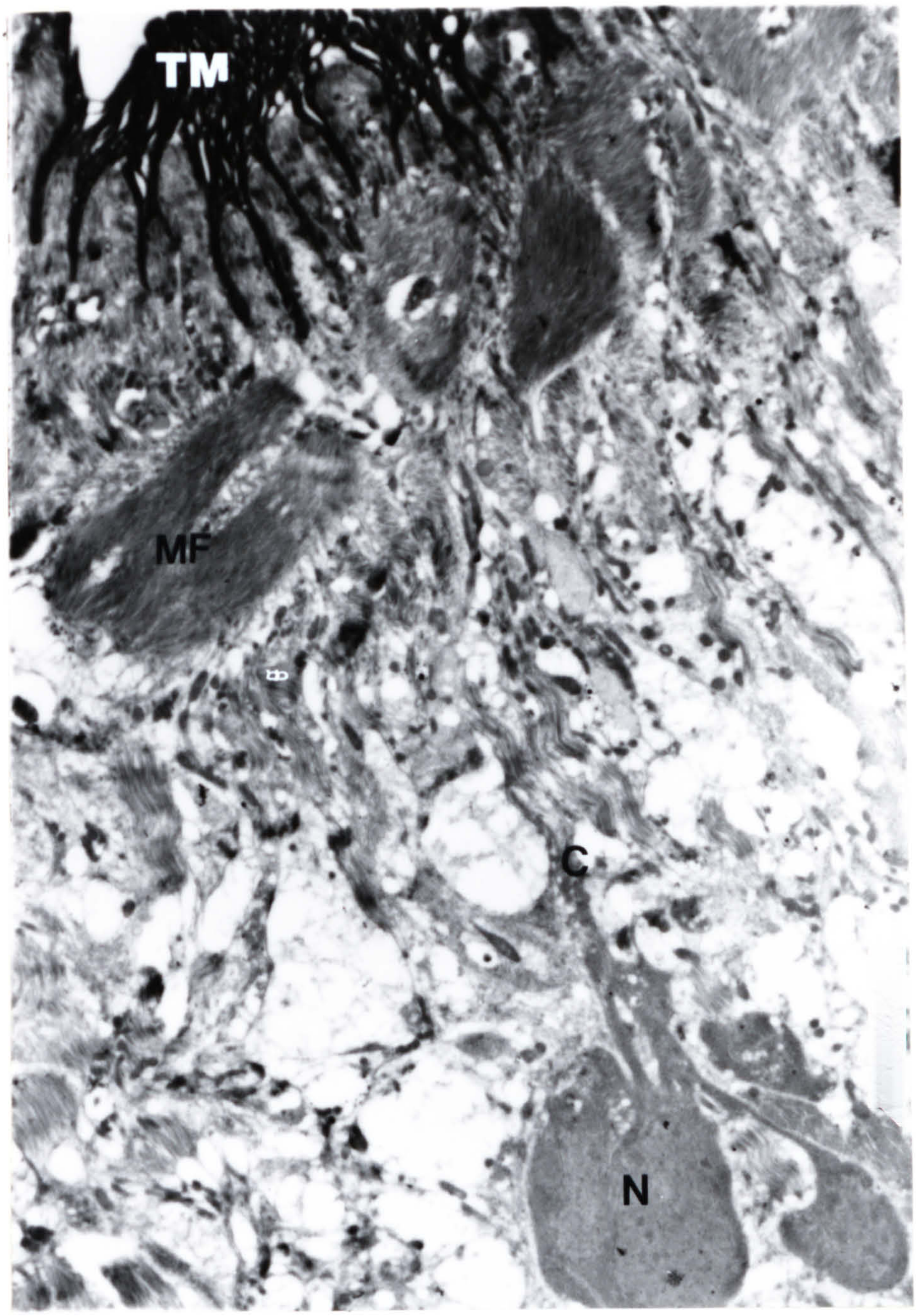
TM
MF
B
C
N

FIGURE 4.4

High magnification of tegument cell body showing a narrow rim of electron-dense perinuclear cytoplasm (*) and irregular nucleus (N) with distributed chromatin. Muscle fibres (MF) and nerve cells with electron-dense droplets (arrow) are also seen in the parenchyma (PT). x 12,100.

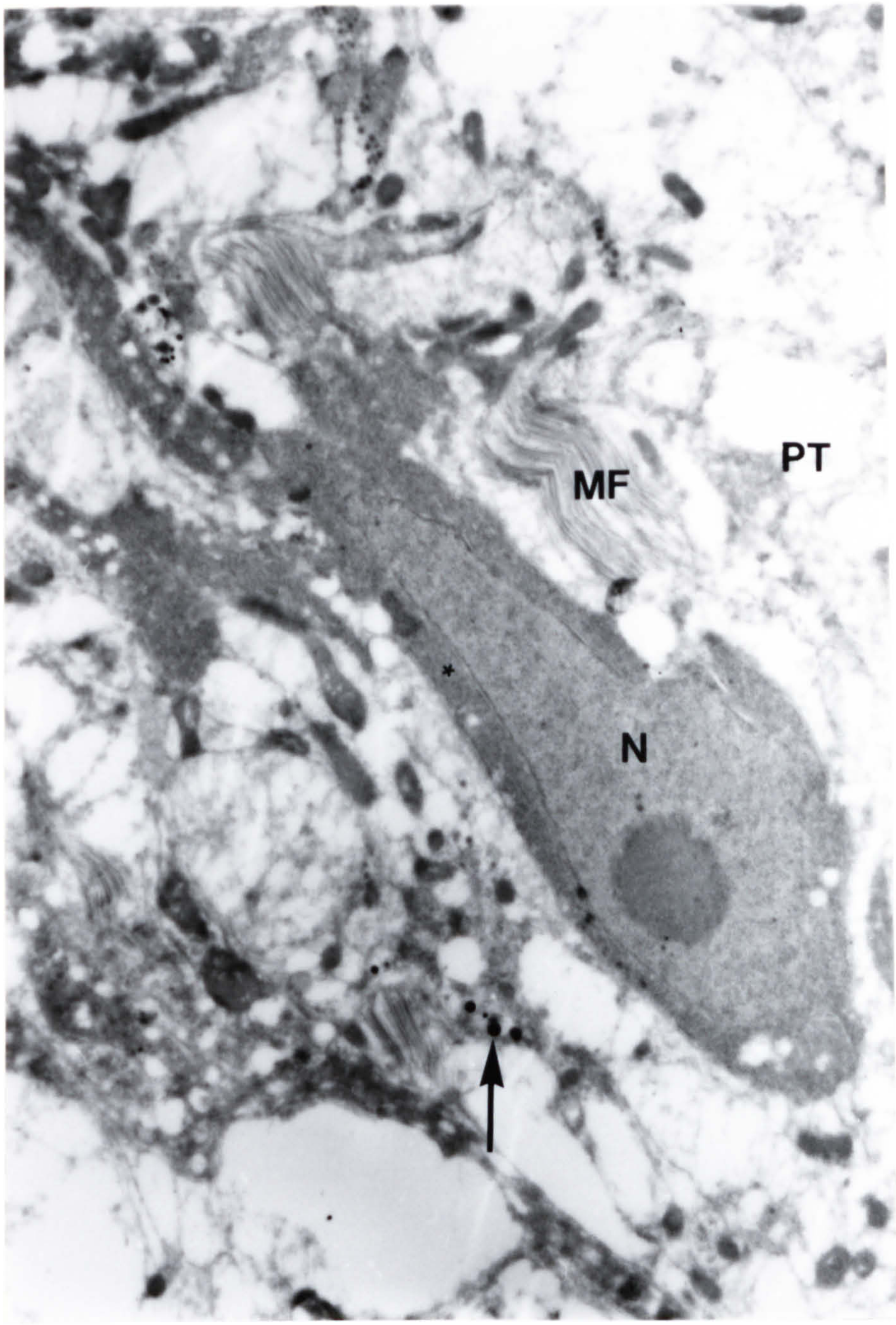
MF
PT
N
*

FIGURE 4.5

High magnification of the tegument (TM) showing numerous discoid bodies (DB) in the cytoplasm. They comprise a trilaminate limiting membrane and dense granular contents. Some regions of the surface plasma membrane have a multilaminate structure (arrow). x 86,000.

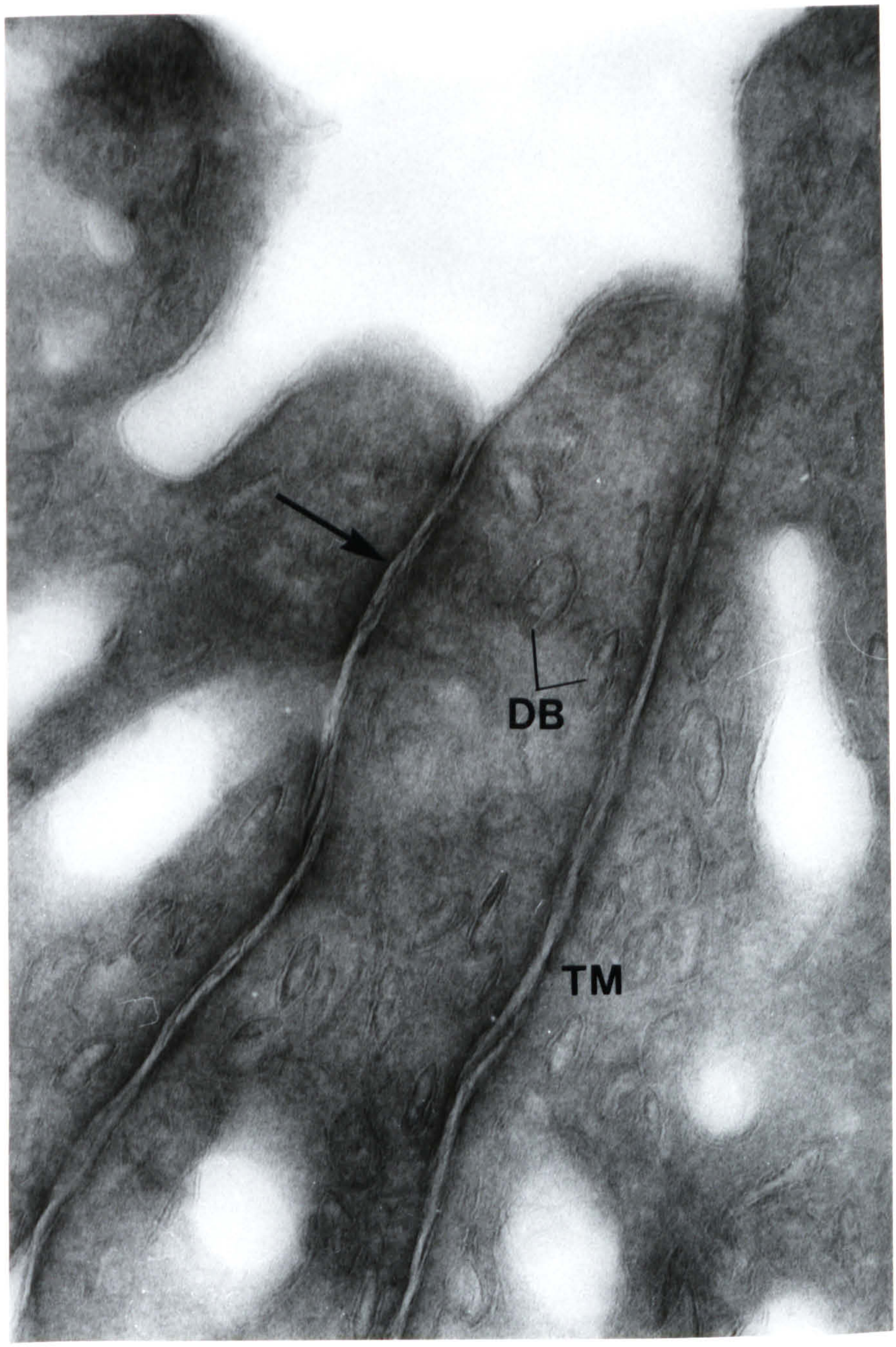
DB
TM

FIGURE 4.6

Gastrodermis is supported by a thin, basal lamina (BL), basal invagination (BI) and a layer of circular and longitudinal muscle fibres (MF). x 9,000.

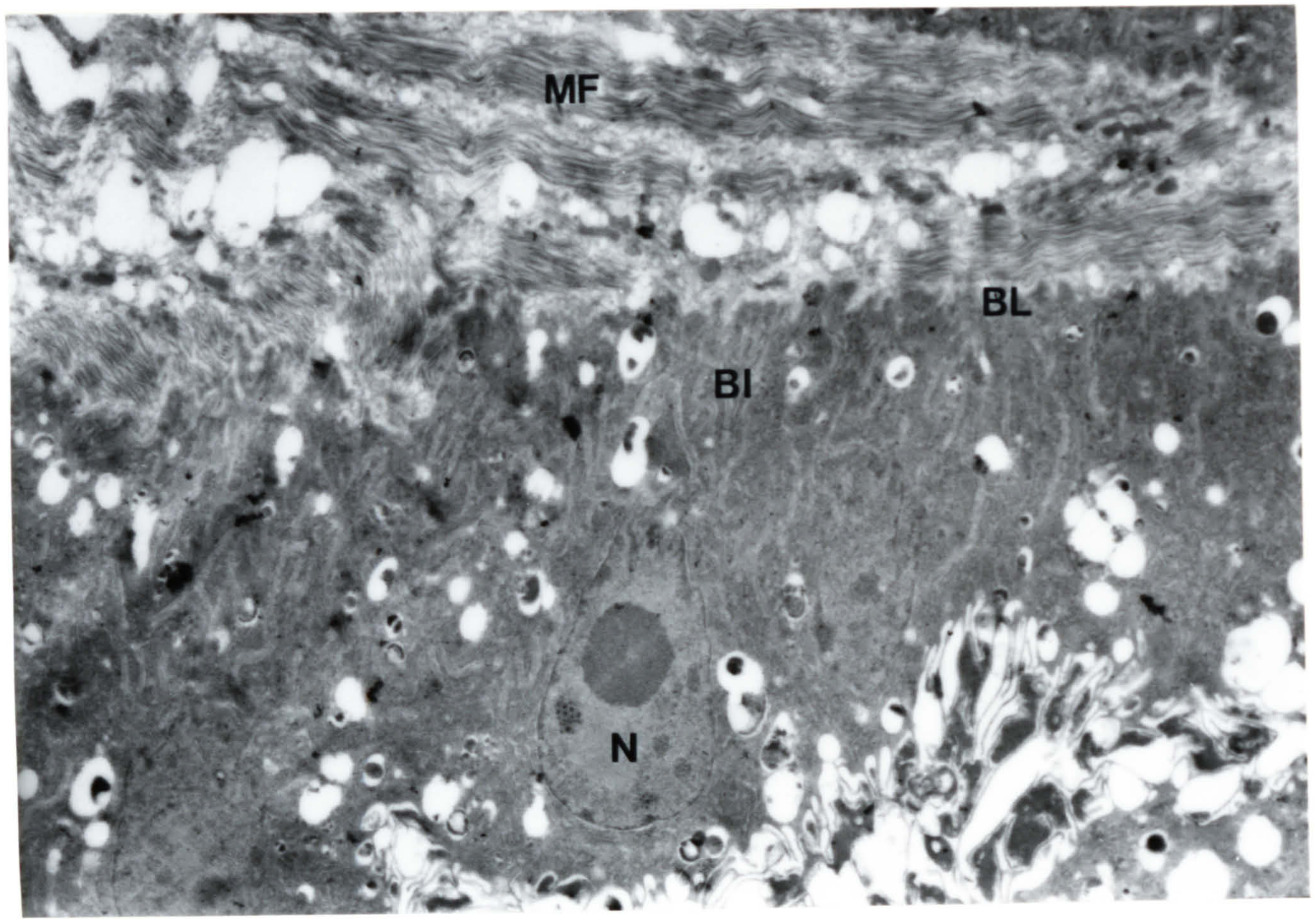
MF
BL
BI
N

FIGURE 4.7

Plate-like invaginations (arrow) of the basal plasma membrane (PM) partly partition the cytoplasm in the syncytial epithelium and separate the nuclei (N). Apart from the large basal nuclei, Golgi (GA) stacks and dense, membrane-bound secretory bodies (SB) are seen in the epithelium (gastrodermis). x 9,300.

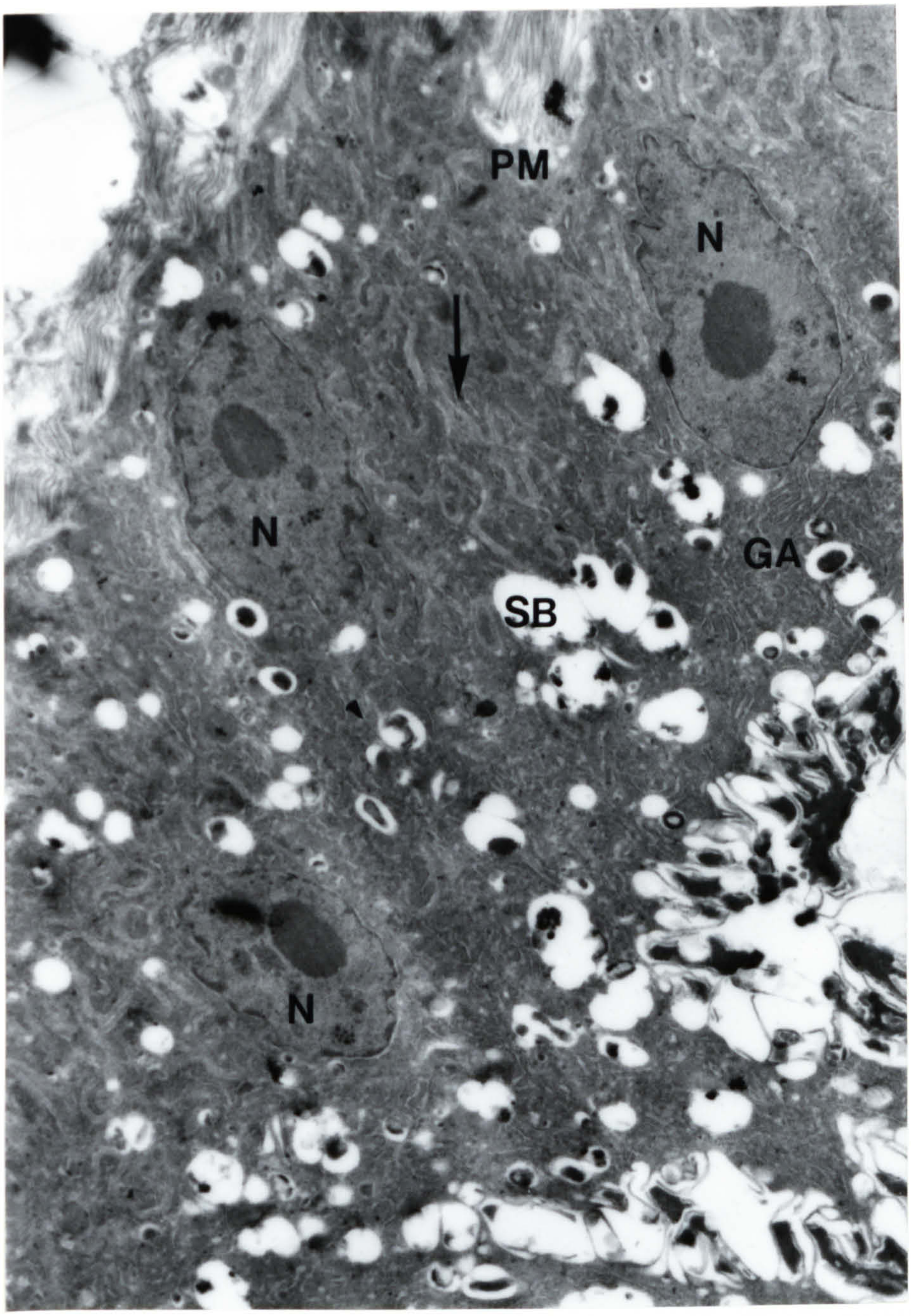
PM
N
N
N
GA
SB
N

FIGURE 4.8

Luminal area contains haemoglobin (Hb) from ingested mouse erythrocytes. The pleomorphic lamellae (L) are broad and sheet-like structures. Nuclei (N), endoplasmic reticulum (ER), basal invagination (BI) and surface microvilli (arrow) are also shown in 4% PF fixed sections. x 7,700.

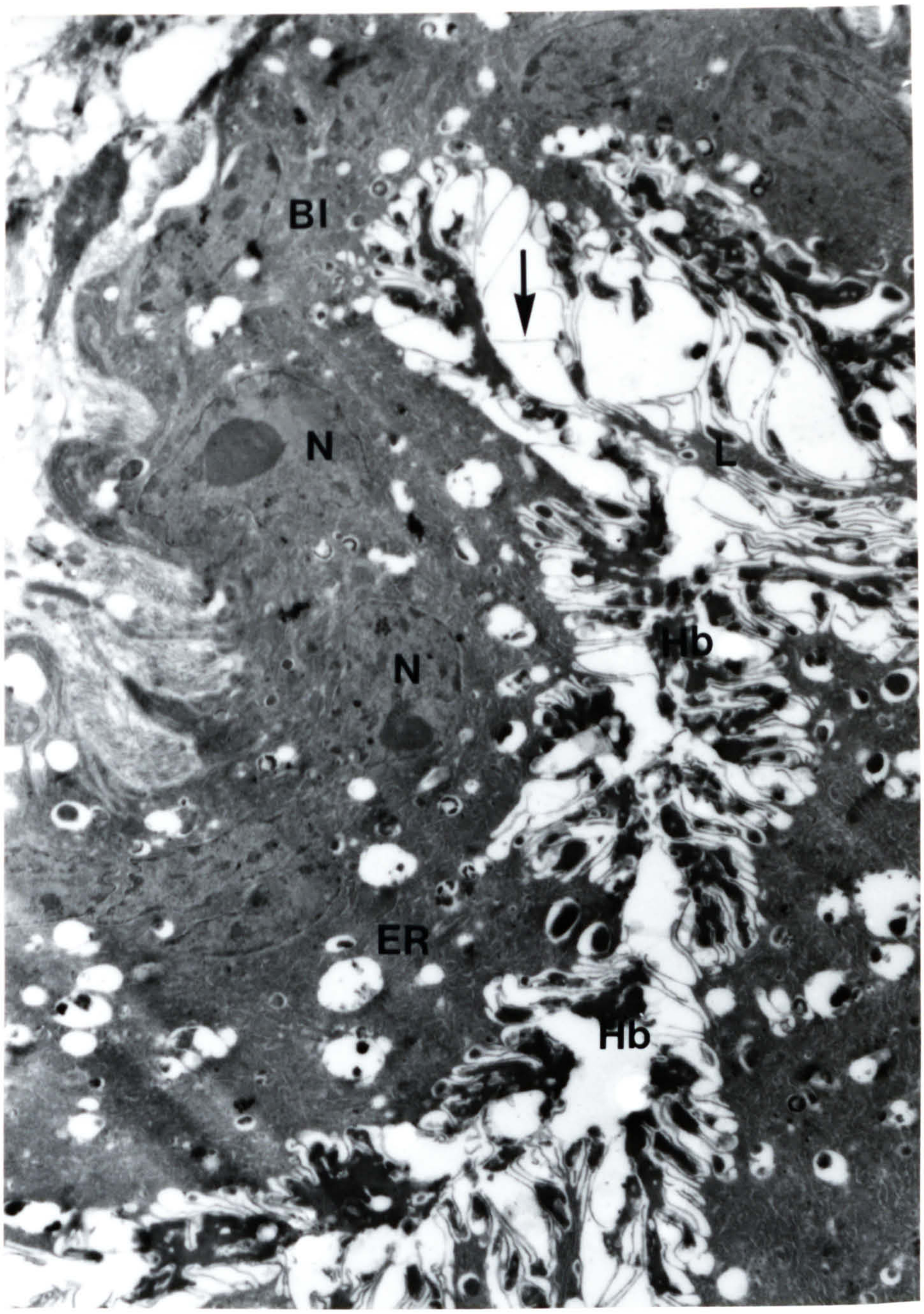
BI
N
L
N
Hb
ER
Hb

FIGURES 4.9 & 4.10

Cryosection of adult worm reacted with MAB D7.2 (1:50) and RAM/Ig/gold (1:25). Note gold particles (arrow) are seen in the tegument (TM) only. Vacuolation (V) are seen in the cytoplasm of the tegument (adult worms were collected by portal perfusion and fixed in 4% PF for 3.5 h at RT). x 9,200 & 13,200.

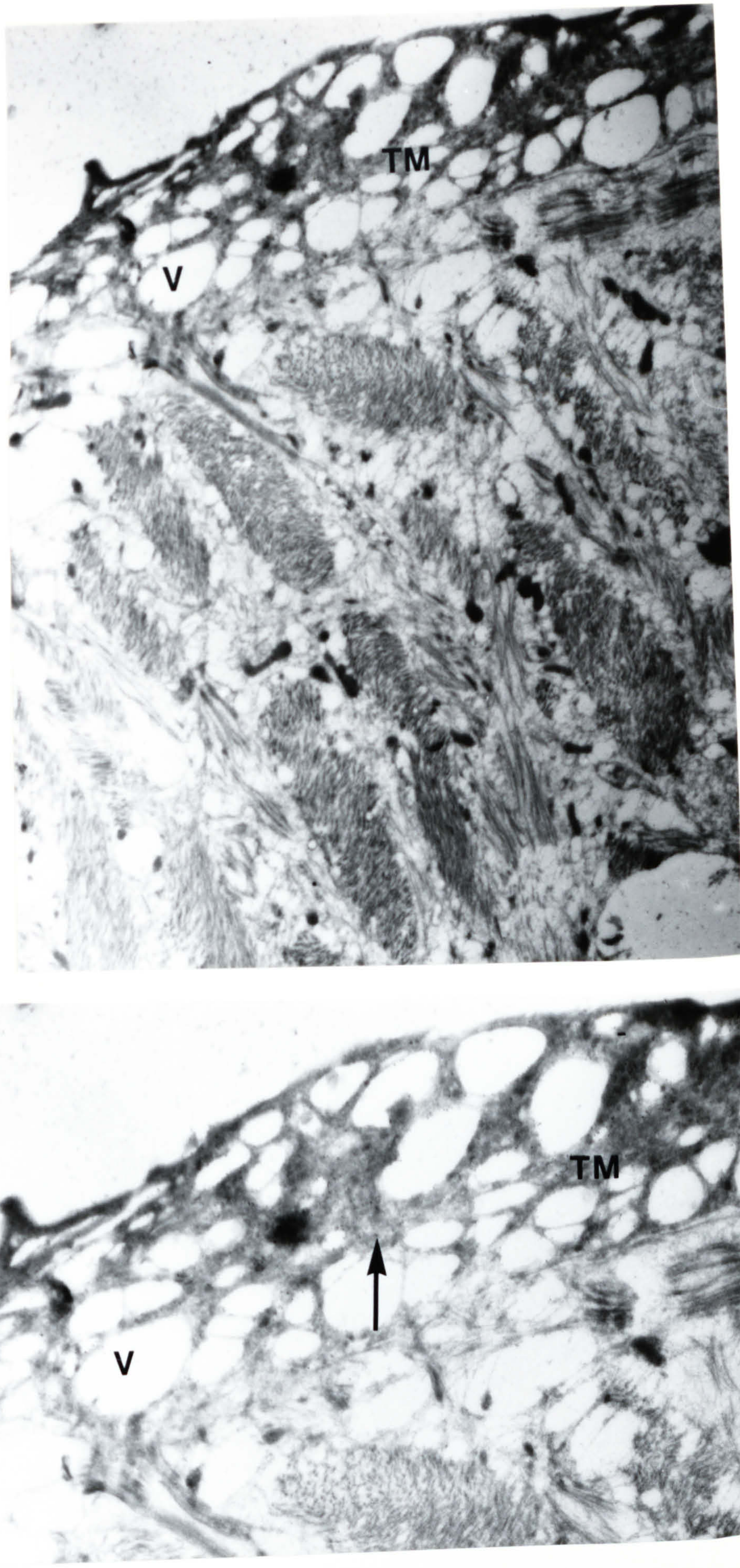
TM
V
TM
V

FIGURE 4.11

Higher magnification of Fig. 4.9 showing gold particles (arrow) in the tegument cytoplasm. The apposing membranes of the basal invaginations of the tegument (TM) become separated and expanded to form extra-tegumental vacuoles (V). x 25,000.

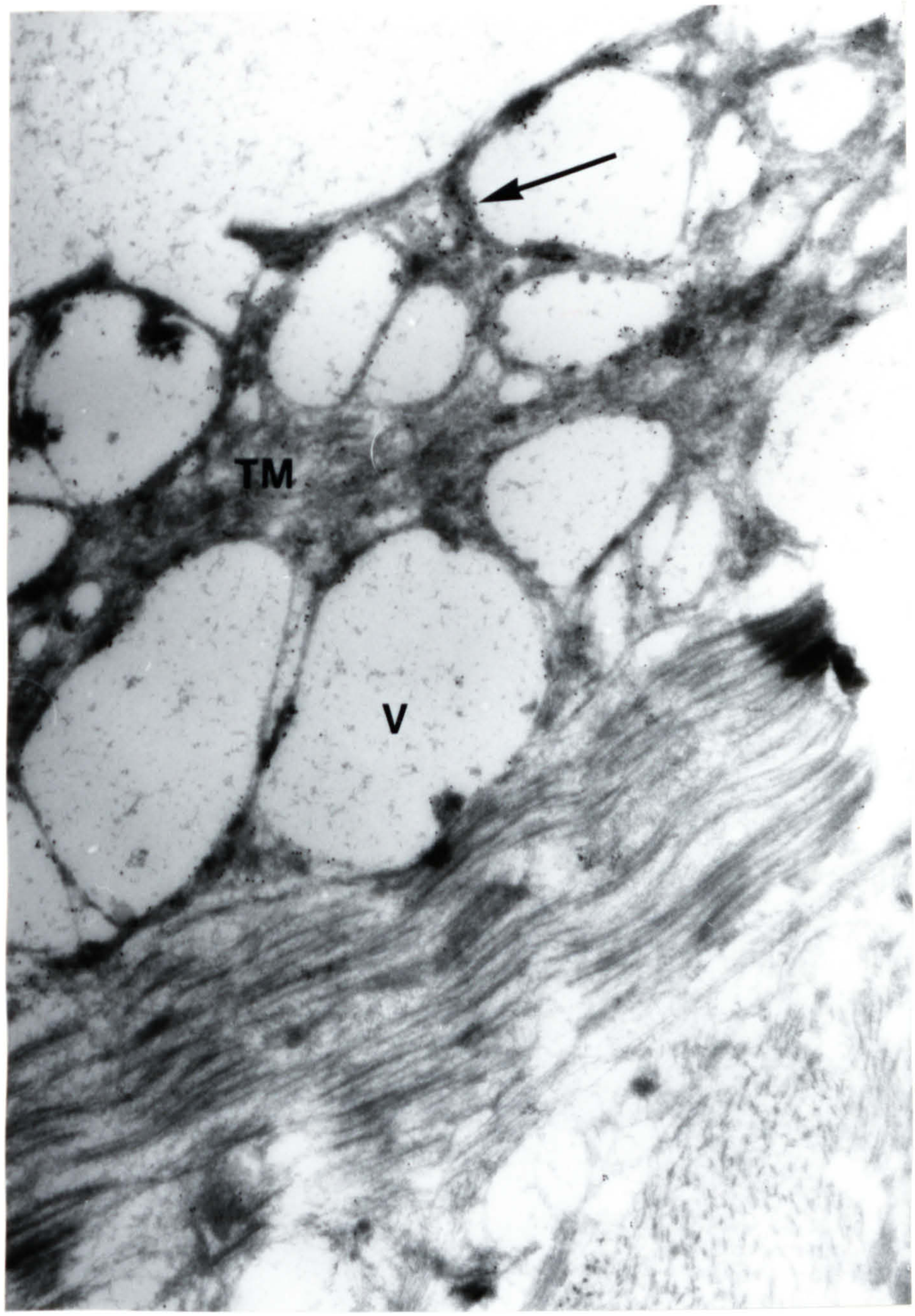
TM
V

FIGURE 4.12

The antigen (arrow) recognized by MAB D7.2 is also seen in the cytoplasmic connection (C) between the tegumental cell body and the tegument (TM). x 22,400.

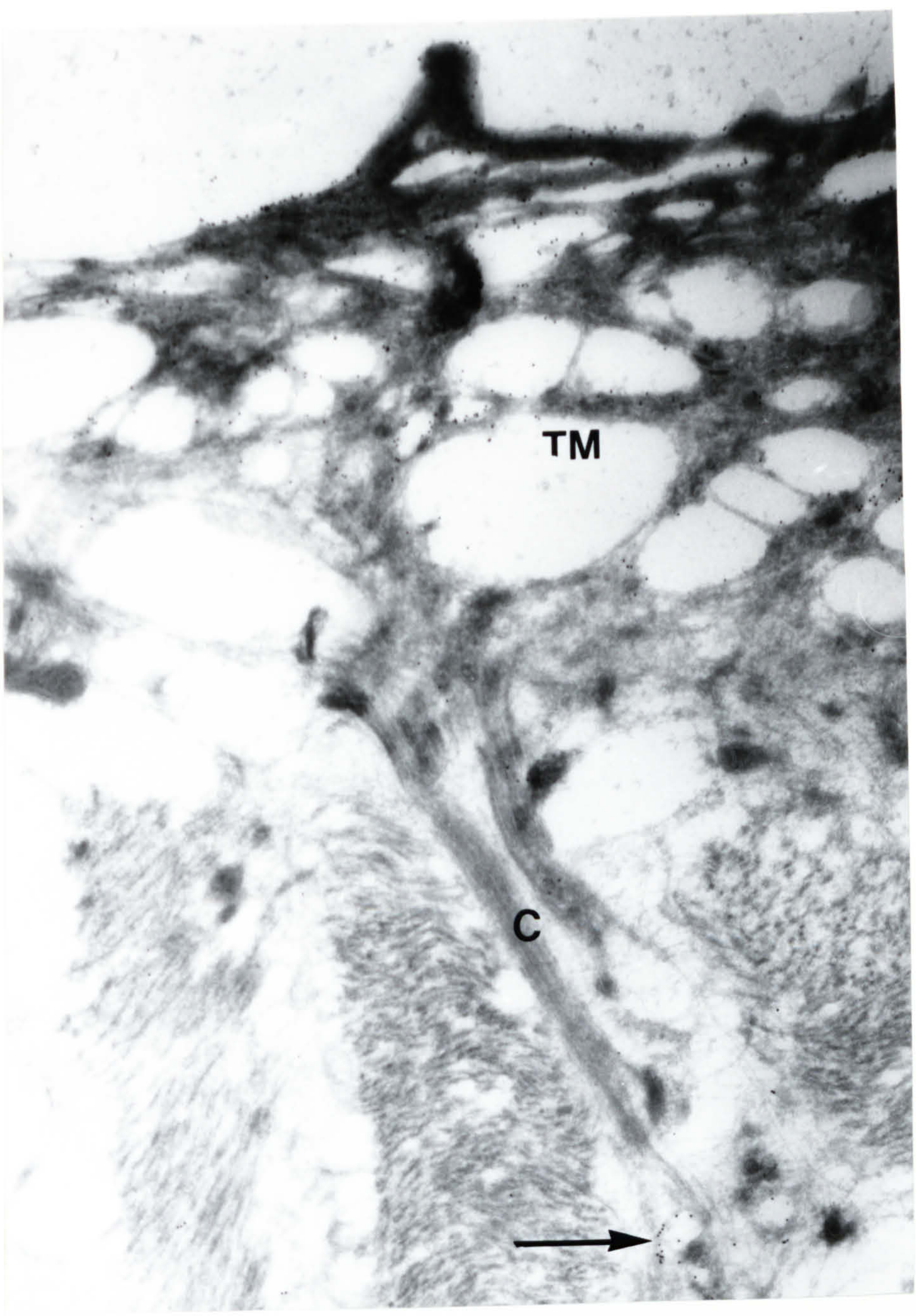
TM
C

FIGURES 4.13 & 4.14

Higher magnification of Fig. 4.9 showing gold particles (arrow) are deposited in the cytoplasmic connections (C) between the tegument (TM) and tegumental cell bodies. x 22,900 & 33,900.

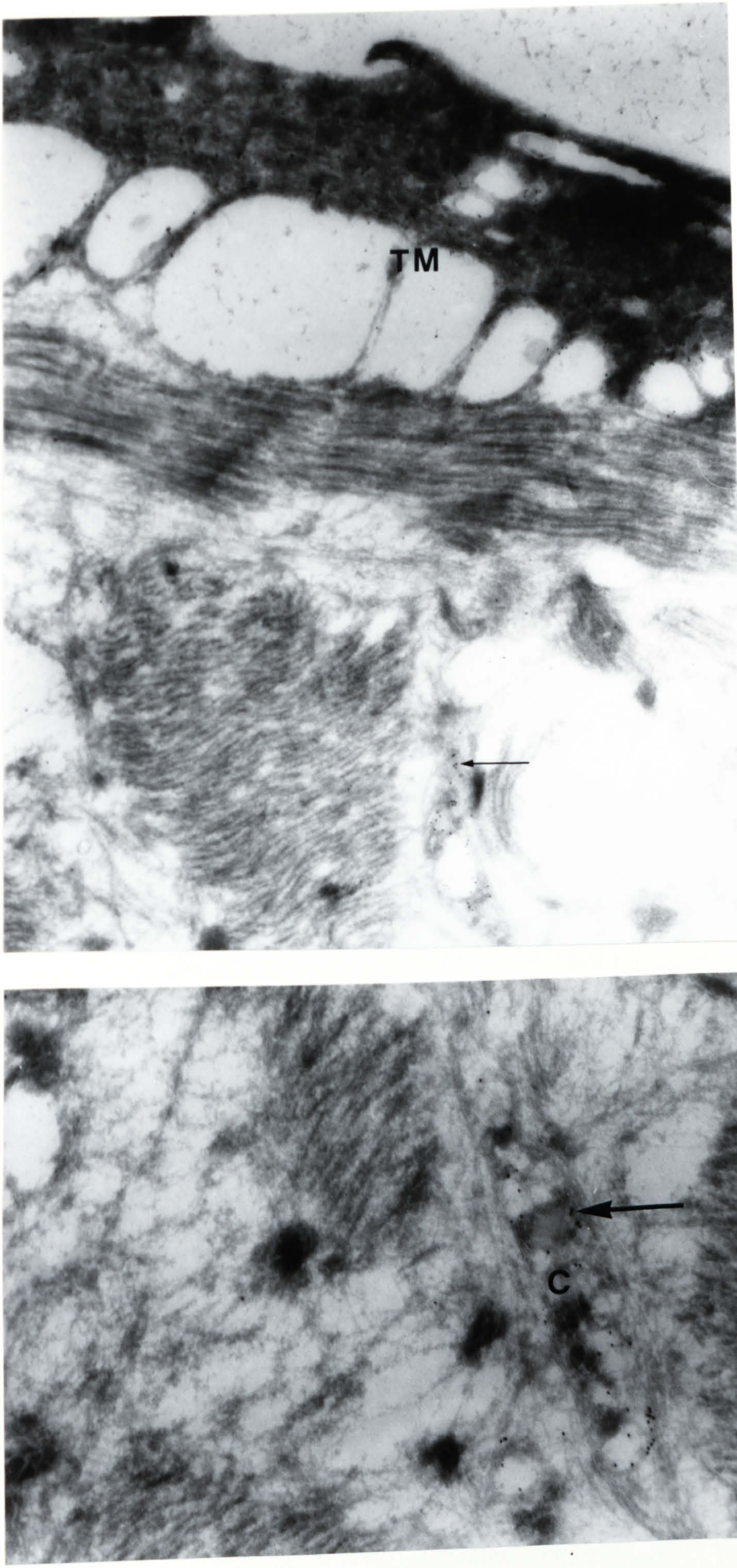
TM
C

FIGURE 4.15

Adult worm collected without portal perfusion and fixed in 4% PF for 4 h at RT. Cryosection was immunostained with MAB D7.2 (1:30) and RAM/Ig/gold (1:25). Note gold particles (arrow) are confined in the tegument (TM). Large vacuoles (V) formed by expanding of the basal invaginations as seen in Fig. 4.11 have disappeared. x 27,000.

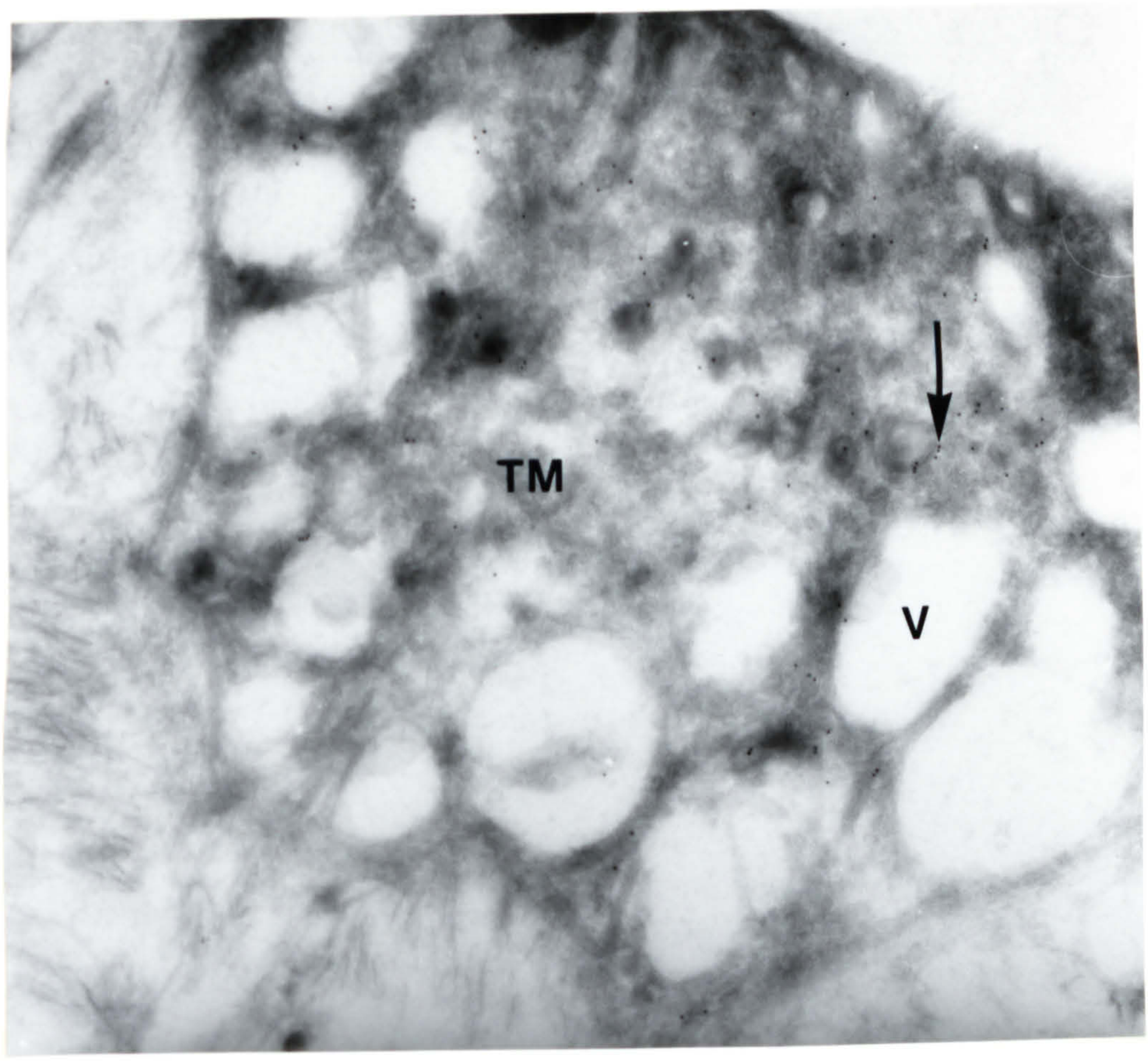
TM
V

FIGURE 4.16

More gold particles are seen in the tegument (TM) and internal tissues (I) of the section stained with AMS (1:80) and RAM/Ig/gold (1:25). Adult worm was fixed in 4% PF for 3.5 h at RT. See Fig. 4.15 (MAB D7.2 which stained tegument only) for comparison. x 25,300.

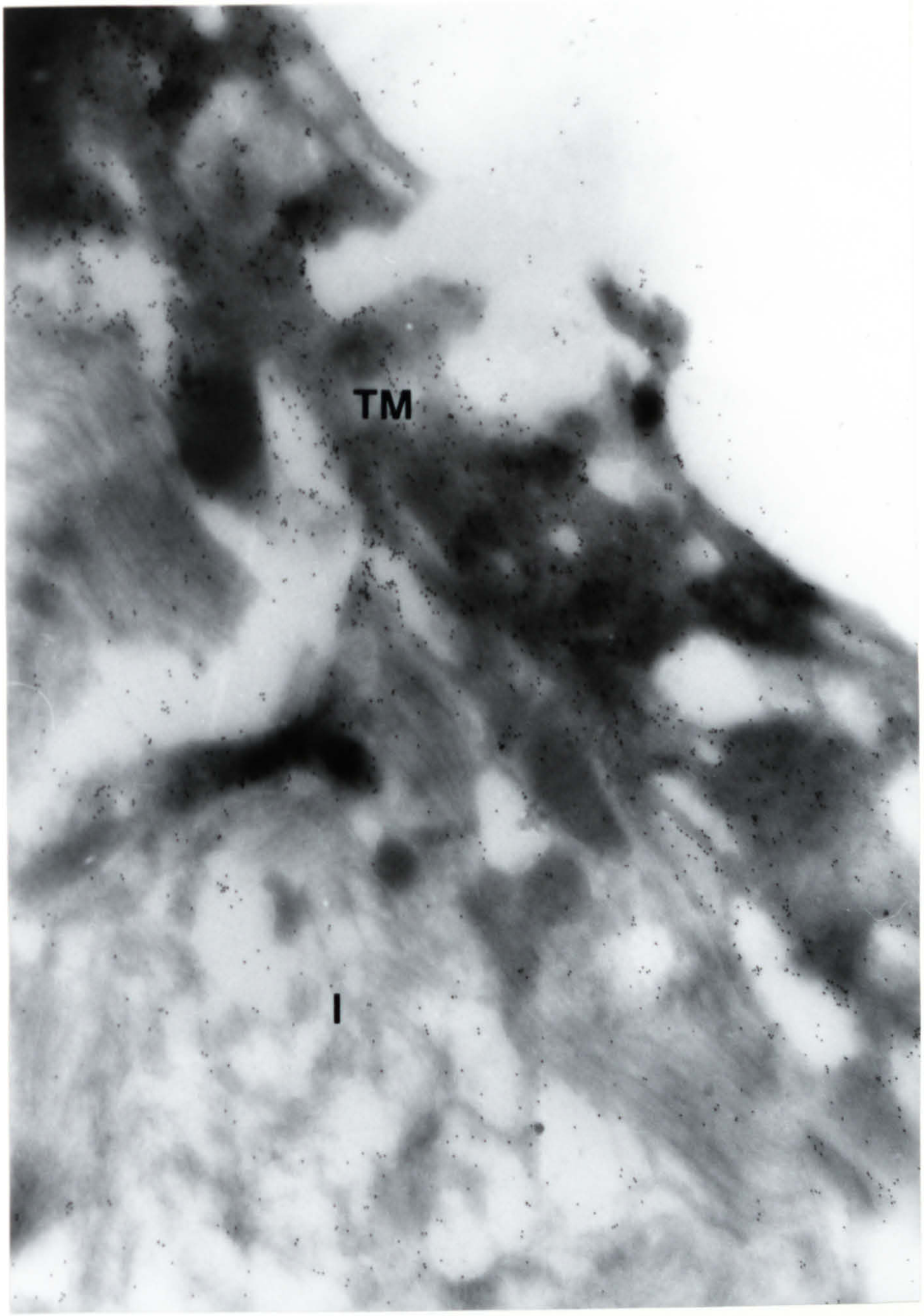
TM

FIGURE 4.17

The target antigens (gold particles, arrow) recognized by MAB D7.4 (1:50) are seen in the tegument cytoplasm and the cytoplasmic connections (C) between tegumental cell bodies and the tegument (TM). x 22,500.

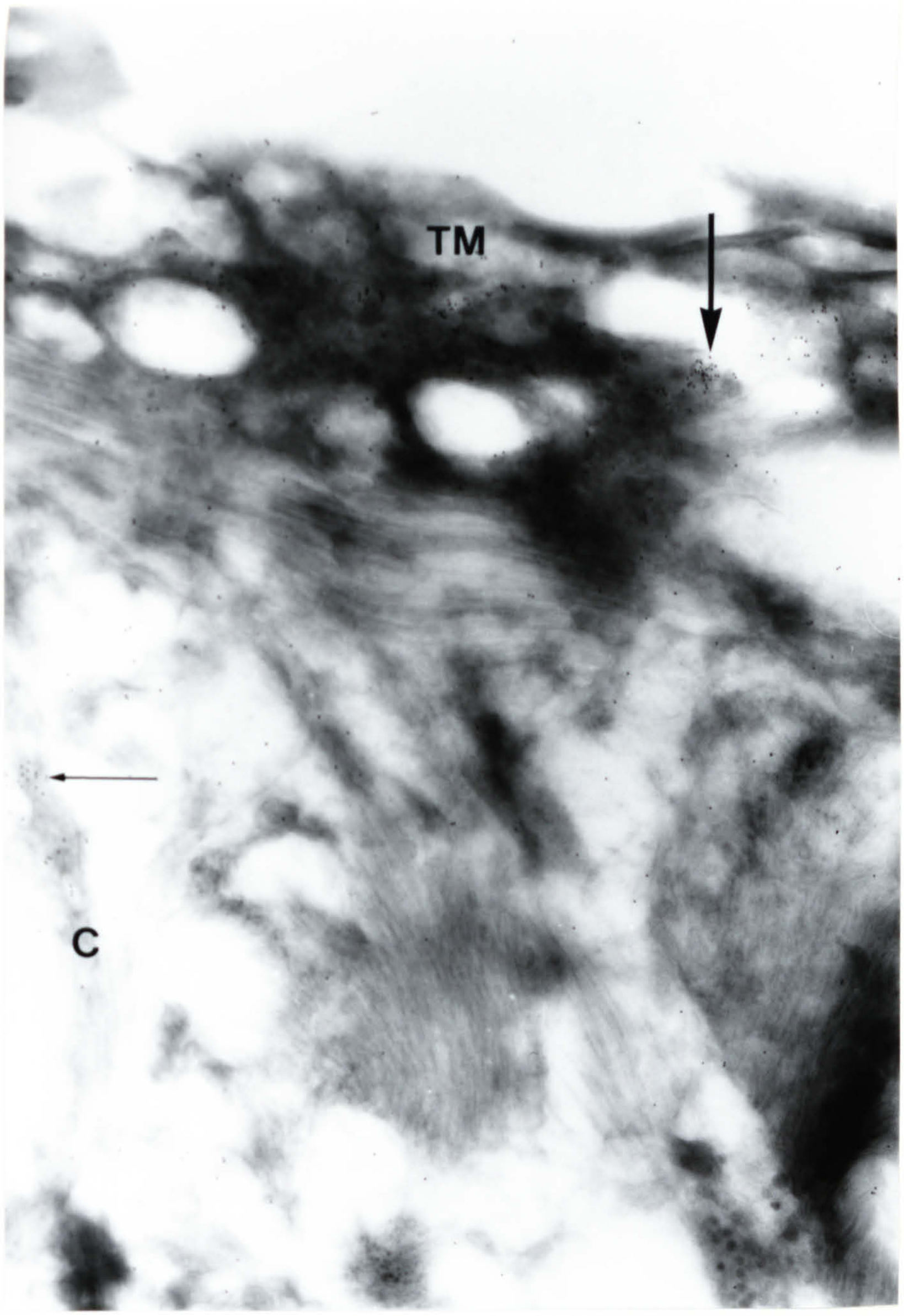
TM
C

FIGURE 4.18

No gold particles are observed in the section which reacted with NMS (1:80) and RAM/Ig/gold (1:25) (TM = Tegument, MF = Myofibres). x 11,700.

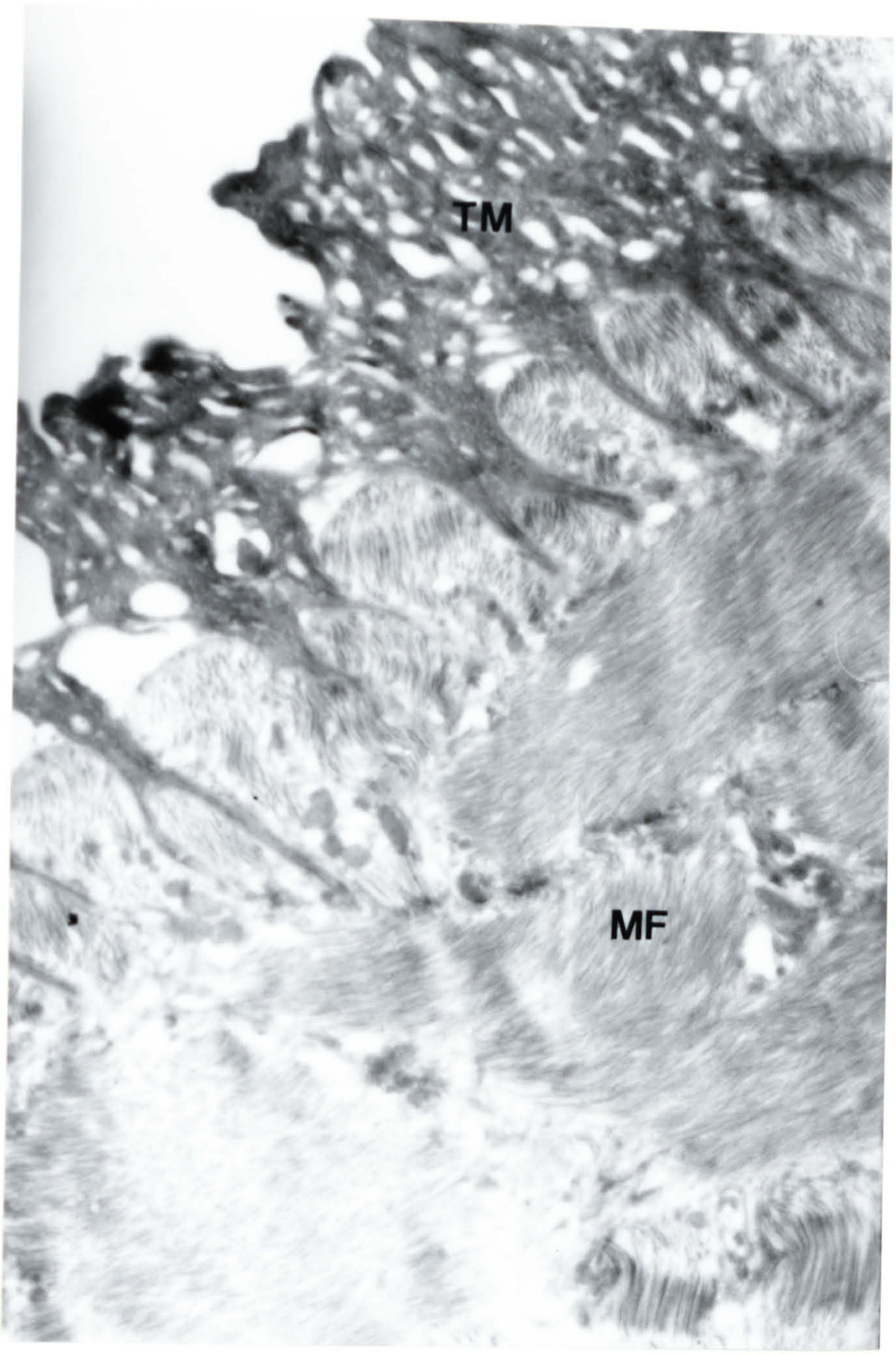
TM
MF

FIGURE 4.19

Cryosection of adult worm immunostained with NS-1 (1:50) and RAM/Ig/gold (1:25). No gold particles are seen in the section. Adult worm was fixed in 4% PF for 3.5 h at RT. (TM = Tegument, MF = Myofibres). x 9,000.

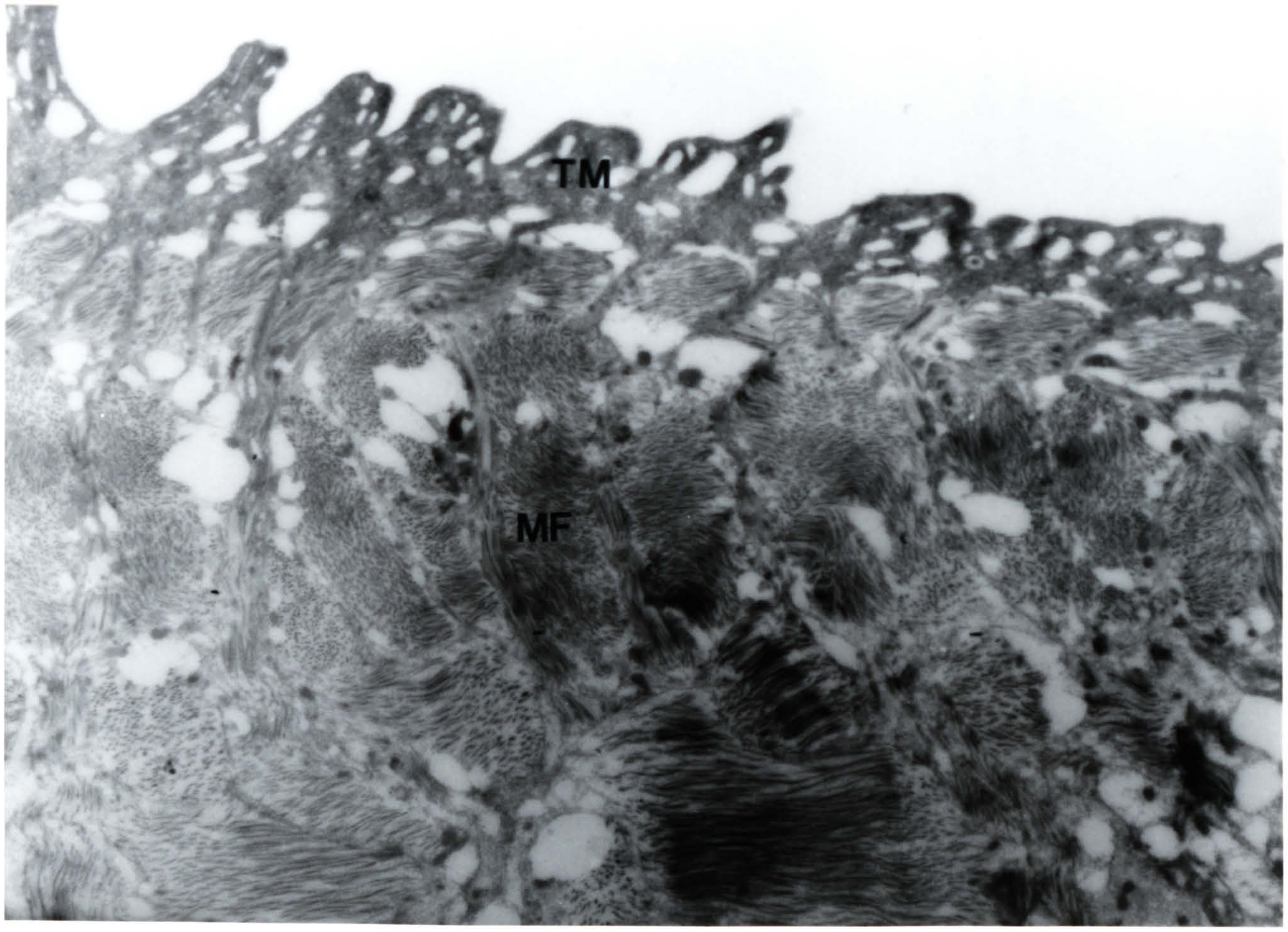
TM
MF